UNIVERSIDADE ESTADUAL PAULISTA
"JÚLIO DE MESQUITA FILHO"
INSTITUTO DE BIOCIÊNCIAS – RIO CLARO

PROGRAMA DE PÓS-GRADUAÇÃO EM ECOLOGIA, EVOLUÇÃO E BIODIVERSIDADE

THERMAL AND HYDRIC PHYSIOLOGY DETERMINE HABITAT OCCUPANCY IN A GROUP OF NEOTROPICAL FROGS AND INFLUENCE THEIR VULNERABILITY TO CLIMATE CHANGE

LUIS MIGUEL SENZANO CASTRO

Rio Claro – SP
2024

UNIVERSIDADE ESTADUAL PAULISTA
"JÚLIO DE MESQUITA FILHO"
INSTITUTO DE BIOCIÊNCIAS – RIO CLARO

PROGRAMA DE PÓS-GRADUAÇÃO EM ECOLOGIA, EVOLUÇÃO E BIODIVERSIDADE

THERMAL AND HYDRIC PHYSIOLOGY DETERMINE HABITAT OCCUPANCY IN A GROUP OF NEOTROPICAL FROGS AND INFLUENCE THEIR VULNERABILITY TO CLIMATE CHANGE

LUIS MIGUEL SENZANO CASTRO

Tese apresentada ao Instituto de Biociências do Câmpus de Rio Claro, Universidade Estadual Paulista, como parte dos requisitos para obtenção do título de Doutor em Ecologia, Evolução e Biodiversidade.

Orientador: Prof. Dr. Denis Otavio Vieira de Andrade.

Rio Claro – SP
2024

C355t

Castro, Luis Miguel Senzano
Thermal and hydric physiology determine habitat occupancy in a group of neotropical frogs and influence their vulnerability to climate change / Luis Miguel Senzano Castro. -- Rio Claro, 2024
127 p. : il., tabs., mapas

Tese (doutorado) - Universidade Estadual Paulista (Unesp), Instituto de Biociências, Rio Claro
Orientador: Denis Otavio Vieira de Andrade

1. Anfíbios. 2. Mudanças climáticas. 3. Modelagem mecanicista. 4. Balanço hídrico. 5. Ontogenia. I. Título.

Sistema de geração automática de fichas catalográficas da Unesp. Biblioteca do Instituto de Biociências, Rio Claro. Dados fornecidos pelo autor(a).

Essa ficha não pode ser modificada.

CERTIFICADO DE APROVAÇÃO

TÍTULO DA TESE: THERMAL AND HYDRIC PHYSIOLOGY DETERMINE HABITAT OCCUPANCY IN A GROUP OF NEOTROPICAL FROGS AND INFLUENCE THEIR VULNERABILITY TO CLIMATE CHANGE

AUTOR: LUIS MIGUEL SENZANO CASTRO

ORIENTADOR: DENIS OTAVIO VIEIRA DE ANDRADE

Aprovado como parte das exigências para obtenção do Título de Doutor em Ecologia, Evolução e Biodiversidade, área: Biodiversidade pela Comissão Examinadora:

Prof. Dr. DENIS OTAVIO VIEIRA DE ANDRADE (Participaçao Presencial)
Departamento de Biodiversidade / Unesp - IB Rio Claro

Prof. Dr. LUARA TOURINHO DE OLIVEIRA PEREIRA (Participaçao Presencial)
Instituto de Estudos Avançados / Universidade de São Paulo

Prof. Dr. CELIO FERNANDO BAPTISTA HADDAD (Participaçao Presencial)
Departamento de Biodiversidade / Unesp - IB Rio Claro

Rio Claro, 17 de novembro de 2023

ACKNOWLEDGEMENTS

Words cannot express the overwhelming amount of support I've received from different people throughout the development of this work. First, I would like to thank my family, especially my parents, for their continual support during this time.

I would like to put my biggest appreciation to my Advisor, Denis Vieira Andrade for the guidance, patience, and very importantly, the open-door policy for discussions about ideas or issues related to this research anytime. At the very end, these fruitful discussions (and even certain liberties) were key for me to define the general scope of this work, which was very exciting -even though a bit more challenging than initially expected- and rewarding.

I wish to thank Milton C. Ribeiro, Sidney F. Gouveia, Rodrigo S. B. Gavira, and Rodolfo C. O. Anderson, Mariana N. Routh, José E. Carvalho, Luisa M. Diele-Viegas, Laura Tourinho and Celio F. B. Haddad for their critical comments and suggestions during different stages and circumstances throughout this time, which helped me to markedly improve this work.

I want to deeply thank Vanesa F. Bejarano Alegre for her understanding and support during the countless hours, weekends, and holydays I spent at the laboratory away from home. Also, I do appreciate her insightful guidance on conceptual analytical tools, which served me as the starting point for subsequent analytical steps.

I am also deeply grateful to my lab-mates, whose insightful comments improved this work. I also appreciate the valuable and memorable extra academic funny moments and activities and the support they've provided along the way. I would like to thank Denis, Rodrigo, Juliana, Amanda, Mariana, Lua, Georgia, Rafael (Urucum), Vanesa, Diogo, Celso and Jacira Gavira, for their involvement during fieldwork, animal maintenance and/or their hospitality at the field site during the collection of animals.

Finally, none of this research could have been possible without the logistic support of some institutions, such as the Programa de Pós-Graduação em Ecologia, Evolução e Biodiversidade (UNESP - Rio Claro, SP), the Centro de Estudos Ambientais (UNESP - Rio Claro, SP), and the Laboratório de Pesquisa Integrativa em Biodiversidade (Universidade Federal de Sergipe - São Cristóvão, SE).

This study was financed in part by the Coordenação de Aperfeiçoamento de Pessoal de Nível Superior - Brasil (CAPES) - Finance Code 001

ABSTRACT

Amphibians balance their thermal and water budgets depending on their physiological state and the physical environment to avoid detrimental consequences in organismal performance. Most mechanistic assessments emphasize thermal over water constraints, potentially overlooking important aspects of the amphibian's particular morpho-physiological attributes. Herein, we evaluated the influence of thermal and hydric constraints, combined and separately, on the activity budget across the geographic distribution of ground-dwelling Neotropical frogs belonging to the *Leptodactylus* genus (*L. fuscus*, *L. mystacinus*, *L. macrosternum* and *L. luctator*). Based on laboratory and field data, we integrated species-specific functional attributes with their ground-level microclimate through a mechanistic modeling procedure. We inferred environmental suitability using principles of heat and mass balances, while allowing for interactive behavioral responses of sheltering during restrictive conditions. Our results show that hydric-related restrictions in activity are influenced by body size and may become an impediment even under conditions considered thermally adequate. We also found that the consideration of shelters as thermal and hydric refugia improved the resilience capacity of frogs to stressful climatic conditions. More strikingly, thermal-induced restrictions in activity were linked to low temperatures rather than warmer conditions, indicating a trade-off in diel activity driven by upper and lower thermal bounds. These findings provide a broader picture of climatic constraints on anuran activity and offer new insights into how species may respond to changing climatic conditions in tropical regions.

Keywords: Amphibians, Climate change, Mechanistic niche modeling, Thermal and water balance, Ontogeny.

RESUMO

Os anfíbios equilibram a manutenção do seu balanço hídrico e térmico dependendo do seu estado fisiológico e do ambiente físico para evitar consequências deletérias no desempenho do organismo. A maioria das avaliações mecanicistas enfatiza as restrições térmicas sobre as hídricas, potencialmente negligenciando aspectos importantes dos atributos morfo-fisiológicos específicos dos anfíbios. Aqui, avaliamos a influência das restrições hídricas e térmicas, combinada e separadamente, no tempo de atividade em toda a distribuição geográfica de rãs neotropicais terrestres pertencentes ao gênero *Leptodactylus* (*L. fuscus, L. mystacinus, L. macrosternum* e *L. luctador*). Com base em dados de laboratório e de campo, integramos atributos funcionais específicos das espécies com seu microclima ao nível do solo usando um procedimento de modelagem mecanicista. Inferimos a adequabilidade ambiental usando princípios de equilíbrio de calor e massa, ao mesmo tempo que permitimos respostas comportamentais interativas de procura de abrigo durante condições restritivas. Nossos resultados mostram que as restrições hídricas na atividade são influenciadas pelo tamanho corporal e podem se tornar um impedimento mesmo em condições consideradas termicamente adequadas. Encontramos também que a inclusão dos abrigos como refúgios térmicos e hídricos melhorou a capacidade de resiliência das rãs a condições climáticas estressantes. Importante, as restrições na atividade induzidas pela troca de calor estavam ligadas a baixas temperaturas e não as condições mais quentes, indicando um compromisso na atividade diária impulsionado pelos limites térmicos superiores e inferiores. Estas descobertas fornecem uma imagem mais ampla das restrições climáticas à atividade dos anuros e oferecem novos insights sobre como as espécies podem responder às mudanças nas condições climáticas nas regiões tropicais.

Palavras-Chave: Anfíbios, Mudanças climáticas, Modelagem mecanicista, Balanço hídrico, Ontogenia.

TABLE OF CONTENTS

GENERAL INTRODUCTION

As most organisms, amphibians are not randomly distributed in space. Rather the observed distribution corresponds to a variety of ecological, behavioral, and physiological processes that, in conjunction with environmental factors, shape their geographic distribution and dispersal abilities (Griffiths et al. 2010, Dabés et al. 2012). The limitations imposed by thermal and hydric constraints are particularly acute because, as ectotherms, their body temperature is highly influenced by the thermal environment and, as moist skinned organisms, cutaneous evaporative water loss expose them to the constant risk of dehydration (Hillman et al. 2009). As such, anuran's survival and fitness are dependent on the selection of microhabitats that provide favourable thermal and moist conditions that allows for activity while minimizing the risks of incurring in excessive water loss (Seebacher and Alford 2002).

Thermal and hydric attributes of microhabitats are usually associated to thermal and hydric physiology variations in anurans (Wells 2007, Pittman et al. 2014). Species occurring in thermally variable environments, for example, generally exhibit both broader thermal tolerances and thermal preferred ranges than species from more stable areas (Calosi et al. 2008, Deutsch et al. 2008). Likewise, species from hotter areas and usually low humidity are more likely to withstand higher rates of evaporative water loss (Cruz-Piedrahita et al. 2018). A remarkable tolerance to dehydration and a rapid water uptake capacity through the pelvic patch may act as adaptive responses to withstand prolonged periods in habitats with water-limiting conditions (Hillman et al. 2000, Titon et al. 2010). Additionally, morphological variations on body size also lead to interspecific differences by effects on the surface-to-volume ratio, a key factor in determining size-dependent rate processes like water loss and uptake (Titon and Gomes 2015) and heat gain/loss balance (Amado et al. 2018).

Under the current global warming scenario, there has been a growing interest on how species fitness will response to rising temperatures, and species' ability to buffer against the detrimental effects associated to higher thermal conditions (Calosi et al. 2008, Sinervo et al. 2010, Scheffers et al. 2013). Amphibian populations are declining globally (Duarte et al. 2012), and species with a narrow thermal and desiccation tolerance, higher rates of dehydration or a lower rehydration capacity might be at special risk of extinction (Huey et al. 2012), unless they are able to find cooler microsites that provide sufficient moisture to rehydrate and prevent excessive water loss (Seebacher and Alford 2002). Most studies on species' vulnerability to climate change correlate

georeferenced occurrence records of species to climatic variables to identify climatically suitable areas (the correlative ecological niche modeling; see Peterson et al. 2011). Although correlative approaches provide insightful information on species' environmental suitability, they do not capture causal aspects relating intrinsic functional properties of organisms and their environment. In this way, species that today occupy similar environmental conditions may not response equally under novel climatic events, which certainly will play a key role in shaping and setting future species distributions (Evans et al. 2015, Elith and Leathwick 2009). Additionally, most correlative studies are based on above-ground coarse macroclimates, which may fail to capture the thermal and hydric conditions at the microhabitat where the organisms thrive (Nadeau et al. 2016), thereby misleading correlations and predictions (Scheffers et al. 2013, Jiménez et al. 2019).

There is a growing consensus on the benefits of considering additional functional parameters when approaching species distribution patterns (Kearney et al. 2010), and mechanistic models incorporating physiological traits of organisms have shown to be a good alternative to this end (Mitchell et al. 2013, Evans et al. 2015). In essence, mechanistic models integrate organismal functional attributes as metrics to set critical environmental constraints and use the outcomes to infer whether an organism can sustain positive balances of mass and/or energy at a given place (reviewed by Briscoe et al. 2023). This approach has been adopted successfully in studies aiming to evaluate reptile vulnerability to climate change (e.g., Huey et al. 2009, Sinervo et al. 2010, Clusella-Trullas and Chown 2014, Ceia-Hasse et al. 2014), with most of them primarily focusing on organismal thermal traits (Evans et al. 2015).

Besides temperature, water balance sensitivity is an equally important and comparatively less explored aspect of organismal response to climate warming. In wet-skinned organisms like amphibians, mechanistic modeling must consider not only heat, but also water relationships when trying to establish a linkage between the physical properties of the environment and organismal functional attributes (Amado et al. 2018). Phenological activities, such as activity time and reproduction, are markedly tied to the availability of water in anurans. As such, drastic changes in rainfall regimes (e.g., droughts) may hamper anurans' ability to regulate their water balance, causing anurans to reduce their activity time or even cease reproduction to avoid desiccation risk. This must be particularly true in species-rich regions like the south American Neotropics, where declining species events has been related to droughts (Stewart 1995, Walls et al. 2013), tied to heat events (Tuff et al. 2016) which are both expected to become more variable in duration,

frequency, and magnitude under a climate change scenario (Nuñez et al. 2009, Stillman 2019). However, there is a paucity of functional trait-based studies assessing climate change risks on amphibians, and even less well-founded studies rooted simultaneously in their thermal and hydric eco-physiological relationships, with mechanistic-based modeling assessments virtually absent for Neotropical anuran species.

In tropical and subtropical regions, daytime temperatures are much higher and variable than at night (Muñoz and Bodensteiner 2019), but most amphibians in these regions are strictly nocturnal (Anderson and Wiens 2017). The thermal consequences of nocturnality have important implications from a thermoregulatory perspective. For example, thermally permissive conditions at night reduce the risk of overheating but also lower thermoregulatory opportunities (Hitchcock and McBrayer 2006, Rock and Cree 2008), which may have important consequences on amphibian physiological performance. Likewise, because of their moist and highly permeable skin, water loss is still an ongoing process that can constraint activity even under conditions considered thermally suitable.

In this thesis work, we aimed to enhance our understanding of the potential interactions between thermal and hydric constraints on anuran activity at the organismal scale (microclimate) and then scale them up to broad-scale distributional patterns to infer environmental suitability. Bridging these fine-scale mechanisms to broad geographical scales allows us to account for a broader spectrum of processes influencing species' distributions, which might improve our ability to predict species' response to climate change. For such a purpose, we employ thermal, hydric, and performance organismal traits from *Leptodactylys* frogs (*L. fuscus*, *L. mystacinus*, *L. macrosternum* and *L. luctator*), and from this, we provide a mechanistic assessment rooted on principles of heat and mass balance to infer environmental optimality under current and future microclimates. Species of this genus are traditionally associated to water bodies (Haddad et al. 2013), although the extent of dependency to moist conditions greatly vary among species. This turns them a good taxon model, as they inhabit a variety of habitats varying in moist and thermal conditions. The strategy of this thesis was to develop three chapters under three-fold approaches. In chapter 1, we measured thermal and water organismal traits that are thought to limit anuran activity and we also explored their interspecific ecological implications. In chapter 2, we gathered this organismal trait information, and linked them to the hourly ground-level microclimate via a mechanistic modeling approach to infer environmental suitability and predict potential species distribution.

Finally, in chapter 3, we decouple the thermal and water sensitivity in a model species (*L. macrosternum*) between young and adult individuals and integrate them to ground-level conditions for present-day and future microclimates to mechanistically forecast the potential consequences of climate change.

REFERENCES

Amado T. F., C. J. Bidau and M. A. Olalla-Tárraga. 2018. Geographic variation of body size in New World anurans: energy and water in a balance. Ecography doi: 10.1111/ecog.03889

Briscoe N. J., J. Elith, R. Salguero-Gómez, J. L. Lahoz-Monfort, J. S. Camac, K. M. Giljohann, M. H. Holden, B. A. Hradsky, M. R. Kearne, S. M. McMAhon, B. L. Phillips, T. J. Regan, J. R. Rhodes, P. A. Vesk, B. A. Wintle, J. D. L. Yen and G. Guillera-Arriota. 2023. Forecasting species range dynamics with process-explicit models: matching methods to applications. *Ecology Letters*, 22: 1940-1956.

Calosi P., D. T. Bilton and J. I. Spicer. 2008. Thermal tolerance, acclimatory capacity and vulnerability to global climate change. Biology letters 4: 99-102.

Ceia-Hasse A., B. Sinervo, L. Vicente and H. M. Pereira. 2014. Integrating ecophysiological models into species distribution projections of European reptile range shifts in response to climate change. Ecography 37: 679-688.

Clusella-Trullas S. and S. L. Chown. 2014. Lizard thermal trait variation at multiple scales: a review. Journal of Comparative Physiology B 184(1): 5-21.

Dabés L., V. M. G. Bonfim, M. F. Napoli and W. Klein. 2012. Water balance and spatial distribution of an anuran community from Brazil. Herpetologica 68(4): 443-455.

Deutsch C. A., J. J. Tewksbury, R. B. Huey, K. S. Sheldon, C. K. Ghalambor, D. C. Haak and P. R. Martin. 2008. Impacts of climate warming on terrestrial ectotherms across latitude. Proceedings of the National Academy of Sciences of the United States of America 105(18): 6668-6672.

Duarte H., M. Tejedo, M. Katzenberger, F. Marangoni, D. Baldo, J.F. Beltrán, D.A. Martí, A. Richter-Boix and A. Gonzales-Voyer. 2012. Can amphibians take the heat? Vulnerability to climate warming in subtropical and temperate larval amphibians communities. Global Change Biology 18(2): 412-421.

Elith J. and J. R. Leathwick. 2009. Species distribution models: ecological explanation and prediction across space and time. Annual Review of Ecology, Evolution, and Systematics 40: 677-697.

Evans T. G., S. E. Diamond and M. W. Kelly. 2015. Mechanistic species distribution modelling as a link between physiology and conservation. Conservation Physiology 3: 1-16.

Griffiths R. A., D. Sewell and R. S. McCrea. 2010. Dynamic of a declining amphibian metapopulation: survival, dispersal and the impact of climate. Biological Conservation 143: 485-491.

Haddad C. F. D., L. F. Toledo, C. P. A. Prado, D. Loebmann, J. L. Gasparini, I. Sazima. 2013. Guia dos anfíbios da Mata Atlântica: diversidade e biologia. Anolisbooks, São Paulo, Brazil.

Hillman S. S., P. C. Withers and R. C. Drewes. 2000. Correlation of ventricle mass and dehydration tolerance in amphibians. Herpetologica 56(4): 413-420.

Hillman S. S., P. C. Withers, R. C. Drewes and S. D. Hillyard. 2009. Ecological and environmental physiology of amphibians. Oxford University Press. New York, USA.

Huey R. B., C. A. Deutsch, J. J. Tewksbury, L. J. Vitt, P. E. Hertz, H. J. A. Pérez and T. Garland. 2009. Why tropical forest lizards are vulnerable to climate warming. Proceedings of the Royal Society B 276: 1939-1948.

Huey R. B., M. R. Kearney, A. Krockenberger, J. A. M. Holtum, M. Jess and S. E. Williams. 2012. Predicting organismal vulnerability to climate warming: roles of behaviour, physiology and adaptation. Philosophical Transactions of the Royal Society B 367: 1665-1679.

Jiménez L., J. Soberón, J. A. Christen and D. Soto. 2019. On the problem of modeling a fundamental niche from occurrence data. Ecological Modelling 397: 74-83.

Kearney M. R., B. A. Wintle and W. P. Porter. 2010. Correlative and mechanistic models of species distribution provide congruent forecasts under climate change. Conservation Letters 3: 203-213.

Mitchell N. et al. 2013. Linking eco-energetics and eco-hydrology to select sites for the assisted colonization of Australia's rarest reptile. Biology 2: 1-25.

Nadeau C. P., M. C. Urban and J. R. Bridle. 2016. Coarse climate change projections for species living in a fine-scaled world. Global Change Biology 23(1): 12-24.

Nuñez M. N., S. A. Solman and M. F. Cabré. 2009. Regional climate change experiments over southern South America. II: climate change scenarios in the late twenty-first century. Climate Dynamics 32(7-8): 1081-1095.

Peterson A. T., J. Soberón, R. G. Pearson, R. P. Anderson, E. Martínez-Meyer, M. Nakamura and M. B. Araújo. 2011. Ecological niches and geographic distributions. Princeton University Press.

Pittman S. E., M. S. Osbourn and R. D. Semlitsch. 2014. Movement ecology of amphibians: a missing component for understanding population declines. Biological Conservation 169: 44-53.

Scheffers B. R., R. M. Brunner, S. D. Ramirez, L. P. Shoo, A. Diesmos and S. E. Williams. 2013. Thermal buffering of microhabitats is a critical factor mediating warming vulnerability of frogs in the Philippine biodiversity hotspot. Biotropica 45(5): 628-635.

Seebacher F. and R. A. Alford. 2002. Shelter microhabitats determine body temperature and dehydration rates of terrestrial amphibian (*Bufo marinus*). Journal of Herpetology 36(1): 69-75.

Sinervo B. et al. 2010. Erosion of lizard diversity by climate change and altered thermal niche. Science 328(5980): 894-899.

Stewart M. M. 1995. Climate driven population fluctuations in rain forest frogs. Journal of Herpetology 29: 437-446.

Stillman J. H. 2019. Heat waves, the new normal: summertime temperature extremes will impact animals, ecosystems, and human communities. Physiology 34: 86-100.

Titon B., C. A. Navas, J. Jim and F. R. Gomes. 2010. Water balance and locomotor performance in three species of neotropical toads that differ in geographical distribution. Comparative Biochemistry and Physiology A 156: 129-135.

Titon B. and F. R. Gomes. 2015. Relation between water balance and climatic variables associated with the geographical distribution of anurans. PLoS ONE 10(10): e0140761.

Tuff K. T., T. Tuff and K. F. Davies. 2016. A framework for integrating thermal biology into fragmentation research. Ecology Letters 19(4): 361-374.

Walls S. C., W. J. Barichivich and M. E. Brown. 2013. Drought, deluge and declines: the impact of precipitation extremes on amphibians in a changing world. Biology 2: 399-418.

Wells K. D. 2007. The ecology and behavior of amphibians. The University of Chicago Press. USA.

CHAPTER I

WATER BALANCE, TEMPERATURE RELATIONS, AND BEHAVIORAL PERFORMANCE IN LEPTODACTYLID FROGS

Luis M. Senzano[1,*], Rodolfo O. Anderson[2], Rodrigo S. B. Gavira[3], Denis V. Andrade[1]

[1]Laboratório de Biologia Experimental e Integrativa, Departamento de Biodiversidade, Universidade Estadual Paulista, Rio Claro, São Paulo, Brazil

[2]School of Biological Sciences, Monash University, 25 Rainforest Walk, Clayton 3800, Victoria, Australia

[3]Centre d'Etudes Biologiques de Chizé, Villiers en Bois, France.

ABSTRACT

The correspondence between species' habitat preferences (e.g., aquatic, terrestrial, arboreal) and their physiological strategies for regulating temperature and water budgets is relatively well-studied in anurans. However, little is known about how thermal and water balance strategies vary among species occupying the same general habitat. Here, we report on the thermal and hydric physiology of four ground-dwelling Neotropical frogs (*Leptodactylus fuscus*, *L. mystacinus*, *L. macrosternum* and *L. luctator*) differing in size and their degree of association with moisture conditions of terrestrial habitats. We focus on ecologically relevant attributes related to body water regulation, thermoregulation, and organismal performance traits. Our results suggests that more terrestrial species varying in size may rely on distinct water balance strategies to cope with desiccation. Large-sized species may benefit from reduced water loss rates, whereas smaller species might counterbalance their high desiccation rates with high levels of dehydration tolerance. On the other hand, thermal preference, thermal optima, and thermal tolerances were less consistent with respect to the species' degree of terrestrialism. This reinforces the view that differences in strategies to maintain thermal and water balance do occur within the same general habitat, although the degree of terrestrialism does not always translate into changes in functional attributes.

INTRODUCTION

The maintenance of water balance is particularly challenging for amphibians because they are susceptible to high rates of evaporative water loss (EWL) due to their highly permeable skin (Wells, 2007). The challenge of regulating water budgets will vary as a function of species-specific behavioral, morphological, and physiological attributes and the physical environmental drivers (e.g., climate) of their habitat (Dabés et al. 2012). Terrestrial and arboreal species, for example, tend to have a higher capacity for water uptake (WU) (Lemenager et al. 2022) and greater tolerance to dehydration (Pough et al. 1977, Hillman 1980) than species closely associated to water bodies. Arboreal species also exhibit high skin resistance to evaporation (Young et al. 2005, Tracy et al. 2010), which allow them to deal with the greater dehydration risks associated with arboreal habitats (Tracy and Christian 2005. Young et al. 2005). These general trends have been drawn mainly from species with contrasting habits (semi-aquatic, terrestrial, arboreal) that are exposed to extreme differences in environmental drivers such as temperature, wind speeds and water availability (see Scheffers et al. 2013).

Differences in thermal and water balance, however, are likely to occur within the same environment even for closely related species. Ground-dwelling species can differ widely in body shape, size, and their degree of association with water bodies (Maragno et al. 2013, Rievers et al. 2014, Luza et al. 2018). From a thermoregulatory perspective, a highly permeable skin can curtail the opportunities to attain high body temperatures (T_b) due to increased rates of EWL and thus higher dehydration risks in warmer conditions (Buttemer and Thomas 2003, Rothermel and Luhring 2005, Mokhatla et al. 2019). These compromises between water balance and body temperature regulation have important implications for the performance of thermosensitive behavioral traits, including locomotion. For example, while warmer conditions usually increase performance, under desiccating conditions anurans shift their T_b toward colder temperatures favoring water preservation at the cost of suboptimal temperatures for activity (Tracy et al. 1993, Walvoord 2003, Mitchell and Bergmann 2016). These responses also vary according to morphological attributes. Smaller-sized frogs have a greater skin surface area relative to body volume compared to larger counterparts, and this purely dimensional consequence of body size influences the rates of EWL and WU, vulnerability to dehydration, and many other physiological processes (see Peterman et al. 2013, Rubalcaba et al. 2019, Castro et al. 2021). As such, focusing on more ecological and taxonomically restricted groups of species might prove valuable in singling out the relative importance of ecological and mechanistic determinants of the physiological

functions and how those are related to habitat use (Prates and Navas 2009, Titon et al. 2010, Liu and Hou 2012).

Here, we report on the thermal and hydric physiology of four ground-dwelling Neotropical frog species: *Leptodactylus fuscus*, *L. mystacinus*, *L. macrosternum* and *L. luctator*. While similar in general ecology and shape morphology, they greatly differ in size, varying from small-to-moderate (*L. fuscus* and *L. mystacinus*, respectively) to large (*L. macrosternum*) and very large species (*L. luctator*) (Sá et al. 2014, Magalhães et al. 2020). These ground-dwelling frogs are generally associated with open habitats near water bodies, although the strength of this association varies among species. Both *L. mystacinus* and *L. luctator* are primarily found along the edges of standing waters (Oliveira-Filho and Giaretta 2008, Bardier et al. 2014, Henrique and Grant 2019), whereas *L. fuscus* and *L. macrosternum* also occupy drier substrates at varying distances from water edges (Hamann et al. 2006, Lucas et al. 2008, Oda et al. 2016). *Leptodactylus fuscus* is also characterized by exhibiting a more terrestrial reproductive behavior related to foam nest construction, usually located at greater distances from pond edges (Méndez-Narváez et al. 2015), as well as having high desiccation-resistance tadpoles among the *Leptodactylus* species (Venturelli et al. 2021).

These variations in body size and microhabitat preferences offer a valuable opportunity to evaluate whether differences in thermal and water balance could be partially explained by a size-effect component and/or the degree of association with aquatic habitats. We focused on ecologically relevant attributes that provide an indication of the thermal suitability of the environment for activity (such as T_{field}, T_{pref} and T_{opt}), body water regulation (including EWL, R_s and WU), and the thermal and hydric limits bounding the overall organismal performance (CT_{min}, CT_{max} and dehydration tolerance, respectively) (see Box 1 for acronyms of biological paramaters). We hypothesized that the moister conditions surrounding pond edges provide better protection against water loss and facilitate rehydration for species remaining along water edge than for species facing the more variable conditions of adjacent terrestrial microhabitats. As such, we expect that the more terrestrial frogs, *L. fuscus* and *L. macrosternum*, have lower rates of EWL, higher R_s, increased WU capacity, and greater dehydration tolerance compared to *L. mystacinus* and *L. luctator*. Additionally, we anticipate that the more terrestrial species (*L. fuscus* and *L. macrosternum*) will exhibit lower values of T_{field}, T_{pref}, T_{opt}, and a wider thermal tolerance, as they may experience wider fluctuations in body temperature and hydration while active.

METHODS

Study species and housing conditions

Leptodactylus genus (Leptodactylidae) is an ecologically diverse group occupying a wide array of habitats in the Neotropics. *Leptodactylus fuscus* occurs from Northern South America to southernmost part of Brazil, *L. macrosternum* (formerly *L. chaquensis*) spans from Northern Brazil to central regions of South America, *L. mystacinus* is more restricted to the mid- and southeastern South America, while *L. luctator* (formerly *L. latrans*) occurs primarily on south-eastern Brazil (for review see Sá et al. 2014, Magalhães et al. 2020). Nevertheless, they all share a large overlap distribution in the central and mideastern portion of South America (Haddad et al. 2013, Magalhães et al. 2020). The four species are morphologically similar in body shape but distinct in size, ranging from the small *L. fuscus* (~44 mm mean, and 32-56 mm range snout–vent length, SVL), and the moderate-sized *L. mystacinus* (~56 mm mean and, 43-67 mm range SVL), to the large *L. macrosternum* (~74 mm mean and, 48-99 mm range SVL), and the very large *L. luctator* (~93 mm mean and, 73-122 mm range SVL) (Sá et al. 2014, Magalhães et al. 2020).

We collected adult individuals of *L. fuscus* (*N* = 46; 8.79 ± 0.97 g body mass; 43.12 ± 1.32 mm SVL) in the municipalities of Rio Claro (22°20’45” S, 47°32’54” W; collecting years, 2012, 2020) and Barbosa (21°15’01” S, 49°54’53” W; collecting year, 2019), while individuals of *L. mystacinus* (*N* = 11; 14.92 ± 1.6 g body mass; 50.55 ± 1.23 mm SVL) were collected solely in the municipality of Rio Claro (collecting years, 2017, 2020). We collected *L. macrosternum* (*N* = 14; 56.87 ± 8.97 g body mass; 81.52 ± 4.97 mm SVL) in the municipality of Barbosa (21°15’01” S, 49°54’53” W; collecting years, 2019, 2022). Finally, we collected *L. luctator* (*N* = 4, 129.73 ± 27.1 g body mass; 116.15 ± 1.09 mm SVL) in the municipality of Itirapina (22°14’43” S, 47°52’5” W; collecting year, 2015). Animal collection occurred during the hot rainy season (November to March), and for some individuals (*L. fuscus*, *N* = 9; *L. mystacinus*, *N* = 5; and *L. macrosternum*, *N* = 13) we also collected data of their cloacal temperature (T_{field}) taken at the time of capture with a digital thermometer (Incoterm, model 6132, 0.1°C accuracy). Freshly caught frogs were taken to the Laboratory (Laboratório de Biologia Experimental e Integrativa – LABEI, São Paulo State University, Rio Claro, Brazil) where they were caged individually in plastic containers (40x30x25 cm) with free access to water and shelter. Containers were maintained at room temperatures varying between 23 and 27°C, and a photoperiod set by natural light from a large glass window. Animals were generally fed once or twice weekly mainly on mealworms and crickets, allowing a minimum fasting period of 4 d

before any experimental trial. Animal collection was issued by the Instituto Chico Mendes da Conservação da Biodiversidade, Brazil (JCMBIO- MMA, no. 22028) and procedures and experimental protocols approved by the UNESP-IB/Rio Claro Animal Ethic and Committee (protocols no. 2570, 6915 and 5909).

Experimental protocols

For the species for which we have a complete dataset (*L. fuscus*, *L. mystacinus* and *L. macrosternum*) the following protocol was adopted. T_{pref} was measured on the second or third night after the arrival of the animals in the laboratory (<5 days of their capture in the field). In the following days, we ran locomotor trials at six different temperatures (10, 15, 20, 25, 30, 35°C) in random order. Each frog was tested only once at each temperature and no frog was tested to more than one temperature a day. We conducted T_{pref} and T_{opt} measurements at night (18:00-23:00 h), which coincides with the peak of activity for *Leptodactylus* (Bardier et al. 2014). After completing T_{pref} and locomotor trials, we allowed four to five days for the frogs to recover and feed before we proceeded with the measurements of EWL and WU rates. These measurements were taken during daytime (09:00-18:00 h), in random order at 20, 25 and 30°C. Each frog was measured only once a day for either EWL or WU at each temperature. Thus, in total, EWL and WU measurements took 6 consecutive days to complete. Finally, we measured dehydration tolerance, critical thermal minimum (CT_{min}), and maximum (CT_{max}), in this order, allowing a resting recovery period of at least two days between measurements. Dehydration tolerance, CT_{min}, and CT_{max} were also measured during the daytime, between 09:00 and 18:00 h. In total, we completed all physiological measurements within a month of the animals' arrival at the laboratory. In this time frame, we prioritized measuring variables more likely to be thermo-sensitive (T_{pref} and T_{opt}) while postponing those more potentially stressful (critical thermal point and dehydration tolerance).

For *L. luctator*, we measured EWL and WU rates (following the same protocol as above) in a group of frogs previously used for metabolic measurements (Timpone et al. 2020) and that had been in captivity for approximately four months at the time of measurements.

All animals were fully hydrated before any experimental procedure. Full hydration was accomplished by placing animals inside a plastic chamber (7x14x10 cm for individuals of *L. fuscus*, *L. mystacinus* and *L. macrosternum*, and 20x12x12 for *L. luctator* frogs) containing enough water to come into contact with the frog's seat patch area, 1 to 2 cm deep, for about 2 hours at the experimental temperature. Thereafter, frogs were removed from the hydrating chamber, carefully

blotted with paper tissue, and weighed after emptying their urinary bladders. We induced urination by gently pressing the frog's pelvic region. For the locomotor performance trials, in the few cases of unsuccessful measurement attempt, the trial was repeated on the same day (see locomotor performance section below). All animals were periodically checked for body weight, general condition, alertness, and behavior. Only individuals judged as healthy and not exhibiting weight loss were included in the experiments.

Preferred temperature

We measured T_{pref} following the procedures outlined in Anderson and Andrade (2017). Briefly, custom-made circular thermal gradients constructed with galvanized steel sheets were equipped with heat (THG 4" heat tapes) and cold sources (synthetic ice packs) arranged at opposite ends of the thermal gradient, providing a uniformly distributed thermal gradient ranging from 7 to 38°C. At the beginning of each trial, animals were placed in the middle portion of the thermal gradient and were left undisturbed for 2 hours with lights off. Room air temperature varied from 24 to 26.5°C, while relative humidity (RH) varied from 50 to 85%. At the end of the 2-hour period, we measured the frog's cloacal temperature with a quick-reading digital thermometer (Incoterm Industry Ltda, Porto Alegre, RS, Brazil, model 6132, 0.1°C accuracy). This temperature was assumed to be the frog's selected body temperature. After being measured, frogs were returned to their cages.

Locomotor performance

We determined locomotor performance as the longest individual jump distance out of five consecutive jumps for each individual at each tested temperature. Jumping trials were conducted in a 5-m long by 1 m wide track built with plywood boards (100 cm height, 1 cm thick) on top of the laboratory porcelain tiles floor (coefficient of friction greater than 0.42). Room air temperature was kept as close as possible to the experimental temperature by using a split-system air conditioner (Midea, MSE1-09CR model, 9000 BTU capacity, control range capacity: from 17 to 30°C). Before trials, animals were allowed to fully hydrate and equilibrate to the test temperature inside a climatic chamber (same as above) for 2h. Then, one at a time, they were removed from their plastic containers, blotted with paper tissue while inducing urination, and transferred to the jumping track arena. They were released at one end of the arena and were induced to jump five consecutive times, while we manually marked the location of jump landings with a piece of chalk. Whenever necessary, we gently tapped the urostyle region of the frog if it was reluctant to jump.

Immediately after the trial, the frog's T_b was measured using a digital thermometer (same as above) connected to a fast-reading probe inserted into the animal´s cloaca. We determined the length of each jump by measuring the distance between chalk marks with a steel tape measure (model FLF519, Uyustools) to the nearest 1 mm. If individuals jumped out of the arena or hit the side walls before completing the five sequential jumps, the trial was discarded, and the individual was retested on the same day after a new 2-hour recovery at the same test temperature. Trials generally occurred within 90sec after a frog had been removed from the climatic chamber, resulting in negligible changes in T_b.

We fitted various thermal performance curve (TPC) models based on the individuals' longest jump at each test temperature against T_b using the 'nls.multstart' and 'rTPC' R-packages following Padfield et al. (2021). For each species, we combined data from all individuals and selected the best-fitting curve model based on Akaike Information Criterion scores corrected for small sample sizes (AICc) (Supporting S2). This curve-fitting procedure allowed us to select a single TPC shape per species that best fit the empirical observations (Supporting S3). Subsequently, the TPC models were used to analyze individual TPCs for each individual frog, estimating its respective T_{opt} as the T_b level at which the animals achieved maximum performance (Huey and Stevenson 1979). From the combined data from all individuals, we calculated the thermal performance breadth (B_{80}) as the range of T_bs across which jumping ability remains at least 80% of its maximum capacity. This parameter serves as a general descriptive trait characterizing the overall thermal sensitivity of performance for each species (Huey and Kingsolver 1989) (see also Supporting S2).

Evaporative water loss

Rates of EWL were determined by using an open flow-through system already detailed in Anderson et al. (2017). In short, a mass flow controller (model SS-4, Sable Systems International, USA) set up inside a climatic chamber (model EL101/2RS, Eletrolab®, Brazil) ventilated a constant airflow (21.6 cm^3/s) through two silica drying columns and then through a respirometry chamber containing the animal (200 ml chamber volume for *L. fuscus*, *L. mystacinus* and *L. macrosternum*; 1 l volume for *L. luctator*). A humidity sensor (model RH-300, Sable Systems International) monitored the chamber's excurrent airflow, with data being recorded on a computer via a universal interface unit (model UI-2, Sable Systems International).

At the beginning of each trial, fully hydrated animals were placed inside the respirometry chamber and the experiment proceeded until we obtained a minimum period of 15 min of steady-state RH

recordings. After a successful trial, we immediately measured the dorsal skin temperature using an infrared thermometer (62 Mini IR, Fluke, 0.1°C accuracy). In cases where we failed to obtain a steady-state RH recording after 2h of initiating the trial, we stopped the measurement, and the data were discarded. The animal was measured again on a different day. Before and after measuring the animal, we recorded baseline RH levels for the empty chamber (about 1-2%).

Relative humidity recordings were converted into water vapor density (WVD) values (g/m^3), and used to calculate absolute EWL ($\mu gH_2O/s$) from the equation: EWL = (VDe − VDi)*F; where VDe and VDi are the WVD of the excurrent and incurrent (baseline) airflow from/to the chamber, respectively, and F is the airflow rate (cm^3/s). To estimate EWL as area-specific rates ($\mu gH2O/cm^2/s$), we divided the absolute EWL by two-thirds of total skin surface area (A_s) calculated following Klein et al. (2016): $A_s = 8.6856Mass^{0.6652}$, representing the skin proportion that remains in direct contact with air when the animal assumes a water conserving posture (Withers et al. 1982).

Skin resistance to evaporation

Total resistance (R_T) to evaporation is the combined result of both skin (R_s) and boundary layer (R_b) resistances. To derive empirical estimations of R_b, we used the agar method described by Spotila and Berman (1976). We constructed agar models by pouring heated 3% agar solution into alginate (type II, AVAGEL) counter molds obtained from real animals. After hardened, the EWL rates from agar replicas were determined at 25°C under the exact same experimental conditions as the living animals.

R_T (s/cm) was calculated as: R = VDD/EWL, where VDD is the water vapor density (WVD) gradient ($\mu g/cm^3$) between the saturated WVD at the skin surface temperature of the animal or the agar model and the partial WVD at experimental temperature, and EWL is the area-specific EWL rate ($\mu gH_2O/cm^2/s$) (Spotila and Berman 1976). Since agar models' resistance is entirely composed by R_b ($R_T = R_b$), then the R_s of each living frog can be estimated by subtracting their empirically determined R_T values from the R_b values yielded by the measurements taken from their respective agar model (i.e., $R_s = R_T - R_b$).

Water uptake

We determined WU rate by measuring the frog's gain in body mass through their ventral region, particularly the pelvic patch, following the method in Maenaka et al. (2023). Shortly, the fully

hydrated animals were exposed to a custom-made wind tunnel and dehydrated at a constant airstream (3.8 m/s) and air temperature (25°C) until reaching 90% body hydration. At this point, they were removed from the wind tunnel and transferred into a plastic chamber (7x14x10 cm) containing water 1-2 cm deep. At 2-minute intervals, animals were removed, blotted with paper tissue, and weighed, repeating this procedure six consecutive times. Individuals of *L. fuscus*, *L. mystacinus* and *L. macrosternum* were weighed to the nearest 0.0001g (Ohaus®, Barueri, SP, Brazil; scale model AR 2140), while *L. luctator* individuals were weighted to the nearest 0.01g (Marte Científica, São Paulo, SP, Brazil; scale model AD5002). We calculated area-specific WU rates ($\mu gH_2O/cm^2/s$) from the regression slope of body mass gain against rehydration time, divided by one-third of the frog´s total skin surface area (estimated as described above), which we assume represents the surface area of the ventral region in contact with water.

Dehydration tolerance

We measured dehydration tolerance by exposing animals to the same dehydrating procedure in a wind tunnel previously described for the WU measurement, but this time they remained in the tunnel until they reached their dehydration tolerance (see below). While in the tunnel, frogs were periodically inspected for the persistence of their righting reflex, i.e., the ability to right the body when flipped to their back. Animals were allowed to dehydrate until they attained their critical threshold for dehydration tolerance, identified as the point in which the frogs failed to perform the righting reflex within 10 seconds after being flipped (Greenberg and Palen 2021). At this point, the dehydration procedure was halted, the frog was weighed, and immediately put in contact with water for rehydration and recovery. Dehydration tolerance was calculated as the percentage of body mass lost relative to the frog's fully hydrated body mass.

Critical thermal limits

We measured critical thermal limits following the same procedure described in Anderson and Andrade (2017). Briefly, animals were allowed to equilibrate at the starting temperature of 25°C for 2h. Subsequently, a temperature ramping software (Sitrad V.4.11, Full Gauge Eletro-Controles, Brazil) either decrease (for CT_{min}) or increase (for CT_{max}) the temperature of the climatic chamber at a rate of 1°C/10 min. Periodically, the animals were examined for signs of muscle spasms or loss of motor coordination by gently flipping their cages. The threshold for CT_{min} and CT_{max} were defined as the point at which the righting reflex was lost, point at which the experiment was interrupted, and the cloacal T_b of the animals immediately measured with a quick-reading digital

thermometer (same as above). Thermal tolerance breadth (T_{br}) was calculated as: $T_{br} = CT_{max} - CT_{min}$. Experimental starting temperature and ramping rates were the same for all species; CT_{min} and CT_{max} were determined for the same group of individuals; CT_{min} was always measured two or more days before CT_{max}.

Statistical analysis

Our data covers phylogenetically related species; thus, data observations are not completely independent due to shared ancestry (Blomberg et al. 2003). However, phylogenetically structured data with small sample sizes (low number of species) can yield biased estimates of phylogenetic signals caused by a lack of statistical power (see Garamszegi and Møller 2010, Frishkoff et al. 2017, Cox and Logan 2021). Therefore, we proceeded with our analysis without phylogeny-informed statistics. Consequently, our results do not provide support for the discussion of evolutionary inferences; instead, we shall limit our later interpretations to the potential ecological implications related to body size and other physiological attributes.

We employed generalized linear mixed-effect models (GLMM; *lmer* function, 'lme4' package) to evaluate the overall effect of temperature and body mass on EWL and WU among species. We fitted separate models with species, temperature, and body mass as the fixed factors, the species-temperature relationship as interaction term, individuals' identities as random factor, and either EWL or WU as the response variables. To evaluate the thermal sensitivity of EWL and WU, we used the *lstrends* function ('lsmeans' package) with Tukey correction to compare models' temperature slopes among species.

Differences in T_{field}, T_{pref}, T_{opt}, R_s, dehydration tolerance, CT_{min}, CT_{max} and T_{br} among *L. fuscus*, *L. mystacinus*, and *L. macrosternum* were evaluated by performing different analysis of covariance tests (ANCOVA; *aov* function), with the species identity as factor and body mass as the covariate. Because data were collected in different years and sites, for some models, we also added either year (T_{pref}, R_s, CT_{max} and T_{br}) or site (T_{field}, CT_{min}, and T_{br}) as factors whenever they were found to be significant, to control for this effect. Distributional assumptions of normality and homoscedasticity in ANCOVA analysis were evaluated via Shapiro–Wilk and Levene's tests, respectively, whereas GLMMs were evaluated through visual examination of model residuals (we log-transformed EWL and R_s to improve their model residual distributions). F-statistic tests were used to evaluate ANCOVA models, while chi-square tests were used on GLMM models. Whenever significant, a *post-hoc* Tukey's test (*emmeans* function, 'emmeans' package) was performed to identify

significant differences between pairs of measurements among species. All analyses were performed in R (v3.3.6; http://www.R-project.org/) employing RStudio (v1.2.5033; http://www.rstudio.com/). In all cases, a significant level of $p < 0.05$ was used. Unless otherwise stated, all values are presented as means ± s.d. (standard deviation).

RESULTS

The rates of EWL differed among species (X^2_3 = 310.16, p < 0.001), and this difference was associated with body mass (X^2_1 = 58.48, p < 0.001), with larger species exhibiting lower rates of EWL (Fig. 1A). Temperature elevation was followed by an increase of EWL rates in all species (X^2_1 = 603.53, p < 0.001). However, the model slope of this relationship did not differ among species (X^2_3 = 4.9, p = 0.18), indicating that the thermal sensitivity of EWL was similar in all of them. There was no difference in WU capacity among species (X^2_3 = 0.65, p = 0.88). Neither body mass (X^2_1 = 0.47, p = 0.49) nor temperature (X^2_2 = 1.62, p = 0.2) affected WU rates (Fig. 1B, Table 1). For *L. fuscus*, *L. mystacinus* and *L. macrosternum*, their R_s differed ($F_{(2,21)}$ = 91.06, p < 0.001), and this result was influenced by differences in body mass ($F_{(1,21)}$ = 7.94, p = 0.01); the smallest species (*L. fuscus*) had the lowest value of R_s compared to the other two larger species (Fig. 2A). Species also differed in their dehydration tolerance ($F_{(2,20)}$ = 14.26, p < 0.001), with *L. fuscus* being the most dehydration-resistant, followed by *L. mystacinus* and *L. macrosternum* (Fig. 2B, Table 1). Body mass, however, did not influence dehydration tolerance ($F_{(1,20)}$ = 1.67, p = 0.209).

T_{field} recorded for *L. fuscus*, *L. mystacinus*, and *L. macrosternum* did not differ among species ($F_{(2,22)}$ = 1.33, p = 0.28) and was not affected by differences in body mass ($F_{(1,22)}$ = 0.9, p = 0.35) (Fig. 3A). We did not find differences in T_{pref} among species ($F_{(2,35)}$ = 0.71, p = 0.5), nor did body mass influence this trait ($F_{(1,35)}$ = 0.007, p = 0.93) (Fig. 3B). However, *L. fuscus*, *L. mystacinus*, and *L. macrosternum* differed in their T_{opt} for locomotion ($F_{(2,20)}$ = 11.78, p < 0.001), with body mass having an influence on it ($F_{(1,20)}$ = 4.12, p = 0.05); T_{opt} was higher in the largest species (*L. macrosternum*) compared to the smaller ones (*L. fuscus* and *L. mystacinus*) (Fig. 3C). The CT_{max} did not differ among species ($F_{(2,31)}$ = 0.27, p = 0.76; Fig. 4A), but CT_{min} was significantly lower in *L. mystacinus* compared to *L. fuscus* and *L. macrosternum* ($F_{(2,31)}$ = 35.79, p < 0.001) (Fig. 4B). Body mass did not affect CT_{min} ($F_{(1,31)}$ = 0.03, p = 0.86), nor did it affect CT_{max} ($F_{(1,31)}$ = 2.25, p = 0.14). Finally, species differed in T_{br} ($F_{(2,30)}$ = 45.86, p < 0.001), showing similar T_{br} values in *L. mystacinus* and *L. macrosternum*, while the lowest T_{br} value (i.e., the narrowest T_{br}) was observed in *L. fuscus* (Fig. 4C; Table 1). The T_{br} was not influenced by differences in body mass ($F_{(1,30)}$ = 1.29, p = 0.266).

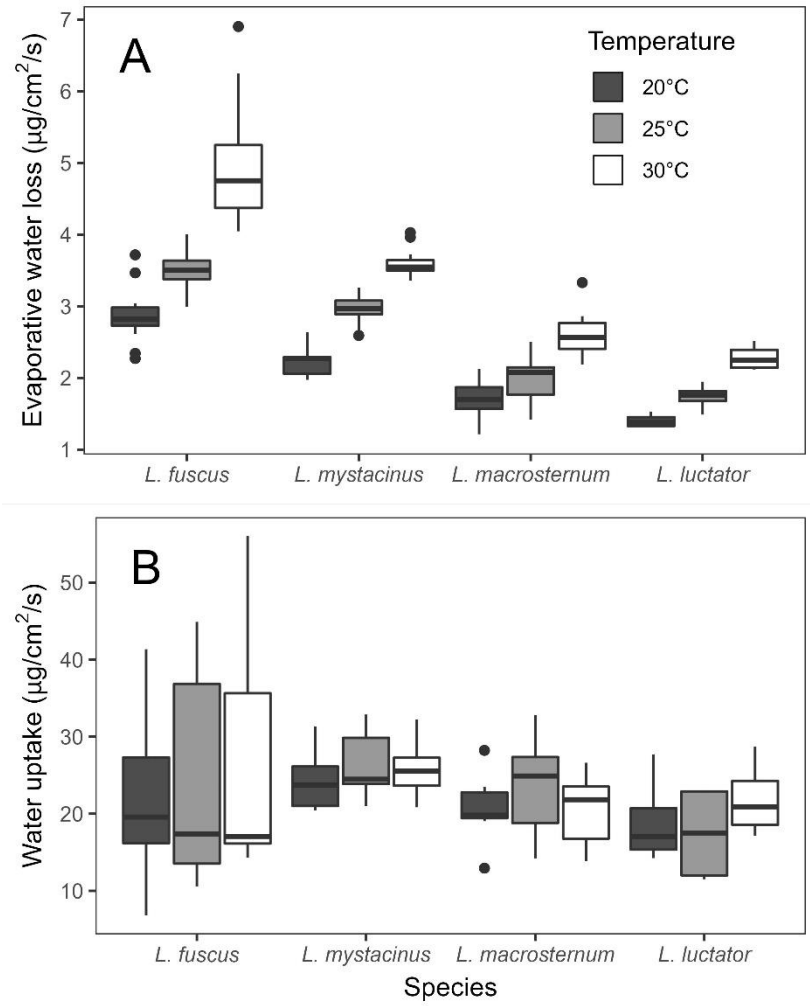

Figure 1. Rates of evaporative water loss (A) and water uptake (B) for *Leptodactylus fuscus*, *L. mystacinus*, *L. macrosternum* and *L. luctator* measured at three temperatures. Boxplot lines indicate medians, the lower and upper borders represent the 25th and 75th percentiles, whiskers are the minimum and maximum range values, and filled circles are outliers.

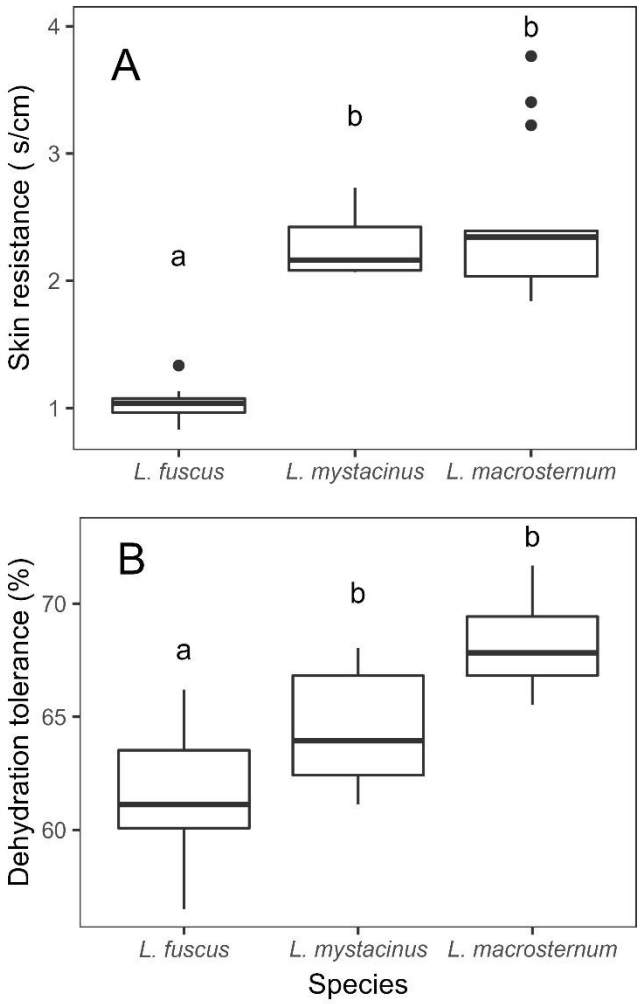

Figure 2. Skin resistance to evaporative water loss (A) and dehydration tolerance (B) for *Leptodactylus fuscus*, *L. mystacinus* and *L. macrosternum*. Different lowercase letters denote statistically significant differences between group means.

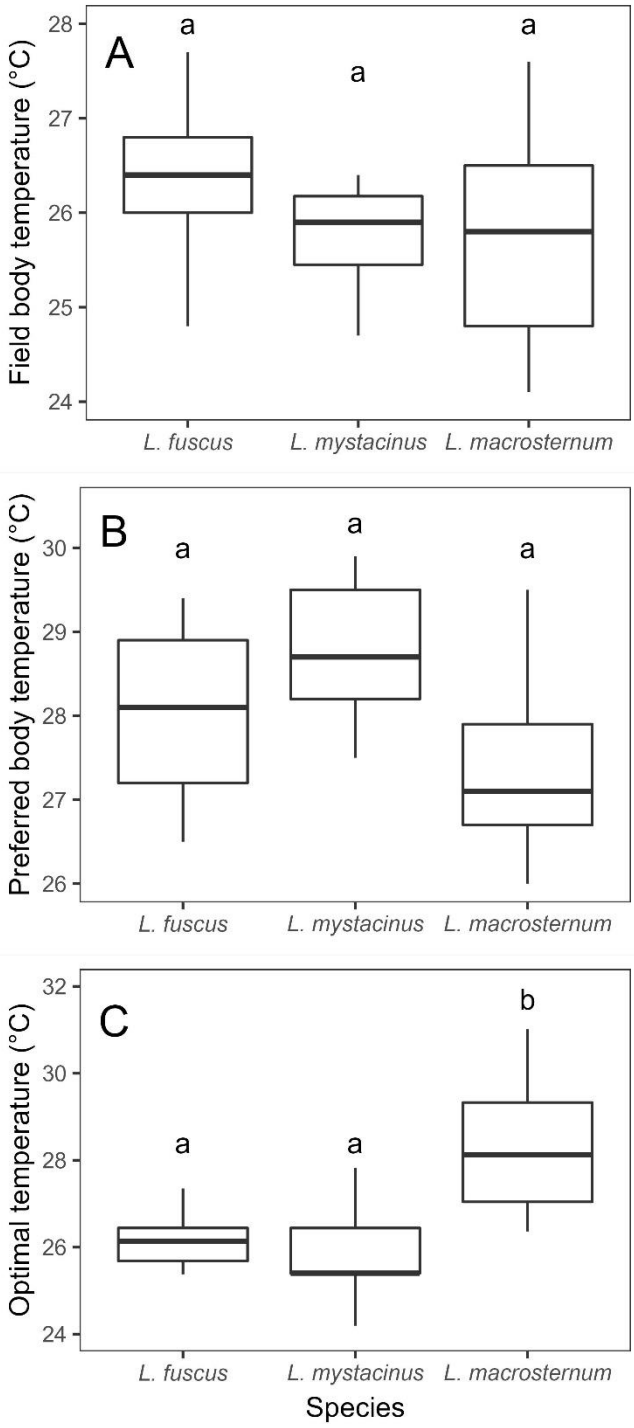

Figure 3. Field body temperature collected at the time of capture (A), preferred body temperature selected in a thermal gradient (B), and optimal temperature for locomotion (C) of *Leptodactylus fuscus*, *L. mystacinus* and *L. macrosternum*. Different lowercase letters denote statistically significant differences between group means.

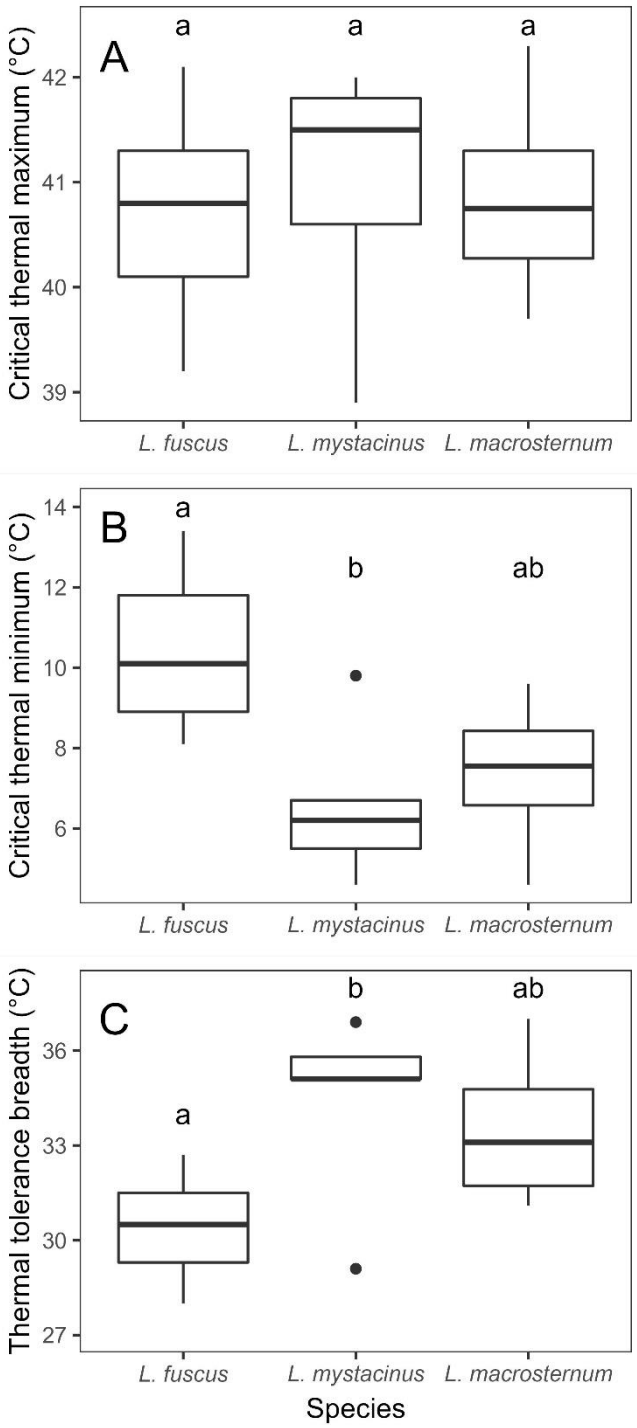

Figure 4. Critical thermal maximum (A), critical thermal minimum (B), and thermal tolerance breadth (C) of *Leptodactylus fuscus*, *L. mystacinus* and *L. macrosternum*. Different lowercase letters denote statistically significant differences between group means.

Table 1. Summary of the physiological traits determined for *Leptodactylus fuscus*, *L. mystacinus*, *L. macrosternum* and *L. luctator*. Evaporative water loss, EWL ($\mu gH_2O/cm^2/s$); water uptake, WU ($\mu gH_2O/cm^2/s$); skin resistamce to evaporation, R_s (s/cm); dehydration tolerance (%); field body temperature, T_{field} (°C); preferred body temperature, T_{pref} (°C); optimum temperature for locomotion, T_{opt} (°C); lower end of thermal performance breadth, B_{80} lower (°C); upper end of thermal performance breadth, B_{80} upper (°C); critical thermal minimum, CT_{min} (°C); critical thermal maximum, CT_{max} (°C); thermal breadth, T_{br} (°C). Traits are presented as mean ± s.d. values.

Species	EWL (20°C)	EWL (25°C)	EWL (30°C)	WU (20°C)	WU (25°C)	WU (30°C)	R_s	Dehydration tolerance	T_{field}	T_{pref}	T_{opt}	B_{80} lower	B_{80} upper	CT_{min}	CT_{max}	T_{br}
L. fuscus	2.87 ± 0.37	3.49 ± 0.24	4.93 ± 0.78	22.91 ± 11.12	23.55 ± 12.75	26.43 ± 14.24	1.04 ± 0.14	61.51 ± 2.84	26.43 ± 0.88	28.1 ± 0.94	26.24 ± 1.04	21.38*	30.37*	10.49 ± 1.75	40.72 ± 0.81	33.51 ± 1.92
L. mystacinus	2.23 ± 0.2	2.96 ± 0.21	3.61 ± 0.21	24.53 ± 4.43	26.42 ± 4.82	25.9 ± 4.27	2.29 ± 0.58	64.47 ± 2.91	26.34 ± 1.52	28.76 ± 0.97	25.92 ± 1.69	19.3*	32*	6.56 ± 1.98	40.96 ± 1.27	30.22 ± 1.42
L. macrosternum	1.70 ± 0.25	1.99 ± 0.29	2.6 ± 0.3	20.77 ± 4.67	23.46 ± 6.64	20.42 ± 4.71	2.46 ± 0.25	68.22 ± 2.2	25.75 ± 1.18	27.29 ± 1.12	28.72 ± 2.62	18.7*	37.08*	7.33 ± 1.48	40.84 ± 0.79	34.4 ± 2.73
L. luctator	1.4 ± 0.1	1.74 ± 0.19	2.28 ± 0.19	19.02 ± 6.05	17.4 ± 6.43	21.93 ± 5.09										

Asterisks represent trait unique (not mean) values derived from the species-specific performance functions described on Supporting S2.

Trait sample size (N):

L. fuscus: EWL (N = 15); WU (N = 9); R_s (N = 8); dehydration tolerance (N = 12); T_{field} (N = 9); T_{pref} (N = 21); T_{opt} (N = 12); CT_{min} (N = 17); CT_{max} (N = 17); T_{br} (N = 17).

L. mystacinus: EWL (N = 11); WU (N = 11); R_s (N = 5); dehydration tolerance (N = 5); T_{field} (N = 5); T_{pref} (N = 25); T_{opt} (N = 5); CT_{min} (N = 5); CT_{max} (N = 5); T_{br} (N = 5).

L. macrosternum: EWL (N = 13); WU (N = 7); R_s (N = 13); dehydration tolerance (N = 7); T_{field} (N = 13); T_{pref} (N = 14); T_{opt} (N = 7); CT_{min} (N = 14); CT_{max} (N = 14); T_{br} (N = 14).

L. luctator: EWL (N = 4); WU (N = 4); R_s (N = 4).

DISCUSSION

We set out to evaluate differences in water balance and thermal physiology among ground-dwelling frogs with distinct body sizes and microhabitat preferences, aiming to understand how local environmental stimuli affect their physiological tolerance. Our results highlight marked and relevant differences among species, yet they only partially support our initial hypothesis relating physiological tolerance and microhabitat preferences. Initially, we anticipated a more water-conserving trend, lower thermoregulatory values, and broader thermal tolerance in species with more terrestrial preferences. While this held true in some cases (e.g., the more terrestrial species, *L. fuscus*, had higher dehydration tolerance), the opposite was observed in others (*L. fuscus* also had the highest EWL, the lowest R_s and the narrowest T_{br}). Moreover, our results indicate that interspecific differences in some traits can be primarily explained by variations in body mass rather than a difference in microhabitat preference.

All species experienced an increase in EWL with rising temperature as a result of the accompanying increase in air water vapor deficit (Riddell et al. 2017), but the rate of increase (i.e., the thermal sensitivity of EWL) remained similar for all of them. This suggests a lack of important water-conserving mechanisms to retard water loss, despite their differences in microhabitat preferences. Anurans have a variety of mechanisms to reduce EWL (Carvalho et al 2010), but an increased skin resistance to water passage (i.e, the R_s) is a common adaptive response in anurans prone to desiccation, which also generally correlates with habitat use (Young et al. 2005). However, the very low values of R_s in our species (<2.5 s/cm) may offer a negligible barrier against the increased EWL with rising temperature, suggesting a poor functional role of R_s against desiccation. This pattern contrasts with some arboreal species, in which thermal sensitivity of EWL and R_s can vary with respect to habitat preferences, even in closely related species (e.g., Buttemer 1990, Buttemer and Thomas 2003). Instead, EWL in our study was mostly related to body mass, which in turn reflects interspecific differences in the body surface-to-volume ratios. As such, EWL among our species is mostly driven by differences in body size rather than differences in R_s and microhabitat preferences.

The rates of WU showed no thermal sensitivity, which is consistent with previous observations in other anurans (Cloudsley-Thompson 1967, Claussen 1969, Tracy 1976, Senzano and Andrade 2018). On the other hand, we were unable to detect differences in WU across species. Smaller frogs have larger surfaces relative to body volume available for water absorption, thus a negative

allometric trend on WU should be expected (Fair 1970). Such negative allometric relation has been reported in other anurans, particularly those with more terrestrial and arboreal habits (Dabés et al. 2012, Titon and Gomes 2015, 2017, Kosmala et al. 2020). The lack of size dependence in WU among our species is unclear, but a possible explanation may relate to their partially overlap in habitat preferences, which may not differ enough to select a clear physiological differentiation on WU (see Dabés et al. 2012). Alternatively, a low variability in WU may merely reflect a trait conservatism shared by other *Leptodactylidae* members. Hence, future research should benefit from the inclusion of more leptodactylid species, particularly if we consider that WU appears to be, to some extent, taxonomically conservative in anurans (Dabés et al. 2012, Titon and Gomes 2015).

Differences in dehydration tolerance have been associated with the degree of terrestriality in anurans (Schmid 1965, Ralin and Rogers 1972, Hillman 1980, Ralin 1981, Beuchat et al. 1984). In agreement with this, we observed the highest dehydration tolerance in the more terrestrial species, *L. fuscus*. This also aligns with the high dehydration resistance that characterizes *L. fuscus* tadpoles when compared to those of other Leptodactilids, including *L. mystacinus* and *L. luctator* (Venturelli et al. 2021). However, contrary to expectations, the other terrestrial species, *L. macrosternum*, was the least dehydration tolerant. Despite their similar microhabitat preference, these two species, *L. fuscus and L. macrosternum*, exhibit notable differences in their dehydration tolerance. A possible explanation may rely on the use of distinct water balance strategies to cope with desiccation conditions. For example, the higher dehydration tolerance of *L. fuscus* may compensate for its smaller body size and, consequently, its higher desiccation rates. Meanwhile, the large size, capable of carrying more bodily water volume and reducing body surface area in *L. macrosternum*, could potentially extend its capability to engage in terrestrial activity well before it reaches its dehydration tolerance limit (e.g., Newman and Dunham 1994). However, due to our limited data, further research involving more species with broader range of body size and habitat preferences is necessary before drawing broader conclusions.

The T_{pref} did not differ among the three measured species (*L. fuscus*, *L. mystacinus*, and *L. macrosternum*). Although data on thermal preference are not available for other leptodactylids, these T_{pref} values fall within the range reported for other Neotropical anurans (Anderson and Andrade 2017, Anderson et al. 2018, Landi 2017, Moretti et al. 2019). The T_{pref} is believed to reflect the T_bs at which various physiological processes function at, or near to, an optimal level

(Martin & Huey, 2008). We observed that the T_{opt} for locomotion remained relatively close (<2.5°C) to their T_{pref} for the three species studied. Anurans often exhibit field activity at T_bs lower than T_{pref} or T_{opt}, a mismatch that has been interpreted as caused by low environmental thermal quality or exceedingly high thermoregulatory costs imposed by functional and/or ecological compromises (see Navas et al. 2021 for a discussion). Two of our species, however, exhibit a T_{field} (26.4 and 26.3°C for *L. fuscus* and *L. mystacinus*, respectively) very close to their T_{opt}, indicating that these two species are capable of achieving their optimal temperatures during activity. Although the difference between T_{field} (25.8°C) and T_{opt} (28.7°C) was slightly higher (~3°C) for *L. macrosternum*, the three species' performance breadths (B_{80}) extended beyond 20-30°C (Table1, Supporting S2), indicating that the three species are likely capable of achieving at least 80% of their maximum performance during activity.

The CT_{max} of the three measured species was similar (~40.8°C) to the values reported for other Leptodactylids (Sanabria et al. 2013, Bovo 2015, Beltrán et al. 2019, May et al. 2019). On the other hand, CT_{min} varied considerably among species, although they remained within the range expected for Leptodactylids (May et al. 2019). Our findings agree with the general view that CT_{max} usually presents a stricter conservatism while CT_{min} is more labile (Pintanel et al. 2019, Bodensteiner et al. 2021). While the CT_{max} was similar among species, *L. fuscus* was the least-cold tolerant (highest value of CT_{min}) among them. As a result, *L. fuscus* exhibited the narrowest T_{br} (the difference between CT_{max} and CT_{min}) among the three species. This unexpected result contrasts with our initial expectations of broader thermal tolerance in *L. fuscus* and *L. macrosternum*, the more terrestrial species. Anurans inhabiting habitats with very contrasting conditions (e.g., forest vs open habitats, elevational gradients) can lead to differences in T_{br} even among closely related species (e.g., Pintanel et al. 2019). Since all our studied species tend to occur in open habitats regardless of their terrestrial preferences, perhaps their critical thermal limits are not under enough selective pressure related to terrestrial preferences because of their shared general habitat use. Differences in thermal tolerance including more species, particularly those markedly differing in habitat preference, constitute an important avenue for further research.

Our study shows that ground-dwelling amphibians occupying the same general habitat can exhibit different strategies to regulate their body temperature and water balance. Leptodactylid frogs, in particular, which are usually associated with water bodies, actually harbor species with a varied degree of association with humid conditions, inhabiting both dry and wet environments (Ponssa et

al. 2017, Venturelli et al. 2021). A more terrestrial habit translates into a higher chance of dehydration (Tracy et al. 2014), and our results indicate that a large body size seems advantageous in terms of water economy by reducing EWL, whereas the disadvantage of higher desiccation rates in smaller species may be counterbalanced by their higher dehydration tolerance. However, the absence of clear patterns in some thermal (CT_{min}, CT_{max}) and water traits (R_s,WU) respective to microhabitat preference suggests that differences in the degree of association to aquatic habitats may not always translate directly into differences on functional attributes. Further studies including thermal and water traits simultaneously on more taxonomically restricted groups with varying habitat preferences should allow for broader generalizations.

REFERENCES

Anderson R. C. O. and D. V. Andrade. 2017. Trading heat and hops for water: Dehydration effects on locomotor performance, thermal limits, and thermoregulatory behavior of a terrestrial toad. *Ecology and Evolution*, 7(21): 9066-9075.

Anderson R. C. O., R. P. Bovo, C. E. Eismann, A. A. Menegario and D. V. Andrade. 2017. Not good, but not all bad: Dehydration effects on body fluids, organ masses, and water flux through the skin of *Rhinella schneideri* (Amphibia, Bufonidae). *Physiological and Biochemical Zoology*, 90(3): 313-320.

Anderson R. C. O., R. P. Bovo and D. V. Andrade. 2018. Seasonal variation in the thermal biology of a terrestrial toad, *Rhinella icterica* (Bufonidae), from the Brazilian Atlantic Forest. *Journal of Thermal Biology*, 74: 77-83.

Bardier C., A. Canavero and R. Maneyro. 2014. Temporal and spatial activity patterns of three species in the *Leptodactylus fuscus* group (Amphibia, Leptodactylidae). *South American Journal of Herpetology*, 9(2): 106–113

Beltrán I., V. Ramírez-Castañeda, C. Rodríguez-López, E. Lasso and A. Amézquita. 2019. Dealing with hot rocky environments: Critical termal maxima and locomotor performance in *Leptodactylus lithonaetes*. *Herpetological Journal*, 29: 155-161.

(Anura: Leptodactylidae)

Beuchat C. A., F. H. Pough and M. M. Stewart. 1984. Response to simultaneous dehydration and thermal stress in three species of Puerto Rican frogs. *Journal of Comparative Physiology B*, 154: 579-585.

Blomberg S. P., T. Garland and A. R. Ives. 2003. Testing for phyllogenetic signal in comparative data: behavioral traits are more labile. *Evolution*, 57(4): 717-745.

Bodensteiner B. L., G. A. Agudelo-Cantero, A. Z. A. Arietta, A. R. Gunderson, M. M. Muñoz, J. M. Refsnider and E. J. Gangloff. 2021. Thermal adaptation revisited: How conserved are thermal traits of reptiles and amphibians? *Journal of Experimental Zoology A*, 335(1): 173-194.

Bovo R. P. 2015. Fisiologia térmica e balanço hídrico em anfíbios anuros. Doctorate Dissertation. Universidade Estadual Paulista. Rio Claro, São Paulo, Brazil.

Bovo R. P., M. N. Simon, D. B. Provete, M. Lyra, C. A. Navas and D. V. Andrade. 2023. Beyond Janzen's hypothesis: How amphibians that climb tropical mountains respond to climate variation. *Integrative Organismal Biology*. obad009.

Buttemer W. A. 1990. Effect of temperature on evaporative water loss of the Australian tree frogs *Litoria caerulea* and *Litoria chloris*. *Physiological Zoology*, 63(5): 1043-1057.

Buttemer W. A. and C. Thomas. 2003. Influence of temperature on evaporative water loss and cutaneous resistance to water vapour diffusion in the orange-thighed frog (*Litoria xanthomera*). *Australian Journal of Zoology*, 51(2): 111-118.

Carvalho J. E., C. A. Navas and I. C. Pereira. 2010. Energy and water in aestivating amphibians. In: A. Navas and J. Carvalho (eds). Aestivation. Progress in molecular and subcellular biology. Springer, Berlin.

Castro K. M. S. A., T. F. Amado, M. A. Olalla-Tárraga, S. F. Gouveia, C. A. Navas and P.A. Martinez. 2021. Water constraints drive allometric patterns in the body shape of tree frogs. *Scientific Reports*, 11: 1218.

Claussen D. L. 1969. Studies on water loss and rehydration in anurans. *Physiological Zoology* 42: 1-14.

Cloudsley-Thompson J. L. 1967. Diurnal rhythm, temperature and water relations of the African toad, *Bufo regularis*. *Journal of Zoology*. 152: 43-54.

Cox C. L. and M. L. Logan. 2021. Using integrative biology to infer adaptation from comparisons of two (or a few) species. *Physiological and Biochemical Zoology*, 94(3): 162-170.

Dabés L., V. M. G. Bonfim, M. F. Napoli and W. Klein. 2012. Water balance and spatial distribution of an anuran community from Brazil. *Herpetologica*, 68(4): 443-455.

Faggioni G. P., F. L. Souza, A. C. Paranhos-Filho, R. M. Gamarra and C. P. A. Prado. 2021. Amount and spatial distribution of habitats influence occupancy and dispersal of frogs at multiple scales in agricultural landscape. *Austral Ecology*, 46(1): 126-138.

Fair J. W. 1970. Comparative rates of rehydration from soil in two species of toads, *Bufo boreas* and *Bufo punctatus*. *Comparative Biochemistry and Physiology*, 34(2): 281-287.

Frishkoff L. O., P. Valpine and L. K. M'Gonigle. 2017. Phylogenetically occupancy models integrate imperfect detection and phylogenetic signal to analyze community structure. *Ecology*, 98(1): 198-210.

Garamszegi L. Z. and A. P. Møller. 2010. Effects of sample size and intraspecific variation in phylogenetic comparative studies: a meta-analytic review. *Biological Reviews*, 85: 797-805.

Grant B.W. 1990. Trade-offs in activity time and physiological performance for thermoregulating desert lizards, *Sceloporus merriami*. *Ecology*, 71(6): 2323-2333.

Greenberg D.A. and W. J. Palen. 2021. Hydrothermal physiology and climate vulnerability in amphibians. *Proceedings of the Royal Society B*, 288: 20202273.

Haddad C. F. D., L. F. Toledo, C. P. A. Prado, D. Loebmann, J. L. Gasparini and I. Sazima. 2013. Guia dos anfíbios da Mata Atlântica: diversidade e biologia. Anolisbooks, São Paulo, Brazil.

Hamann M. I., A. I. Kehr and C. E. Gonzáles. 2006. Species affinity and infracommunity ordination of helminths of *Leptodactylus chaquensis* (Anura: leptodactylidae) in two contrasting environments from northeastern Argentina. *Journal of Parasitology*, 92(6): 1171-1179.

Henrique R. S. and T. Grant. 2019. Influence of environmental factors on short-term movements of butter frogs (*Leptodactylus latrans*). *Herpetologica*, 75(1): 38-46.

Hillman S. S. 1980. Physiological correlates of differential dehydration tolerance in anuran amphibians. *Copeia*, 1980(1): 128-129.

Huey R. B. and R. D. Stevenson. 1979. Integrating thermal physiology and ecology of ectotherms: a discussion of approaches. *American Zoologist*, 19(1): 357-366.

Huey R. B. and J. G. Kingsolver. 1989. Evolution of thermal sensitivity of ectotherm performance. *Trends in Ecology and Evolution*, 4(5): 131-135.

Klein W., L. Dabés, V. M. G. Bonfim, L. Magrini and M. F. Napoli. 2016. Allometric relationships between cutaneous surface area and body mass in anuran amphibians. *Zoologischer Anzeiger - A Journal of Comparative Zoology*, 263: 45-54.

Kosmala G. K., G. P. Brown, R. Shine and K. Christian. 2020. Skin resistance to water gain and loss has changed in cane toads (Rhinella marina) during their Australian invasion. *Ecology and Evolution*, 10: 13071-13079.

Landi P. A. C. 2017. Fisiología térmica de un depredador *Dasythemis* sp. (Odonata: Libellulidae) y su presa *Hypsiboas pellucens* (Anura: Hylidae) y sus posibles implicaciones frente al cambio climático. Graduate Dissertation. Pontificia Universidad Católica del Ecuador. Quito, Ecuador. http://repositorio.puce.edu.ec/handle/22000/13208

Lemenager L. A., C. R. Tracy, K. A. Christian and C. R. Tracy. 2022. Physiological control of water exchange in anurans. *Ecology and Evolution*, 12(2): e8597.

Liu J. and P. L. Hou. 2012. Cutaneous resistance to evaporative water loss in Taiwanese arboreal Rhacophorid frogs. *Zoological Studies*, 51(7): 988-995.

Lucas E. M., C. A. Brasileiro, H. M. Oyamaguchi and M. Martins. 2008. The reproductive ecology of *Leptodactylus fuscus* (Anura, Leptodactylidae): new data from natural temporary ponds in the Brazilian Cerrado and a review throughout its distribution. *Journal of Natural History*, 42(35-36): 2305-2320.

Luza A. L., F. A. Gonçalvez and N. Zanella. 2018. Seasonal variation in the composition of ground-dwelling anuran (Amphibia) assemblages in southern Brazil. *Neotropical Biology and Conservation*, 13(4): 303-312.

Maenaka B. M., L. M. Senzano and D. V. Andrade. 2023. Seasonal variation in thermal biology and water balance in a year-round active Neotropical treefrog, *Scinax fuscovarius*. *Herpetologica*, 79(4): 155-165.

Magalhães F. M., M. L. Lyra, T. R. Carvalho, D. Baldo, F. Brusquetti, P. Burella, G. R. Colli, M. C. Gehara, A. A. Giaretta, C. F. B. Haddad, J. A. Langone, J. A. López, M. F Napoli., D. J. Santana, R. O. Sá, A. A. Garda. 2020. Taxonomic review of South American butter frogs: phylogeny, geographic patterns, and species delimitation in the *Leptodactylus latrans* species group (Anura: Leptodactylidae). *Herpetological Monographs*, 34: 131-177.

Maragno F. P., T. G. Santos and S. Z. Cechin. 2013. The role of phytophysiognomies and seasonality on the structure of ground-dwelling anuran (Amphibia) in the Pampa biome, southern Brazil. *Annals of the Brazilian Academy of Sciences*, 85(3): 1105-1115.

Martin T. L. and R. B. Huey. 2008. Why “suboptimal” is optimal: Jensen’s inequality and ectotherm thermal preferences. *The American Naturalist*, 171(3): E102-E118.

May R., A. Catenazzi, R. Santa-Cruz, A. S. Gutierrez, C. Moritz and D. L. Rabosky. 2019. Thermal physiological traits in tropical lowland amphibians: Vulnerability to climate warming and cooling. *PLoS ONE*, 14(8): e0219759.

Méndez-Narváez J., S. V. Flechas and A. Amézquita. 2015. Foam nests provide context-dependent thermal insulation to embryos of three Leptodactylids frogs. *Physiological and Biochemical Zoology*, 88(3): 246-253.

Mitchell A. and P. J. Bergmann. 2016. Thermal and habitat preferences do not maximize jumping performance in frogs. *Functional Ecology*, 30: 733-742.

Mokhatla M., J. Measey and B. Smit. 2019. The role of ambient temperature and body mass on body temperature, standard metabolic rate and evaporative water loss in southern African anurans of different habitat specialization. *PeerJ*, 7: e7885.

Moretti E. H., S. C. M. Titon, B. T. Junior, F. S. Marques and F. R. Gomes. 2019. Thermal sensitivity of innate immune response in three species of *Rhinella* toads. *Comparative Biochemistry and Physiology Part A*, 237: 110542.

Navas C. A., S. F. Gouveia, J. J. Solano-Iguarán, M. A. Vidal, L. D. Bacigalupe. 2021. Amphibian responses in experimental thermal gradients: Concepts and limits for inference. *Comparative Biochemistry and Physiology B*, 254: 110576.

Newman R. A. and A. E. Dunham. 1994. Size at metamorphosis and water loss in a desert anuran (*Scaphiopus couchii*). *Copeia*, 2: 372-381.

Oda F. H., V. G. Batista, P. G. Gambale, F. T. Mise, F. Souza, S. Bellay, J. C. G. Ortega and R. M. Takemoto. 2016. Anuran species richness, composition, and breeding habitat preferences: a comparison between forest remmants and agricultural landscapes in southern Brazil. *Zoological Studies*, 55: e34.

Padfield D., H. O'Sullivan and S. Pawar 2021. rTPC and nls.multstart: a new pipeline to fit thermal performance curves in R. *Methods in Ecology and Evolution*, 12(6): 1138-1143.

Peterman W. E., J. L. Locke and R. D. Semlitsch. 2013. Spatial and temporal patterns of water loss in heterogeneous landscapes: using plaster models as amphibian analogues. *Canadian Journal of Zoology*, 91(3): 135-140.

Ponssa M. L., J. S. Barrionuevo, F. P. Alcaide and A. P. Alcaide. 2017. Morphometric variations in the skin layers of frogs: An exploration into their relation with ecological parameters in *Leptodactylus* (Anura, Leptodactylidae), with an emphasis on the Eberth-Kastschenko layer. *The Anatomical Record*, 300: 1895-1909.

Prado C. P., M. Uetanabaro and F. S. Lopes. 2000. Reproductive strategies of Leptodactylus chaquensis and L. podicipinus in the Pantanal, Brazil. *Journal of Herpetology*, 34(1): 135-139.

Riddell E. A., E. K. Apanovitch, J. P. Odom and M. W. Sears. 2017. Physical calculations of resistance to water loss improve predictions of species range models. *Ecological Monographs*, 87(1): 21-33.

Rothermel B. B. and T. M. Luhring. 2005. Burrow ability and desiccation risk of Mole salamander (*Ambystoma talpoideum*) in harvested versus unharvested forest stands. *Journal of Herpetology*, 39(4): 619-626.

Rubalcaba J. G., S. F. Gouveia and M. A. Ollaga-Tárraga. 2019. A mechanistic model to scale up biophysical processes into geographical size gradients in ectotherms. *Global Ecology and Biogeography*, 28(6): 793-803.

Senzano L. M. and D. V. Andrade. 2018. Temperature and dehydration effects on metabolism, water uptake and the partitioning between respiratory and cutaneous evaporative water loss in a terrestrial toad. *Journal of Experimental Biology*, 221: jeb188482.

Titon B., C. A. Navas, J. Jim and F. R. Gomes. 2010. Water balance and locomotor performance in three species of neotropical toads that differ in geographical distributions. Comparative Biochemistry and Physiology Part A, 156(1): 129-135.

Titon B. J. and F. R. Gomes. 2015. Relation between water balance and climatic variables associated with the geographical distribution of anurans. *PLoS ONE*, 10(10): e0140761.

Titon B. J. and F. R. Gomes. 2017. Associations of water balance and thermal sensitivity of toads with macroclimatic characteristics of geographical distribution. *Comparative Biochemistry and Physiology A*, 208: 54-60.

Tracy C. R. 1976. A model of the dynamic exchanges of water and energy between a terrestrial amphibian and its environment. *Ecological Monographs*, 46: 293-326.

Tracy C. R., K. A. Christian, M. P. O'Connor and C. R. Tracy. 1993. Behavioral thermoregulation by *Bufo americanus*: The importance of hydric environment. *Herpetologica*, 49(3): 375-382.

Tracy C. R. and K. A. Christian. 2005. Preferred temperature correlates with evaporative water loss in Hylid frogs from northern Australia. *Physiological and Biochemical Zoology*, 78(5): 839-846.

Tracy C. R., K. A. Christian and C. R. Tracy. 2010. Not just small, wet, and cold: effects of body size, and skin resistance on thermoregulation and arboreality of frogs. *Ecology*, 91(5): 1477-1484.

Tracy C. R., T. Tixier, C. L. Nöene and K. A. Christian. 2014. Field hydration state varies among tropical frog species with different habitat use. *Physiological and Biochemical Zoology*, 87(2): 197-202.

Oliveira-Filho J. C. and A. A. Giaretta. 2008. Reproductive behavior of *Leptodactylus mystacinus* (Anura, Leptodactylidae) with notes on courtship call of other Leptodactylus species. *Iheringia, Série Zoologia*, 98(4): 508-515.

Pintanel P., M. Tejedo, S. R. Ron, G. A. Llorente and A. Merino-Viteri. 2019. Elevational and microclimatic drivers of thermal tolerance in Andean *Pristimantis* frogs. *Journal of Biogeography*, 46(8): 1664-1675.

Prates I. and C. A. Navas. 2009. Cutaneous resistance to evaporative water loss in Brazilian Rhinella (Anura: Bufonidae) from contrasting environments. *Copeia*, 3: 618-622.

Pough F. H., M. M. Stewart and R. G. Thomas. 1977. Physiological basis of habitat partitioning in Jamaican *Eleutherodactylus*. *Oecologia*, 27: 285-293.

Ralin D. B. 1981. Ecophysiological adaptation in a diploid-tetraploid complex of treefrogs (Hylidae). *Comparative Biochemistry and Physiolgy A*, 68(2): 175-179.

Ralin D. B. and J. S. Rogers. 1972. Aspects of tolerance to desiccation in *Acris crepitans* and *Pseudacris streckeri*. *Copeia*, 1972(3): 519-525.

Rievers C. R., M. R. S. Pires and P. C. Eterovick. 2014. Habitat, food, and climate affecting leaf litter anuran assemblages in an Atlantic Forest remnant. *Acta Oecologica*, 58: 12-21.

Sá R. 0., T. Grant, A. Camargo, W. R. Heyer, M. L. Ponssa and E. Stanley. 2014. Systematics of the Neotropical Genus *Leptodactylus* Fitzinger, 1826 (Anura: Leptodactylidae): phylogeny, the

relevance of non-molecular evidence, and species accounts. *South American Journal of Herpetology*, 9(1): S1-S128.

Sanabria E. A., L. B. Quiroga, E. Gonzáles, D. Moreno and A. Cataldo. 2013. Thermal parameters and locomotor performance in juvenile of *Pleurodema nebulosum* (Anura: Leptodactylidae) from the Monte Desert. *Journal of Thermal Biology*, 38(7): 390-395.

Scheffers B. R., B. L. Phillips, W. F. Laurance, N. S. Sodhi, A. Diesmos and S. E. Williams. 2013. Increasing arboreality with altitude: a novel biogeographic dimension. *Proceedings of the Royal Society B*, 280: 20131581.

Schmid W. D. 1965. Some aspects of the water economies of nine species of amphibians. Ecology, 46(3): 261-269.

Timpone L. T., R. S. B. Gavira and D. V. Andrade. 2020. Effects of temperature and meal size on the postprandial metabolic response of *Leptodactylus latrans* (Anura, Leptodactylidae). *Journal of Experimental Zoology* A, 333(2): 79-87.

Venturelli D. P., V. R. Silva and A. A. Giaretta. Tadpoles' resistance to desiccation in species of *Leptodactylus* (Anura, Leptodactylidae). *Journal of Herpetology*, 55(3): 265-270.

Walvoord M. E. 2003. Cricket frogs maintain body hydration and temperature near levels allowing maximum jump performance. *Physiological and Biochemical Zoology*, 76(6): 825-835.

Wells K. D. 2007. The ecology and behavior of amphibians. Chicago, USA: The University of Chicago Press.

Withers P. C., S. S. Hillman, R. C. Drewes and O. M. Sokol. 1982. Nitrogen excretion in sharp-nosed reed frogs (Hyperolius nasutus: Anura, Hyperoliidae). *Journal of Experimental Biology*, 97: 335-343.

Young J. E., K. A. Christian, S. Donnellan, C. R. Tracy and D. Parry. 2005. Comparative analysis of cutaneous evaporative water loss in frogs demonstrates correlation with ecological habits. *Physiological and Biochemical Zoology*, 78(5): 847-856.

SUPPORTING INFORMATION

Supporting S1. Summary of the thermal performance curve (TPC) models fitted to each species

TPC models are ranked based on their Akaike Information Criterion scores corrected for small sample sizes (AICc), with lower scores indicating a better fit of model to empirical observations. See Padfield et al. (2021)* for TPC descriptions, equations, and references therein.

L. fuscus		*L. mystacinus*		*L. macrosternum*	
TPC model	**AICc**	**TPC model**	**AICc**	**TPC model**	**AICc**
gaussian	620.56	gaussian	178.46	quadratic	288.41
oneill	622.1	quadratic	179.22	gaussian	289.79
weibull	622.22	weibull	181.26	boatman	290.79
ratkowsky	624.37	oneill	181.27	kamykowski	290.88
boatman	624.45	ratkowsky	181.33	beta	291.1
beta	624.57	briere2	181.74	ratkowsky	291.43
delong	625.68	rezende	182.25	weibull	291.48
briere2	627.61	spain	182.78	briere2	292.05
joehnk	629.05	hinshelwood	183.45	oneill	292.45
thomas_2017	629.07	boatman	184.42	spain	292.73
kamykowski	629.12	beta	184.42	thomas_2017	293.49
quadratic	631.26	joehnk	184.57	delong	294.98
rezende	632.13	thomas_2017	184.57	rezende	296.21
johnson_lewin	634.42	kamykowski	184.58	johnson_lewin	304.43
spain	634.77	delong	184.58	joehnk	304.6
hinshelwood	638.54	lactin2	185.41	lactin2	308.98
lactin2	647.37	johnson_lewin	193.65	hinshelwood	468.19

*Padfield D., H. O'Sullivan and S. Pawar. 2021. rTPC and nls.multstart: a new pipeline to fit thermal performance curves in R. *Methods in Ecology and Evolution*, 12(6): 1138-1143.

Supporting S2. Species-specific thermal performance curve (TPC) models

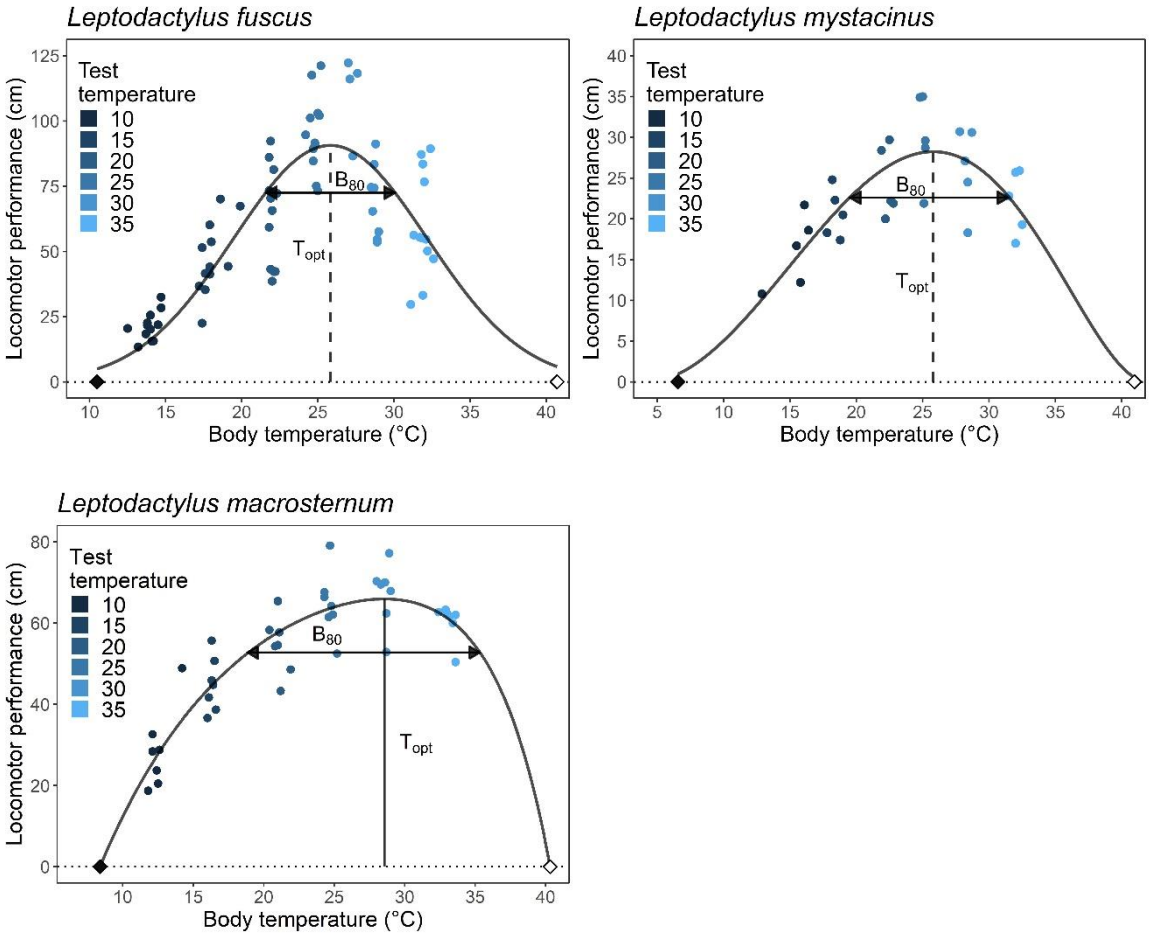

Figure S2. Each curve describes the best TPC model found to *Leptodactylus fuscus* (TPC model, gaussian), *L. mystacinus* (TPC model, gaussian), and *L. macrosternum* (TPC model, quadratic) based on their AICc scores (see Supporting S1). Locomotor performance represents the longest distance jumped by each individual at each test temperature. Points indicate individuals' body temperature collected at the end of each temperature trial. The vertical dashed line indicates the species-specific optimal temperature (T_{opt}) for locomotion. Horizontal double headed arrows represent the lower (left side arrow) and upper (right side arrow) ends of the performance breadth (B_{80}) (the range of T_bs across which jumping ability remains at least 80% of its maximum capacity).

CHAPTER II

COLD TROPICAL NIGHTS: THERMAL AND HYDRIC CONSTRAINTS ON ACTIVITY OF NEOTROPICAL FROGS AT THE GEOGRAPHIC SCALE

Luis M. Senzano[1], Milton C. Ribeiro[2], Sidney F. Gouveia[3], Denis V. Andrade[1]

[1]Laboratório de Biologia Experimental e Integrativa, Departamento de Biodiversidade, Universidade Estadual Paulista, Rio Claro, São Paulo, Brazil

[2]Laboratório de Ecologia Espacial e Conservação (LEEC), Departamento de Biodiversidade, Universidade Estadual Paulista, Rio Claro, São Paulo, Brazil

[3] Laboratório de Pesquisa Integrativa em Biodiversidade. Departamento de Ecologia, Universidade Federal de Sergipe, São Cristóvão, Sergipe, Brazil.

ABSTRACT

Amphibians balance their thermal and water budgets depending on their physiological state and the physical environment so that these factors constrain organismal performance. Most mechanistic assessments emphasize the thermal over water constraints, potentially missing important aspects of amphibian ecophysiological patterns. Here, we evaluate the potential role of thermal and hydric constraints on the activity budget across the geographic distribution of three Neotropical frogs (*Leptodactylus fuscus*, *L. mystacinus,* and *L. macrosternum*). We infer environmental suitability based on principles of heat and mass balances through a mechanistic modeling procedure coupled to laboratory and field data. We integrated species-specific functional attributes with their immediate physical environment (ground-level microclimate) under nocturnal conditions while allowing for interactive behavioral responses of sheltering during harmful and daytime conditions. Our results evidence the roles played by body size on hydric restrictions and inhibition of activity even under thermally adequate conditions, and by shelters as thermal and hydric refugia. More strikingly, thermal-induced restrictions in activity were linked to low temperatures rather than warmer conditions, indicating a trade-off in diel activity driven by upper and lower thermal bounds. These findings provide a broader picture of climatic constraints on anuran activity and distribution and insights into how species may respond to changing climatic conditions.

INTRODUCTION

Thermal and hydric constraints are key drivers of ectotherm activity (Kearney 2013, Gunderson and Leal 2016) and several ecological and geographic patterns (Rozen-Rechels et al. 2019). In general, ectotherms engage in activity when conditions allow keeping their body temperature (T_b) within certain thermal thresholds, retreating to refuges if the conditions become threatening (Kearney et al. 2018, Huey and Kingsolver 2019). The sensitivity of their performance to changes in body temperature (T_b) is often described using a thermal performance curve (TPC). This curve typically increases from a critical minimum temperature (CT_{min}) until it peaks at an optimal temperature (T_{opt}) and then decreases until it reaches a critical thermal maximum (CT_{max}) (Huey and Stevenson 1979). Owing to their usually permeable skin (Wells 2007), amphibians are also heavily constrained by water supply. Because environmental water is temperature sensitive, these organisms must be active at sites and periods that balance humidity and temperature. As such, field-active anurans generally operate within a narrow range of temperatures that provide enough heat to activate metabolism but not to cause dehydration (Seebacher and Alford 2002, Mitchell and Bergmann 2016).

The anurans' ability to maintain their T_b close to their T_{opt} can thus be constrained by water and other competing thermal-dependent physiological demands (Mitchell and Bergmann 2016, Anderson and Andrade 2017) or by the availability of suitable sites (Seebacher and Alford 2002). As microclimatic conditions constantly change, animal thermal and hydric states vary with environmental surroundings, thus further constraining their activity pattern (Tracy et al. 2014, Ruthsatz et al. 2022). Restrictions on activity time resulting from thermal or hydric trade-offs can potentially lead to reduced food intake, energy deficits, and increased reproductive costs (Huey and Kingsolver 2019), ultimately leading to reduced fitness and local population extirpation (Bestion et al. 2015). Among amphibians from tropical and subtropical regions, where daytime temperatures are higher and more variable than those at night (Schwarzkopf and Alford 1996, Muñoz and Bodensteiner 2019), most species are strictly nocturnal (Anderson and Wiens 2017). Although nocturnality may buffer against the higher water costs found during the daytime, anurans are not free from water stress during nighttime. Such nocturnality has significant consequences for amphibian physiological performance, such as reducing the risk of overheating, but also thermoregulatory opportunities (Hitchcock and McBrayer 2006, Rock and Cree 2008). Specifically, the higher water demand throughout activity may lead to reduced opportunities to keep T_b close to its optimal function (O'Connor and Tracy 1992), reduce, or even fully restrict

activity time (Feder and Londos 1984, Peterman and Semlitsch 2014), potentially compromising immediate and long-term survival of frogs (Geise and Linsenmair 1988).

These thermal and hydric constraints at the scale of individual activity can sum-up and affect the amphibians' niche and geographic distribution (Rubalcaba et al. 2019a). Bridging activity patterns of individuals locally with broad-scale patterns is challenging but essential for grasping climatic effects on species' local survival. Mechanistic models are a powerful tool to integrate the biophysical and physiological information of the animals with microclimatic conditions and scale them up to larger extents (Kearney & Porter 2009). Such models have been deployed to investigate the anuran activity based on the potential interactions between thermal and hydric constraints (e.g., Enriquez-Urzelai et al. 2019, Rubalcaba et al. 2019a, Ginal et al. 2021, Greenberg and Palen 2021). However, none has focused on tropical species, and most are focused primarily on thermal constraints for activity and less on the potential effects of hydric constraints (e.g., Kearney et al. 2008, Beukema et al. 2021).

Here, we use thermal and hydric organismal traits from three nocturnal Neotropical frogs (*Leptodactylus fuscus*, *L. mystacinus,* and *L. macrosternum*) and combine multiple modeling approaches to identify potential thermal and hydric constraints on activity throughout their geographic distribution. We integrated biophysical aspects of the species with physiological information on thermal (CT_{min} and CT_{max}), hydric (evaporative water loss and dehydration tolerance; EWL and EWL_{tol}), performance traits (thermal performance breadth; B_{80}), and hourly, ground-level microclimate (Kearney et al. 2014) in a mechanistic modeling approach (Rubalcaba et al. 2019b). We identified physiologically limiting constraints on activity under strictly nocturnal conditions, allowing for interactive responses of sheltering during harmful and daytime conditions. This mechanistic approach enabled us to evaluate the potential role of thermal and hydric constraints on anuran activity at scales (ground-level microclimate) and diel conditions (nocturnal activity) typically experienced by many Neotropical anurans and to provide a mechanistic assessment based on principles of heat and mass balances to infer environmental optimality and sub-optimality in areas potentially accessible to the species.

METHODS

Frog species

Leptodactylus frogs (Anura, Leptodactylidae) are a morphologically and ecologically diverse genus occupying various habitats throughout the Neotropics, particularly abundant in lowland and montane tropical forests (Wells 2007). We focused on three leptodactylid frog species: the small-sized *Leptodactylus fuscus* (5-9 g body mass; snout–vent length (SVL) 32-56 mm), the moderate-sized *L. mystacinus* (14-18 g mass; SVL 43-67 mm), and the moderate-to-large-size *L. macrosternum* (55-80 g mass; SVL 65-97 mm) (Sá et al. 2014). Apart from the size, these frogs are generally similar in morphology and natural history. They lack integumental adaptations to reduce EWL, being considered "typical" amphibians, exhibit ground-dwelling nocturnal habits, and spend most of their time in highly to moderately moist areas (Solano 1887, Silva and Giaretta 2008). They are generally associated with habitats near standing waters. However, *L. fuscus* can occur at greater distances from the water edges (more terrestrial habits) than the other two species (Méndez-Narváez et al. 2015, Venturelli et al. 2021). Their activity and reproductive periods also coincide during the warmest and wettest months of the year (Haddad et al. 2013).

Physiological data

Details of the animal housing conditions and protocols for experimental data collection are virtually the same as those provided elsewhere (Maenaka et al. 2023), but here we describe them briefly. We employed adult individuals of both sexes of *Leptodactylus fuscus* (N = 46; 8.79 ± 1.6 g; 43.12 ± 1.32 mm of SVL), *L. mystacinus* (N = 11; 14.92 ± 1.83 g; 50.55 ± 1.23 mm), and *L. macrosternum* (N = 14; 56.87 ± 8.97 g; 81.52 ± 4.97 mm) collected in São Paulo State, southeastern Brazil. Physiological data comprise critical components of thermal, water balance, and locomotor functions related to ambient constraints or necessary as inputs to solve the ectotherm heat model.

The behavioral performance of anuran amphibians is highly influenced by temperature. We empirically quantified this response by obtaining the thermal performance curves (TPC) for the locomotor/escape response. More specifically, we determined the maximum jump distance (out of five jumps) achieved by the animals at different temperatures, which was then used to construct species-specific TPCs. All trials were conducted at night in a jumping arena at six test temperatures (10, 15, 20, 25, 30, and 35°C). The jumping arena consisted of a 5-m long, 1-m wide track built with plywood boards on top of the laboratory floor, with the room air temperature kept

as close as possible to the experimental temperature using a split-system air conditioner. Individual frogs were tested once at each temperature and no more than one temperature per day. The trial order was randomized, and only individuals tested at all temperatures were included in the analyses. From the TPCs, we extracted the frog temperature at which optimal performance was attained (T_{opt}) and the thermal performance breadth (B_{80}; the range of T_b across which jumping ability remained at least 80% of T_{opt}) (Fig. 1). Even though it represents a performance decrease compared to T_{opt}, B_{80} is generally interpreted as the thermal range at which animals perform 'well' (Huey and Stevenson 1979). Beyond the B_{80} limits, performance drops toward the critical thermal minimum (CT_{min}) or maximum (CT_{max}), the physiological endpoints at which locomotor failure occurs. The CT_{min} and CT_{max} were determined by gradually decreasing or increasing T_b at a constant cooling/heating rate (1°C/10 min) until attaining the non-lethal point of righting reflex loss (a temporal loss of muscle coordination judged by the animals' incapacity to right their body after being flipped onto their back) (Fig. 1). Because activity cannot occur beyond these critical limits, we used them as the lower and upper thermal thresholds for activity in our simulations.

The rates of EWL from the animals were measured at different temperatures (15°C, 20°C, and 25°C) using an open flow-through system. This system consisted of a continuous dry airflow that ventilated a chamber containing the animal while the air humidity leaving the chamber was continuously monitored using an RH analyzer connected to a computer. We calculated the absolute EWL (gH_2O/h) rates for each species from these data (see Maenaka et al. 2023). As hydric deficits can compromise activity by affecting organismal performance (Rozen-Rechels et al. 2019), we also determined the species' ability to tolerate dehydration. For this, fully hydrated animals were weighed and then subjected to a desiccating procedure by exposing them to a wind tunnel until they attained the point of righting reflex loss analogous to the critical thermal limits. At this point, they were weighed again, and their dehydration tolerance (EWL_{tol}) was quantified as the percentage (%) of body mass lost relative to their fully hydrated mass. EWL_{tol} was used as the hydric physiological threshold for the cessation of activity in our simulations.

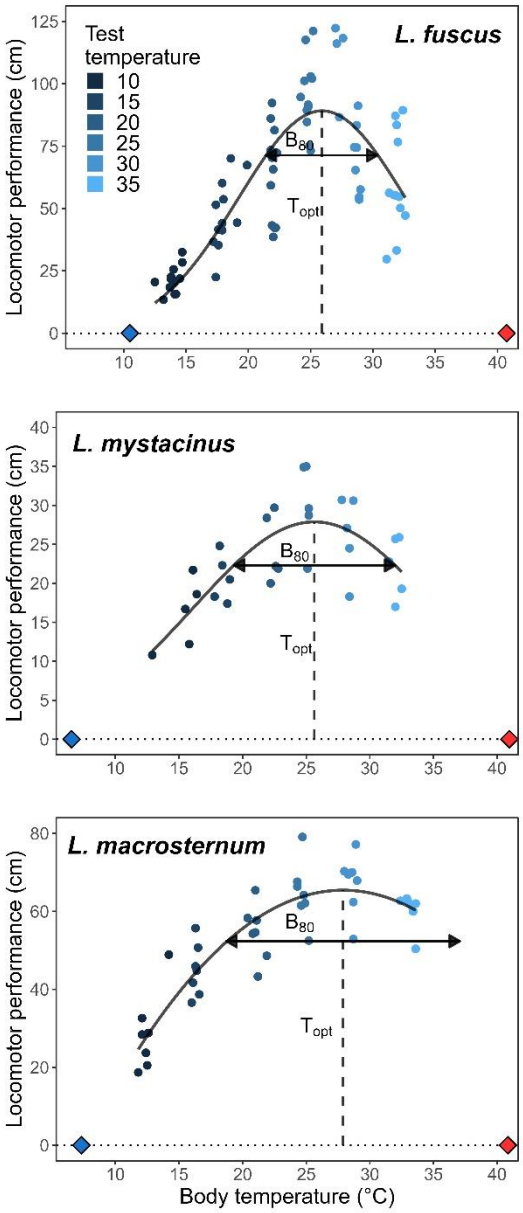

Figure 1. Locomotor performance represents the longest distance jumped by each individual at each test temperature. Points indicate individuals' body temperature collected at the end of each temperature trial. Vertical dashed lines indicate the optimal temperature (T_{opt}) for *L. fuscus* (26.24 °C), *L. mystacinus* (25.92°C) and *L. macrosternum* (28.72°C). Horizontal arrows indicate the thermal range at which locomotory function remains above 80% of its maximum capacity (i.e., the B_{80}). Head arrows indicate the B_{80} lower (21.38, 19.3, 18.7 °C) and upper (30.37, 32, 37.08 °C) ends for the respectively *L. fuscus*, *L. mystacinus* and *L. macrosternum*. Rhombuses are the point at which locomotor function fails. Blue rhombous indicates the empirically determined CT_{min} (10.49, 6.56, 7.33°C, respectively) and red rhombous the CT_{max} (40.72, 40.96, 40.84°C, respectively).

Thermal and hydric ecological modeling

Species distributional areas

We restricted our mechanistic modeling to the South American region, which encompasses the currently known distribution of our model species (see Sá et al. 2014, Magalhães et al. 2020). We delineated the distributional areas for each species based on the α-hull method (Burgman and Fox 2003). This technique yields geographical range estimates by fitting Delauney α-hull polygons (Delauney triangulation) around species presence records (Supporting S2). Presence records were obtained from the Global Biodiversity Information Facility portal (GIBIF; http://www.gbif.org/) for *L*. *fuscus* and *L. mystacinus*. For *L. macrosternum*, we used georeferenced records from Magalhães et al. (2020), which offer updated and revised occurrence data for this species. After a data cleaning, we used 2901 records for *L. fuscus*, 258 for *L. mystacinus*, and 265 for *L. macrosternum* (detailed in Supporting S2).

Because available occurrence data constrain polygonal range delimitations, spatial coverage can suffer discontinuities due to sampling gaps in areas that may represent feasible locations for species presence (Marsh et al. 2023), especially in under-sampled regions such as the Neotropics (Fouquet et al. 2007). We used predicted presences from species distribution models (SDM) to reduce these potential geographical gaps to complement our previous polygonal range delimitations (Pena et al. 2014, Syfert et al. 2014). We constructed SDMs by relating species presence records (used for polygonal range delimitations) to bioclimatic variables obtained from the WorldClim database (http://www.worldclim.org/). We selected them for their ecological relevance and low spatial collinearity. We used an ensemble modeling technique (Araújo and New 2007), in which the outputs of multiple predictive models were combined to estimate species habitat suitability, with values ranging between 0 and 1 (see Supporting S2 for full details on bioclimatic variable selection and SDM procedures). Suitability maps were then converted into binary maps (presence/absence) by applying the lowest presence threshold (LPT; Pearson et al. 2007), a method that sets the lowest suitability value by which all grid cells equal to (or better than) those containing a species record are retained, thus minimizing omission error (Pearson et al. 2007). The LPT also accounts for moderately suitable yet feasible locations for the species presence that more restrictive methods would otherwise overlook (see Peterson and Raghavan 2017). Finally, the LPT maps were superimposed on polygonal range estimates to produce a derived range delimitation. Although SDM presence predictions can suffer from the same under-

sampling issues as polygonal delimitations, SDMs are a relatively robust alternative to complement polygonal range estimates (Pena et al. 2014, Syfert et al. 2014). Furthermore, this combined approach yielded better spatial continuity with broader environmental conditions, which is well suited for this study, which is inferring environmental optimality and sub-optimality of locations.

Microclimatic conditions

We used the microclimate described by Kearney et al. (2014) to estimate species responses to ambient conditions at the organismal scale. This dataset is built on the 'NicheMapR' r-package (Kearney and Porter 2017). It uses biophysical modeling to estimate climatic parameters at the microhabitat level, based on the input of various descriptors for a 24-hour period of a monthly day at a 15 km spatial resolution. We extracted microclimatic conditions at various shading levels (0, 25, 50, 75, and 90%) of wind speed, relative humidity, solar radiation, soil surface (and 5 cm below surface) temperatures, and air temperature 1 cm above the ground (Kearney et al. 2014). The species exhibit a wide geographical distribution (Sá et al. 2014, Magalhães et al. 2020), which covers different biomes with contrasting vegetation structures (Hansen et al. 2013). Therefore, we assigned shade-specific values for the microclimatic conditions to each grid cell. To achieve this, a 30m tree cover map (Hansen et al. 2013) was upscaled to 15 km resolution using bilinear resampling, and the continuous output (ranging from 0 to 100%) was reclassified to represent five categorical canopy classes: 0-20% tree cover (0% canopy), 21-40% tree cover (25% canopy), 41-60% tree cover (50% canopy), 61-80% tree cover (75% canopy) and 81-100% tree cover (90% canopy). We then matched (stacked) this discretized canopy map to our rasterized microclimate dataset. We decomposed the grid rasters into individual cell-based column layers, with each cell column containing all combinations of hourly shading conditions for each monthly microclimate (12 months). Finally, we derived a rearranged new microclimate dataset in which each grid cell only maintained its most representative shade level (0%, 25%, 50%, 75%, or 90%) of microclimate based on the canopy map.

A second issue with the wide distribution of our species is related to their seasonal period of activity. For example, in the southernmost portion of their distribution, *L. fuscus* and *L. mystacinus* are primarily active between December and March (Abe and Garcia 1991, Lucas et al. 2008, Oliveira-Filho et al. 2008). In contrast, in the central region of their distribution, they are mainly active between August and November (De-Carvalho et al. 2008). Finally, in the northern portion, *L. fuscus* is primarily active between March and July (Solano 1987, Martins 1988, Méndez-Narváez et

al. 2015). Similarly, the period of activity of *L. macrosternum* differs between its southern and northern distributions, beginning in December in the former (Prado et al. 2000) and May in the latter (Chaves et al. 2021), coinciding with the rainy months in these regions (Alvarez et al. 2014). To account for this regional effect on phenology, the activity time in each grid cell was restricted to the most humid month. This period coincides with the most favorable time of the year for frogs to be active. This was accomplished by decomposing the microclimate rasters again (similar procedure described above for canopy shade), but only the month with the highest 24-hour mean RH was preserved at each location.

Body temperature and evaporative water loss evaluation

To link frogs to the ground-level microclimate, we first solved the expected inflows and outflows of heat energy for T_b using the biophysical model described by Rubalcaba et al. (2019b). The model builds upon heat mechanisms for ectotherms as described by Porter et al. (1973), relating the body heat/mass flux to local microclimates (solar radiation, longwave radiation, convective heat flow, conduction to the ground, and cooling evaporation) at a given time while accounting for species-specific morphological features and thermoregulatory behavior (see Rubalcaba et al. 2019b for a detailed explanation). This biophysical model has already been validated by empirical observations of more than 40 lizards (Rubalcaba et al. 2019b) and here we evaluated its predictive performance using thermal data from wet-skinned models (agar replicas) deployed under field conditions. Agar replicas mimic the shape and size of amphibians while incorporating evaporative properties equivalent to those of a living animal and are a well-established method for field thermal studies (Nowakowski et al. 2017, Anderson et al. 2018, Lertzman-Lepofsky et al. 2020, Ortega-Chinchilla et al. 2022). This agar approach allowed us to evaluate the biophysical model over a wide temporal window (various days), as it provides continuous operative thermal measures. We deployed agar replicas of various sizes (5, 23, 28, and 112 g) in the field over sunny and shady locations and monitored their core temperatures using thermal data loggers for six consecutive days (Supporting S3 includes further details). Concurrently, using the biophysical modeling described above, we estimated the expected hourly temperatures for similar-sized hypothetical agars at the same sunny and shady locations as the empirical agar models. To compare the congruency between these two approaches, we generated temperature curves from simulations and mean hourly field observations (T_b collected from agar replicas) and evaluated the similarity between them via Discrete Fréchet Distance (DFD) analysis (see Eiter and Mannila 1994,

Cui et al. 2022). This metric measures the dissimilarity between two curve shapes, the lower the value, the more similar the curves are.

Evaporative cooling is an essential component of the organismal heat budget. The biophysical model incorporates this effect by estimating the expected rate of cutaneous EWL based on key organismal attributes (body mass, skin surface and its resistance to evaporation (R_s), and body posture), environmental conditions, and physical principles governing mass transfer. We used the empirically determined EWL rates of the three species to evaluate the accuracy of the biophysical modeling. For this, we first identified grid cells in our microclimate dataset that had a combined profile of wind speed (1 ±0.1 m/s) and air and ground temperatures (15, 20, 25°C with a ±1°C variation) that closely matched our experimental conditions of airflow rate (21 cm^3/s) and test temperatures (15, 20, 25°C) with living frogs. For these same grid cells, we used the biophysical model to simulate the expected EWL for a theoretical 9g *L. fuscus*, 15g *L. mystacinus*, and 57g *L. macrosternum* (the average mass of our measured living frogs) represented by an anuran-like ectotherm with species-specific morphological characteristics (see Supporting S4 for model settings). We then compared the evaporative water loss at different temperatures between these two approaches. This was done by performing generalized linear mixed-effect models (GLMM) run separately for each species, with the interaction between source (simulations vs. empirical measures) and temperature (15°C, 20°C, and 25°C) as fixed factors, the identity of living frogs as a random factor, and EWL as the response variable. GLMMs were followed by Tukey's tests to identify significant differences at each temperature. The distributional normality assumption was verified by visually examining the model residuals and the Shapiro–Wilk test.

The empirically derived and biophysically calculated levels of T_b and EWL were compared using DFD and GLMM analyses, respectively, as global measures of congruency, and the hourly average temperature deviations as diagnostic measures of congruency for hourly T_b. While not identical, the level of congruency between empirical and biophysical T_b estimations (particularly in shady conditions) deviated, on average, equal to or less than 2.7°C. Similarly, although the EWL differed at some species-specific test temperatures, the empirical and biophysical calculations coincided with others (see Results sections). Based on these results, we accepted the level of congruency for the empirical vs. biophysical estimations (but see Discussion section) and proceeded with biophysical projections for all further analysis.

Activity and environmental restrictions

We simulated the hourly T_b distribution for a theoretical 9 g *L. fuscus*, 15 g *L. mystacinus,* and 57 g *L. macrosternum* at 1cm above ground conditions. As nocturnal frogs, we allowed surface activity across all nighttime hours (18:00 – 05:00 h) and assumed that animals retreat to underground refugia (become inactive) during the daylight hours (06:00 – 17:00) (Silva and Giaretta 2008, Henrique and Grant 2019). Because simulations incorporate a body thermal inertia (i.e., the T_b at a given hour is influenced by the T_b in the previous time step hour), we assumed that animals start activity (18:00 h) with a T_b matching their retreat site temperature the hour before emergence (17:00 h) (detailed below). To infer environmental constraints, our simulations focused primarily on organismal-based heat and water exchange processes. We implemented two interactive subroutines that simulated simple behavioral responses based on the organism's internal temperature state (thermal sensitivity of locomotor performance) and hydration (dehydration thresholds derived from cumulative EWL).

First, we used the thermal sensitivity of locomotor performance from empirical TPCs to infer habitat thermal suitability. We set CT_{min} and CT_{max} as the lower and upper thermal thresholds at which activity ceases due to locomotor impairment (i.e., the 'thermal activity timeframe' in our simulations). Within this thermal timeframe, we adopted a temperature-dependent probability of activity following Gunderson and Leal (2016), in which the surface activity transitions from zero (defined by physiological limits) to greater than zero (dictated by organismal performance capabilities). This smooth transitional model of activity patterns has proven to be very effective in predicting empirical observations of lizard species (Rozen-Rechels et al. 2020). In this way, our models assume that frogs with a T_b within their thermal performance breadth (B_{80}) are physiologically capable of conducting most ecological tasks and, as a result, are always active at the surface (100% probability of activity) unless severely dehydrated (see below). Beyond these limits, performance, and hence the probability of activity, rapidly decreases following the descending portions of locomotor TPCs until performance reaches zero (i.e., as set by the lower and upper thermal thresholds). To account for the potential costs associated with hydric stress, we incorporated the sensitivity to EWL (derived from the EWL simulated by the biophysical model) as a potential constraint for activity. We assumed that the animals were fully hydrated at the time of emergence. From this point on, we computed the hourly cumulative EWL (gH_2O/h) until it reached the maximum body water loss tolerance (EWL_{tol}) by *L. fuscus* (61.51%), *L. mystacinus* (64.47%), and

L. macrosternum (68.22%). The 'hydric activity timeframe' was defined as the time (total hours) between emergence and reaching the dehydration threshold (EWL_{tol}), assuming no further activity beyond this point. Regardless of the hydration level, this hydric activity timeframe can be curtailed at any time if the animal attains a critical thermal threshold (explained above). In summary, we considered that frogs would retreat to underground refugia if they experienced harmful temperatures (CT_{min} or CT_{max}), chronic hydric deficits (EWL_{tol}), or during the daytime.

Although nocturnally active, daytime shelters can also affect frogs' thermal budgets (Forget-Klein and Green 2021). In nature, our species tend to build burrows in highly wet soils (Solano 1887, Silva and Giaretta 2008) at depths of about 5-9 cm, depending on the species (Martins 1988, Oliveira-Filho and Giaretta 2008, Lucas et al. 2008). Based on their burrow characteristics, frogs were assumed to be 5 cm deep and fully hydrated when sheltered. We used the hourly substrate temperature 5 cm below the surface as a proxy measure for sheltering T_b because animals may attain thermal equilibrium with their shelter (Smits 1984). Note that 'sheltering' is a facultative state during activity that permits animals to escape harmful surface conditions. However, sheltered, inactive animals may not escape harmful T_b during thermal stress. Therefore, we also set unsuitable locations (grid cells) where frogs exceeded their CT_{min} or CT_{max} when sheltered during daytime hours.

Suitability maps

To identify the physiologically limiting constraints on activity across the entire distribution of the species, we searched for grid cells in which the activity time was curtailed before nighttime hours were completed and the hours of restrictions (Hr; nighttime hours of inactivity due to thermal and hydric constraints) and the respective traits responsible for this cessation (CT_{min}, $CT_{max,}$ or EWL_{tol}) were identified. The resulting grid cell output was then rasterized into new raster layers to represent the potential physiological constraints on activity in a geographic space. Based on these spatial physiological outputs, we also calculated the percentage that represented these grid cells with the detected Hr concerning the total geographical distribution of the species.

The production of suitability maps involved two steps. First, a thermal and hydric suitability map was produced separately for more straightforward interpretation when addressing the two primary criteria used to infer the environmental constraints in our simulations. Then, the resulting suitability maps were overlaid to produce a derived map representing the joint suitability as a function of the thermal and hydric criteria. From a thermal standpoint, our mechanistic models

were constructed based on thermal thresholds bounding temperature-dependent activity probabilities (dictated by organismal performance capabilities), all related to the hourly microclimate. Hence, for a continuously active frog, the thermal thresholds and probabilities of activity will vary hourly as the nightly thermal conditions change over time. For this reason, we quantified a location's thermal suitability by scaling hourly surface activity scores between 0 (least suitable) if the animal was impeded from engaging in activity (0h of activity) due to thermal restrictions, and 1 (most suitable) if the animal achieved at least 6h of activity with its T_b kept within the B_{80} limits, which is a time assumed to be sufficient for performing most relevant ecological tasks. This assumption is based on field observations of some leptodactylid species, in which a large proportion of activity occurs primarily during the first half of the night (Woolbright 1985, De-Carvalho et al. 2008, Bardier et al. 2014). On the other hand, unlike thermal traits, EWL is a cumulative process that occurs hourly (sum across hours) until it attains the physiological endpoint defined by EWL_{tol}. Hence, the hydric suitability of locations was estimated by scaling the total cumulative EWL scores into relative scores ranging from 0 (least suitable) when the cumulative EWL reached EWL_{tol} during the first hour of activity (0h of activity due to hydric restrictions) to 1 (most suitable) if the animal was able to be active at night with a cumulative EWL approximating its initial state of complete hydration. Note that because EWL is an unavoidable process, even locations considered highly suitable from a hydric perspective will exhibit values close to 1 but not 1. Finally, we combined the thermal and hydric suitability maps by averaging their scores to produce a joint suitability map ranging from 0, where activity was curtailed by both thermal or hydric restrictions, and 1, representing locations where animals could maintain an optimal range of T_b (at least 6h of activity within their B_{80} limits) and a good hydration level.

RESULTS

Comparisons of T_b from biophysical simulations and empirical field observations showed a congruence pattern along the daily cycle (Supporting S5). In general, the overall agreement of hourly predictions and observations was better in shady (DFD = 1.48 for 28g agars; DFD = 1.56 for 5g agars) than sunny locations (DFD = 5.36 for 112g agars; DFD = 5.83 for 23g agars), with an average hourly deviation of 1.28°C for 28g agars (maximum deviation of 3.09°C), 1.32°C for 5g agars (maximum of 3.16°C), 2.67°C for 112g agars (maximum of 6.96°C), and 2.56°C for 23g agars (maximum of 7.42°C). Simulated and empirical EWL differed for *L. fuscus* (X^2_2 = 57.06, P < 0.001), *L. mystacinus* (X^2_2 = 41.27, P < 0.001), and *L. macrosternum* (X^2_2 = 41.98, P <0.001), being this difference significant (P < 0.05) at 20°C for *L. fuscus*, at 15°C and 25°C for *L. mystacinus*, and 15°C and 20°C for *L. macrosternum*. In contrast, no significant differences were found in the remaining temperature comparisons (Supporting S6).

Considering only the period in which frogs were active, CT_{min} imposed a variable number of hours of restriction on all species within their current geographic distribution. EWL_{tol} also imposed restrictions, but only on *L. fuscus*. On average, considering only the cells where the animals experienced some level of restriction, *L. fuscus* was restricted by an Hr of 3.17 ± 2.64 hours, *L. mystacinus* by an Hr of 6.08 ± 3.29 hours, and *L. macrosternum* by an Hr of 4.11 ± 2.78. These restrictions in activity covered an area that represented 10.2%, 14.3%, and 6% of the total distribution of the three species, respectively.

The spatial distribution of cells in which the animals experienced some level of restriction was not uniform. In *L. fuscus,* restriction occurred mainly in the southern distribution as a function of CT_{min} (Fig. 2A), and due to EWL_{tol} in the central and eastern distributions (Fig. 2B). In *L. mystacinus* and *L. macrosternum,* restriction occurred mainly in their southern distributions and was solely due to CT_{min} limitations (Fig. 2C and 2D, respectively), with only a few locations in northern Argentina for *L. mystacinus*. None of the species attained CT_{max} during activity across their entire distribution.

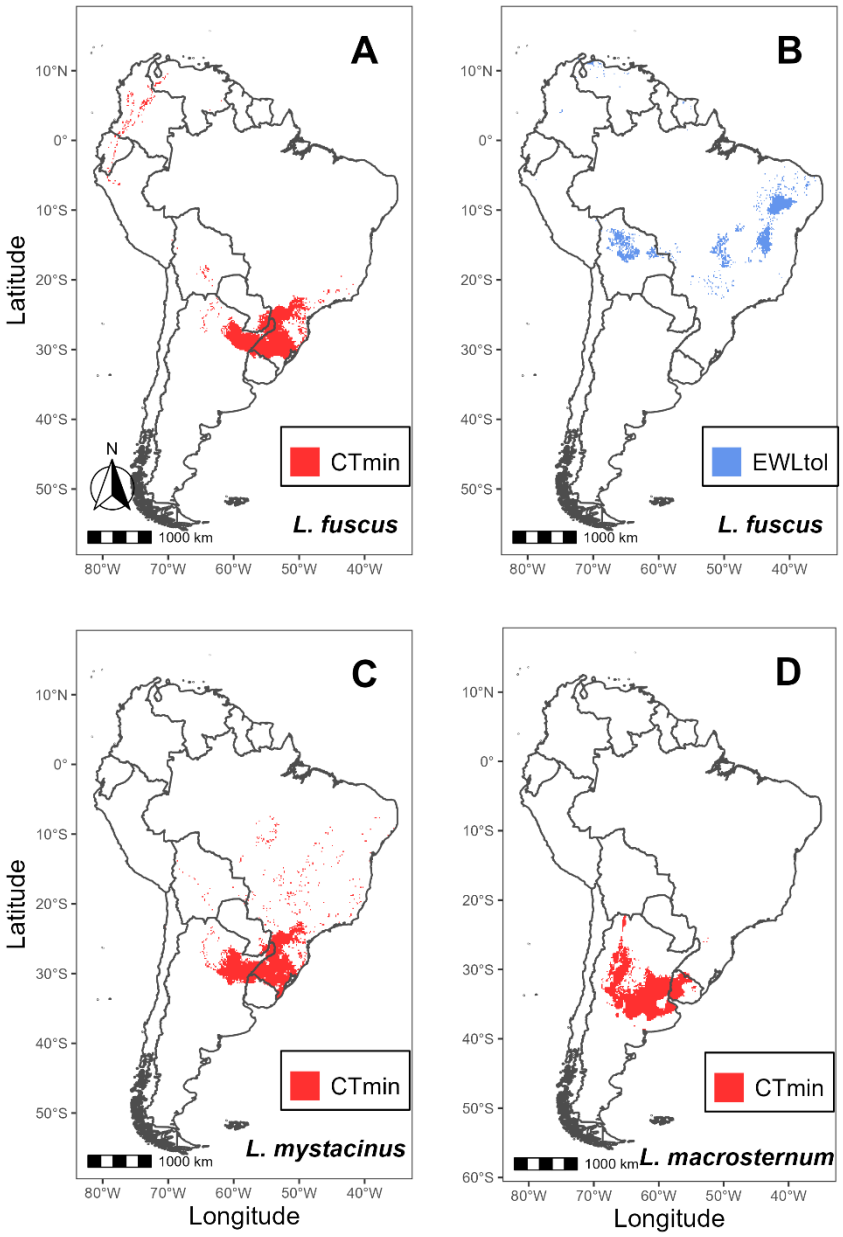

Figure 2. Physiological constraints on activity time derived from mechanistic simulations for *Leptodactylus fuscus* (A and B), *L. mystacinus* (C), and *L. macrosternum* (D). The indicated areas represent locations where the animals reached their physiological endpoints (CT_{min} and EWL_{tol}) during activity, regardless of the total number of hours they experienced restrictions. As a result, these areas also represent locations in which species presence is mediated through the buffering effect of shelter use.

Suitability maps revealed that central and northern regions provide suitable thermal conditions for the three species, where animals can maintain at least 6h of activity within an optimal range of T_b (i.e., within their B_{80} limits) (Fig. 3A, 3D, 3G). On the other hand, hydric conditions were more suitable (i.e., areas with lower cumulative EWL during activity) in the southern limits of *L. fuscus* (Fig. 3B), the southern portion of the distribution of *L. mystacinus* (Fig. 3E), and almost the entire distribution of *L. macrosternum* (Fig. 3H). The combination of the thermal and hydric suitability maps clearly showed that the level of suitability varied spatially based on species-specific temperature locomotor sensitivity and hydric requirements (Figs. 3C, 3F, and 3I).

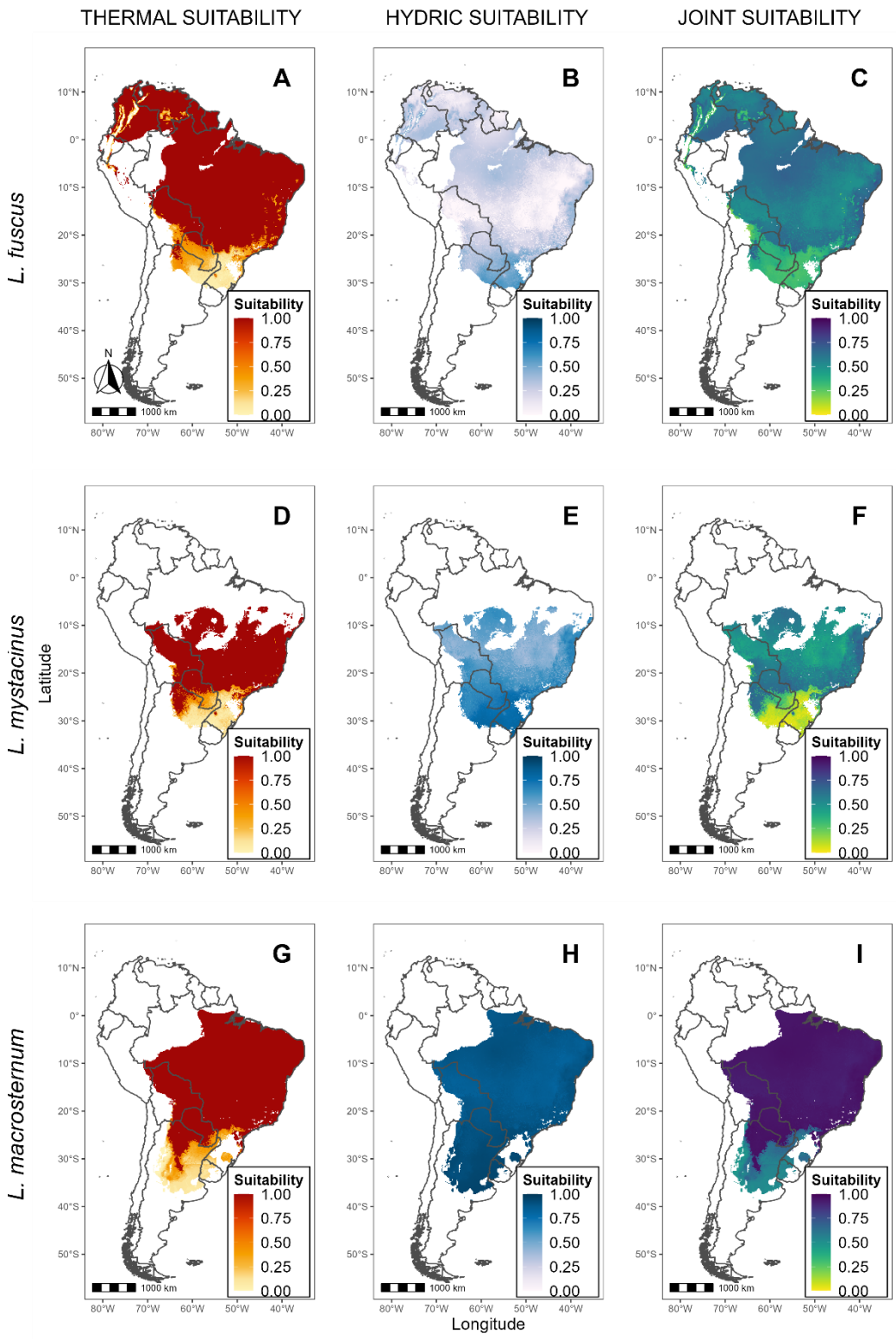

Figure 3. Hydric suitability (A, D, and G), thermal suitability (B, E, and H), and joint suitability (a combination of hydric and thermal suitability) for *Leptodactylus fuscus*, *L. mystacinus,* and *L. macrosternum*.

DISCUSSION

We found an overall good match between the biophysically modeled and empirical data for the daily T_b fluctuations in agar models and EWL rates for living organisms. For daily T_b, wider deviations (>4°C) were mainly at sunny locations and during the daytime. This may result from the usually higher and more variable diurnal temperature (Muñoz and Bodensteiner 2019) and wind speed (Trebs et al. 2005) than in shady locations, where canopies buffer against temperature extremes and high humidity variations (Frenne et al. 2021), thus offering more stable operative temperatures (see Köhler et al. 2011, Nowakowski et al. 2017). For EWL rates, discrepancies between the empirical and biophysical estimations may arise, for example, because the biophysical modeling disregards the contribution of pulmonary water loss, which can account for up to 8% of total evaporation in a typical anuran (Lillywhite 1975, Senzano and Andrade 2018). Also, both the biophysical model and empirical approaches assume an unlike fixed, water-conserving posture of animals. While such factors can vary haphazardly and are hardly captured by ours or any other mechanistic approach (Briscoe et al. 2023), we reached fair and promising levels of agreement between empirical and biophysical estimates of T_b and EWL rates. For instance, both the general shape pattern of daily T_bs and its deviations were within the natural range expected for field active anurans in this region (e.g., Noronha-de-Souza et al. 2015, Maenaka et al. 2023) and the voluntary thermal maximum of various Neotropical anurans do not surpass this same range (Díaz-Ricaurte et al. 2022). Likewise, both approaches accurately agreed on the negative effect of body size on EWL rates (Supporting S6), which was a crucial component in determining water budgets in our simulations. Therefore, despite some discrepancy between modeled and empirical data, our mechanistic model is still within biologically realistic values of T_b and EWL and thus it provides biologically meaningful estimates.

The three studied species experienced different levels of restriction in their activity. Such differences may stem from their different sensitivity to the thermal and hydric conditions. For instance, *L. mystacinus* had, on average, the highest restrictions in activity time (6 h), followed by *L. macrosternum* (ca. 4 h), and *L. fuscus* with the lowest hours of restrictions (ca. 3 h). Because restrictions in foraging activity compromise food acquisition, energetics, growth, and reproduction in anurans (Geise and Linsenmair 1988, Bartelt et al. 2010), *L. mystacinus* appears to have fewer foraging opportunities than the other species. Most *Leptodactylus* frogs are more active during the first half of the night (Woolbright 1985, De-Carvalho et al. 2008, Bardier et al. 2014), coinciding with the warmest night hours, which favor reproductive (Zina and Haddad 2005, Chaves et al.

2017) and locomotor activity (Henrique and Grant 2019). In agreement, most constraints on activity were predicted in our simulations to occur at the end of the night (Supporting S6), indicating that the species, particularly *L. mystacinus,* may adjust their activity to the early night hours in areas where conditions are less restrictive. Furthermore, our modeling estimations were restricted to the most humid time of the year, when hydric and thermal conditions are usually milder. As such, because reproductive periods extend for longer than we considered (see Heyer and Giaretta 2009, Camurugi et al. 2017), reductions in ambient humidity throughout the months of activity could further constraint their foraging activity time, thereby determining not only their phenology but also other essential functions (e.g., Geise and Linsenmair 1988, Senenayake et al. 2019).

Restriction in activity was linked to CT_{min} for all three species and EWL_{tol} for *L. fuscus*. This is surprising because most assessments link activity restrictions to warm conditions, including for reptiles (e.g., Sinervo et al. 2010, Kearney 2013, Sears et al. 2016, Kearney et al. 2018), and anurans (Enriquez-Urzelai et al. 2019, Lertzman-Lepofsky et al. 2020). This is even more striking for tropical species, which are believed to often operate at temperatures closer to their upper thermal tolerance. Instead, none of the three species reached the upper thermal threshold for activity (CT_{max}). In fact, their T_b distribution during activity was below their optimal temperature for performance and its upper thermal limit (B_{80} upper; see Supporting S7). This indicates that their activity appears to be dictated by lower temperatures, particularly on the southern border of their distribution. We shall notice, however, that a large proportion of their T_b distribution is still above their lower limit B_{80}, suggesting that species are capable of sustaining performance, if not at the best levels, at least within considerably high levels. Beukema et al. (2021) also found that a salamander (*Salamandra Salamandra*) was thermally constrained by its microclimate from achieving favorable warmer T_b. Our findings do not oppose previous claims on the susceptibility of tropical species to climate change (Deutsch et al. 2008). Instead, they highlight the pervasiveness of the lower thermal bound for activity and thus the distribution of tropical anurans, thus suggesting that the overemphasis on the upper thermal limits such as CT_{max} (e.g., Duarte et al. 2012, Scheffers et al. 2013, Simon et al. 2015, Turriago et al. 2022) may provide an incomplete understanding of climatic constraints on anurans.

Suitable regions have average conditions generally below the species' T_{opt}, and these lower temperatures also account for lower EWL rates, thus partially explaining why species were less

constrained by water. The unfavorable surface to volume ratio of smaller species also leads to faster dehydration, which result in interspecific differences in the maginitude of such water constraints. This is reflected in the smaller species, *L. fuscus* and *L. mystacinus*, for which thermally suitable regions become unsuitable owing to drier conditions. This occurs mainly in Brazil's central and northernmost regions, where the drier seasons are more pronounced, and the gradual and cumulative loss of body water by evaporation constrains activity even in locations considered thermally suitable for performance. For organisms subject to these conditions, shelters play a crucial role against heat stress during daytime (Spieler and Linsenmair 1998, Forget-Klein and Green 2021) and colder and drier conditions at nighttime. This was evident in some central and southern regions, where the use of shelter buffered species from the harmful nightly conditions during activity (see Fig. 1), though this buffering capacity may still have some limitations, as species reached their CT_{max} during daytime in a few locations (Supporting S8). As a result, temperatures above CT_{max} may still be threatening if diurnal conditions become warmer, particularly during climate heat events, which are expected to become more frequent as climate change progresses (Stillman 2019).

In summary, our mechanistic assessment, combined with physiological and field data on the thermal sensitivity of organismal performance and water needs, provides novel insights into how the activity of Neotropical anurans is constrained by temperature and water across their geographic range. Body size imposes a hydric risk, with smaller species being more vulnerable to dehydration and activity inhibition, even under thermally adequate conditions. Strikingly, these species' thermal-induced activity restrictions were mainly linked to low temperatures rather than warmer conditions. Just as the upper thermal constraints from heat and radiation during the daytime lead most anurans to nocturnality, lower night temperatures also impose a lower thermal constraint that appears to determine their overall activity. This finding highlights the importance of accounting for multiple constraints, such as temperature and water, and full diel activity patterns in mechanistic models for a better understanding of the influence of climate on species' activity, thermal niche, and geographic distribution.

REFERENCES

Abe A. S. and L. S. Garcia. 1991. Response to temperature in the oxygen uptake of awake and dormant frogs (Amphibia, Leptodactylidae). *Studies on Neotropical Fauna and Environment* 26(3): 135-141.

Alvarez C. A., J. L. Stape, P. C. Sentelhas, J. L. M. Gonçalves and G. Sparovek. 2014. Köeppen's climate classification map for Brazil. Meteorologische Zeitschrift 22(6): 711-728.

Anderson R. C. O., R. P. Bovo and D. V. Andrade. 2018. Seasonal variation in the thermal biology of a terrestrial toad, *Rhinella icterica* (Bufonidae), from the Brazilian Atlantic Forest. *Journal of Thermal Biology*, 74: 77-83.

Anderson S.R. and J.J. Wiens. 2017. Out of the dark: 350 million years of conservatism and evolution in diel activity patterns in vertebrates. *Evolution*, 71(8): 1944-1959.

Araújo M. B. and M. New. 2007. Ensemble forecasting of species distributions. *Trends in Ecology and Evolution*, 22(1): 42-47.

Bardier C., A. Canavero and R. Maneyro. 2014. Temporal and spatial activity patterns of three species in the *Leptodactylus fuscus* group (Amphibia, Leptodactylidae). *South American Journal of Herpetology*, 9(2): 106-113.

Bartelt P. E., R. W. Klaver and W. P. Porter. 2010. Modeling amphibian energetics, habitat suitability, and movements of western toads, *Anaxyrus* (=*Bufo*) *boreas*, across present and future landscapes. *Ecological Modelling*, 221: 2675-2686.

Bestion E., A. Teyssier, M. Richard, J. Clobert and J. Cote. 2015. Live fast, die young: Experimental evidence of population extinction risk due to climate change. PLoS Biology, 13(10): e1002281

Beukema W., F. Pasmans, S. V. Praet, F. Ferri-Yáñez, M. Kelly, A. E. Laking, J. Erens, J. Speybroeck, K. Verheyen, L. Lens and A. Martel. 2021. Microclimate limits thermal behaviour favourable to disease control in a nocturnal amphibian. *Ecology Letters*, 24: 27-37.

Briscoe N.J., J. Elith, R. Salguero-Gómez, J.L. Lahoz-Monfort, J.S. Camac, K.M. Giljohann, M.H. Holden, B.A. Hradsky, M.R. Kearne, S.M. McMAhon, B.L. Phillips, T.J. Regan, J.R. Rhodes, P.A. Vesk, B.A. Wintle, J.D.L. Yen and G. Guillera-Arriota. 2019. Forecasting species range dynamics with process-explicit models: matching methods to applications. *Ecology Letters*, 22: 1940-1956.

Burgman M.A. and J.C. Fox. 2003. Bias in species range estimates from minimum convex polygons: implications for conservation and options for improved planning. *Animal Conservation*, 6: 19-28.

Chaves M. F., G. J. B. Moura, F. C .M. A. Tenório, J. S. Baptista, C. J. C. L. Neto, V. W. T. Texeira and A. A. C. Texeira. 2017. Influence of rainfall and temperature on the spermatogenesis of *Leptodactylus macrosternum* (Anura: Leptodactylidae). *Zoologia*, 34: e20782.

Chaves M. F., G. J. B. Moura, J. S. Baptista, A. P. Dantas, V. W. Texeira and A. A. C. Teixeira. 2021. Environmental and abiotic factors interfere in *Leptodactylus macrosternum* (Anura, Leptodactylidae) reproduction despite no changes in sexual hormones levels. *Research, Society and Development* 10(8): e46110817627.

Cui Z., W. Li, S. Yu and M Jin. 2022. Similarity analysis of dynamic temperature measurements. Meteorology and Measurement Systems, 29(2): 283-300.

De-Carvalho C. B., E. B. Freitas, R. G. Faria, R. C. Batista, C. C. Batista, W. A. Coelho and A. Bocchiglieri. 2008. História natural de *Leptodactylus mystacinus* e *Leptodactylus fuscus* (Anura: Leptodactylidae) no Cerrado do Brasil Central. Biota Neotropica 8(3): 105-115.

Deutsch C.A., J.J. Tewksbury, R.B. Huey, K.S. Sheldon, C.K. Ghalambor, D.C. Haak and P.R. Martin. 2008. Impacts of climate warning on terrestrial ectotherms across latitude. *Proceedings of the National Academy of Sciences of the United States of America*, 105(18): 6668-6672.

Díaz-Ricaurte J. C., F. C. Serrano and M. Martins. 2022. VTMaxHerp: A data set of voluntary thermal maximum temperatures of amphibians and reptiles from two Brazilian hotspots. *Ecology*, 103(3): e3602.

Duarte H., M. Tejedo, M. Katzenberger, F. Marangoni, D. Baldo, J. F. Beltrán, D. A. Martí, A. Richter-Boix and A. Gonzalez-Voyer. 2012. Can amphibians take the heat? Vulnerability to climate warming in subtropical and temperate larval amphibian communities. *Global Change Biology*, 18: 412-421.

Enriquez-Urzelai U., M. R. Kearney, A. G. Nicieza and R. Tingley. 2019. Integrating mechanistic and correlative niche models to unravel range-limiting processes in a temperate amphibian. *Global Change Biology*, 25(8): 2633-2647.

Feder M. E. and P. L. Londos. 1984. Hydric constraints upon foraging in a terrestrial salamander, *Desmognathus ochrophaeus* (Amphibia: Plethodontidae). *Oecologia*, 64: 413-418.

Forget-Klein É. and D.M. Green. 2021. Toads use the subsurface thermal gradient for temperature regulation underground. *Journal of thermal Biology*, 99: 102956. *Proceedings of the National Academy of Sciences of the United States of America*, 105(18): 6668-6672.

Fouquet A., A. Gilles, M. Vences, C Marty, , Blanc and N. J. Gemmell. 2007. Underestimation of species richness in Neotropical frogs revealed by mtDNA Analyses. *PLoS ONE*, 2(10): e1109.

Frenne P., J. Lenoir, M. Luoto, et al. 2021. Forest microclimates and climate change: Importance, drivers and future research agenda. *Global Change Biology*, 27: 2279-2297.

Geise W. and K. E. Linsenmair. 1988. Adaptations of the reed frog *Hyperolius viridiflavus* (Amphibia, Anura, Hyperoliidae) to its arid environment. IV. Ecological significance of water economy with comments on thermoregulation and energy allocation. *Oecologia*, 77: 327-338.

Ginal P., M. Mokhatla, N. Kruger, J. Secondi, A. Herrel, J. Measey and D. Rödder. 2021. Ecophysiological models for global invaders: Is Europe a big playground for the African clawed frog? Journal of Experimental Zoology A, 335(1): 158-172.

Greenberg D.A. and W.J. Palen. 2021. Hydrothermal physiology and climate vulnerability in amphibians. *Proceedings of the Royal Society B*, 288: 20202273.

Gunderson A.R. and M. Leal. 2016. A conceptual framework for understanding thermal constraints on ectotherm activity with implications for predicting responses to global change. *Ecology letters*, 19: 111-120.

Haddad C.F.D., L.F. Toledo, C.P.A. Prado, D. Loebmann, J.L. Gasparini and I. Sazima. 2013. Guia dos anfíbios da Mata Atlântica: diversidade e biologia. Anolisbooks, São Paulo, Brazil.

Hansen M.C. et al. 2013. High resolution global maps of 21st-century forest cover change. Science, 342(6160): 850-853.

Henrique R.S. and T. Grant. 2019. Influence of environmental factors on short-term movements of butter frogs (*Leptodactylus latrans*). *Herpetologica*, 75(1): 38-46.

Heyer W. R. and A. A. Giaretta. 2009. Advertisement calls, notes on natural history, and distribution of *Leptodactylus chaquensis* (Amphibia: Anura: Leptodactylidae) in Brasil. *Proceedings of the Biological Society of Washington*, 122(3): 292-305.

Hitchcock M. A. and L. D. McBrayer. 2006. Thermoregulation in nocturnal ecthotherms: Seasonal and intraspecific variation in the mediterranean gecko (*Hemidactylus turcicus*). *Journal of Herpetology*, 40(2): 185-195.

Huey R. B. and R. D. Stevenson. 1979. Integrating thermal physiology and ecology of ectotherms: a discussion of approaches. *American Zoologist*, 19(1): 357-366.

Huey R. B. and J. G. Kingsolver. 2019. Climate warming, resource availability, and the metabolic meltdown of ectotherms. *The American Naturalist*, 194(6): E000–E000

Kearney M. R. 2013. Activity restriction and the mechanistic basis for extinctions under climate warming. *Ecology Letters*, 16(12): 1470-1479.

Kearney M.R., A.P. Isaac and W.P. Porter. 2014. microclim: global estimates of hourly microclimate based on long-term monthly climate averages. *Scientific Data*, 1: 140006.

Kearney M.R. and W.P. Porter. 2017. NicheMapR – an R package for biophysical modelling: the microclimate model. *Ecography*, 40: 664-674.

Kearney M.R., B.L. Phillips, C.R. Tracy, K.A. Christian, G. Betts and W.P. Porter. 2008. Modelling species distributions without using species distributions: the cane toad in Australia under current and future climates. *Ecography*, 31(4): 423-434.

Kearney M.R., S.L. Munns, D. Moore, M. Malishev and C. Bull. 2018. Field tests of a general ectotherm niche model show how water can limit lizard activity and distribution. *Ecological Monographs*, 88(4): 672-693.

Köhler A., J. Sadowska, J. Olszewska, P. Trzeciak, O. Berger-Tal and C. R. Tracy. 2011. Staying warm or moist? Operative temperature and thermal preferences of common frogs (*Rana temporaria*), and effects on locomotion. *Herpetological Journal*, 21: 17-26.

Lertzman-Lepofsky G.F., A.M. Kissel and B. Sinervo. 2020. Water loss and temperature interact to compound amphibian vulnerability to climate change. Global Change Biology, 26(9): 4868-4879.

Lillywhite H. B. 1975. Physiological correlates of basking in amphibians. *Comparative Biochemestry and Physiology Part A*, 52(2): 323-330.

Lucas E. M., C. A. Brasileiro, H. M. Oyamaguchi and M. Martins. 2008. The reproductive ecology of *Leptodactylus fuscus* (Anura, Leptodactylidae): new data from natural temporary ponds in the

Brazilian Cerrado and a review throughout its distribution. *Journal of Natural History*, 42(35-36): 2305-2320.

Maenaka B. M., L. M. Senzano and D. V. Andrade. 2023. Seasonal variation in thermal biology and water balance in a Year-Round active Neotropical treefrog, *Scinax fuscovarius*. *Herpetologica*, 00: 00-00.

Magalhães F. M., Lyra M. L., Carvalho T. R., Baldo D., Brusquetti F., Burella P., Colli G. R., Gehara M. C., Giaretta A. A., Haddad C. F. B., Langone J. A., López J. A., Napoli M. F., Santana D. J., Sá R. O., Garda A. A. 2020. Taxonomic review of South American butter frogs: phylogeny, geographic patterns, and species delimitation in the *Leptodactylus latrans* species group (Anura: Leptodactylidae). *Herpetological Monographs*, 34: 131-177.

Maenaka B. M., L. M. Senzano and D. V. Andrade. 2023. Seasonal variation in thermal biology and water balance in a year-round active Neotropical treefrog, *Scinax fuscovarius*. *Herpetologica*, 00(0): 1-11.

Marsh C. J., M. M. Syfert, E. Aletrari, Y. Gavish, W. E. Kunin and N. Brummitt. 2023. The effect of sampling effort and methodology on range size estimates of poorly-recorded species for IUCN Red List assessments. Biodiversity and Conservation, 32: 1105-1123.

Martins M. 1988. Biologia reprodutiva de *Leptodactylus fuscus* em Boa Vista, Roraima (Amphibia: Anura). Revista Brazileira de Biologia 48(4): 969-977.

Marvin G.A., K. Davis and J. Dawson. 2016. Effect of acute low body temperature on predatory behavior and prey-capture efficiency in a plethodontid salamander. *Physiology and Behavior*, 158: 121-127.

Méndez-Narváez J., S. V. Flechas and A. Amézquita. 2015. Foam nests provide context-dependent thermal insulation to embryos of three Leptodactylid frogs. *Physiological and Biochemical Zoology* 88(3): 246-253.

Mitchell A. and P. J. Bergmann. 2016. Thermal and habitat preferences do not maximize jumping performance in frogs. *Functional Ecology*, 30: 733-742.

Muñoz M.M. and B.L. Bodensteiner 2019. Janzen's hypothesis meets the Bogert effect: connecting climate variation, thermoregulatory behavior, and rates of physiological evolution. *Integrative Organismal Biology*, 1(1): 1-12.

Noronha-de-Souza C. R., R. P. Bovo, L. H. Gargaglioni, D. V. Andrade and K. C. Bícego. 2015. Thermal biology of the toad *Rhinella schneideri* in a seminatural environment in southeastern Brazil. *Temperature*, 2(4): 554-562.

Nowakowski A.J., J.I. Watling, S.M. Whitfield, B.D. Todd, D.J. Kurz and M.A. Donnelly. 2017. Tropical amphibians in shifting thermal landscapes under land-use and climate change. *Conservation Biology*, 31(1): 96-105.

O'Connor M. P. and C. R. Tracy. 1992. Thermoregulation by juvenile toads of Bufo woodhousei in the field and in the laboratory. *Copeia*, 1992(3): 865-876.

Oliveira-Filho J.C. and A.A. Giaretta. 2008. Reproductive behavior of *Leptodactylus mystacinus* (Anura, Leptodactylidae) with notes on courtship call of other Leptodactylus species. *Iheringia, Série Zoologia*, 98(4): 508-515.

Ortega-Chinchilla J. E., L. C. Cabanzo-Olarte, R. Vaz, F. Lamadrid-Feris, C. R. Bevier and C. A. Navas. 2022. Behavioral models of hydrothermal regulation in anurans: A field study in the Atlantic Forest, Brazil. *Biotropica*. DOI: https://doi.org/10.1111/btp.13187

Pearson R. G., C. J. Raxworthy, M. Nakamura and A. T. Peterson. 2007. Predicting species distributions from small numbers of occurrence records: a test case using cryptic geckos in Madagascar. *Journal of Biogeography*, 34: 102-117.

Pena J. C. C., L. H. Y. Kamino, M. Rodriguez, E. Mariano-Neto and M. F. Siqueira. 2014. Assessing the conservation status of species with limited available data and disjunct distribution. *Biological Conservation*, 170: 130-136.

Peterman W. E. and R. D. Semlitsch. 2014. Spatial variation in water loss predicts terrestrial salamander distribution and population dynamics. *Oecologia*, 176: 357-369.

Peterson A. T. and R. K. Raghavan. 2017. The geographic distribution of *Ixodes scapularis* (Acari: Ixodidae) revisited: The importance of assumptions about error balance. *Journal of Medical Entomology*, 54(4): 1080-1084.

Porter W.P., J.W. Mitchell, W.A. Beckman and C.B. DeWitt. 1973. Behavioral implications of mechanistic ecology. *Oecologia*, 13:1-54.

Prado C. P. A., M. Uetanabaro and F. S. Lopes. 2000. Reproductive strategies of *Leptodactylus chaquensis* and *L. podicipinus* in the Pantanal, Brazil. Journal of Herpetology 34(1): 135-139.

Rock J. and A. Cree. 2008. Extreme variation in body temperature in a nocturnal thigmothermic lizard. *Herpetological Journal*, 18: 69-76.

Rozen-Rechels D., A. Dupoué, O. Lourdais, S. Chamaillé, S. Meylan, J. Clobert and J. Le Galliard. 2019. When water interacts with temperature: ecological and evolutionary implications of thermo-hydroregulation in terrestrial ectotherms. *Ecology and Evolution*, 9(17): 10029-10043.

Rozen-Rechels D., P. Farigoule, S. Agostini, A. Badiane, S. Meylan and J.F. Le Galliard. 2020. Short-term change in water availability influences thermoregulation behaviours in a dry-skinned ectotherm. *Journal of Animal Ecology*, 89(9): 2099-2110.

Rubalcaba J.G., S.F. Gouveia and M.A. Ollaga-Tárraga. 2019a. A mechanistic model to scale up biophysical processes into geographical size gradients in ectotherms. *Global Ecology and Biogeography*, 28(6): 793-803.

Rubalcaba J.G., S.F. Gouveia and M.A. Ollaga-Tárraga. 2019b. Upscaling microclimatic conditions into body temperature distributions of ectotherms. *The American Naturalist*, 193(5): 677-687.

Ruthsatz K., A. Rakotoarison, J. Razafimampiandra, V. S. Randriamahefa, F. Rabemananjara, F. Rakotondraparany, M. C. Bletz and M. Vences. 2022. Field body temperatures in Malagasy rainforest frogs. *Herpetology Notes*, 15: 565-578.

Sá R.0., T. Grant, A. Camargo, W.R. Heyer, M.L. Ponssa and E. Stanley. Systematics of the Neotropical Genus *Leptodactylus* Fitzinger, 1826 (Anura: Leptodactylidae): phylogeny, the relevance of Non-molecular evidence, and species accounts. *South American Journal of Herpetology*, 9(1): S1-S128.

Scheffers B. R., R. M. Brunner, S. D. Ramirez, L. P. Shoo, A. Diesmos and S. E. Willians. 2013. Thermal buffering of microhabitats is a critical factor mediating warming vulnerability of frogs in the Philippine biodiversity hotspot. *Biotropica*, 45: 628-635.

Schwarzkopf L. and R. A. Alford. 1996. Desiccation and shelter-site use in a tropical amphibian: comparing toads with physical models. *Functional Ecology*, 10: 193-200.

Sears M.W., M.J. Angilletta, M.S. Schuler, J. Borchert, K.F. Dilliplane, M. Stegman, T.W. Rusch and W.A. Mitchell. 2016. Configuration of the thermal landscape determines thermoregulatory performance of ectotherms. *Proceedings of the National Academy of Sciences of the United States of America*, 113(38): 10595-10600.

Seebacher F. and R. A. Alford. 2002. Shelter microhabitats determine body temperature and dehydration rates of a terrestrial amphibian (*Bufo marinus*). *Journal of Herpetology*, 36: 69-75.

Senenayake U. I., S. Siriwardana, D. K. Weerakoon and M. R. Wijesinghe. 2019. Combating extreme tropical seasonality: Use of rock crevices by the critically endangered frog *Nannophrys marmorata* in Sri Lanka. *Herpetological Conservation and Biology*, 14(1): 261-268.

Senzano L.M. and D.V. Andrade. 2018. Temperature and dehydration effects on metabolism, water uptake and the partitioning between respiratory and cutaneous evaporative water loss in a terrestrial toad. Journal of Experimental Biology, 221: 188482.

Silva W.R. and A.A. Giaretta. 2008. Further notes on the natural history of the South American pepper frog, *Leptodactylus labyrinthicus* (Spix, 1824) (Anura, Leptodactylidae). Brazilian Journal of Biology 68(2): 403-407.

Simon M. N., P. L. Ribeiro and C. A. Navas. 2015. Upper thermal tolerance plasticity in tropical amphibian species from contrasting habitats: Implications for warming impact prediction. *Journal of Thermal Biology*, 48: 36-44.

Sinervo B. et al. 2010. Erosion of lizard diversity by climate change and altered thermal niches. *Science*, 328: 894-899.

Smits 1984. Activity patterns and thermal biology of the toad *Bufo boreas halophilus*. *Copeia*, 3: 689-696.

Solano H. 1987. Algunos aspectos de la biología reproductiva del sapito silvador *Leptodactylus fuscus* (Schneider) (Amphibia: Leptodactylidae). *Amphibia-Reptilia*, 8: 111-128.

Spieler M. and K. E. Linsenmair. 1998. Migration patterns and diurnal use of shelter in a ranid frog of a West African savannah: a telemetric study. *Amphibia-Reptilia*, 19: 43-64.

Stillman J. H. 2019. Heat waves, the new normal: summertime temperature extremes will impact animals, ecosystems, and human communities. *Physiology* 34: 86-100.

Syfert M. M., L. Joppa, M. J. Smith, D. A. Coomes, A. P. Bachman and N. A. Brummitt. 2014. Using species distribution models to inform IUCN Red List assessments. *Biological Conservation*, 177: 174-184.

Tracy C.R., T.Tixier, C.L. Nöene and K.A. Christian. 2014. Field hydration state varies among tropical frog species with different habitat use. *Physiological and Biochemical Zoology*, 87(2): 197-202.

Trebs V., S. Metzger, F. X. Meixner, G. Helas, A. Hoffer, Y. Rudich, A. H. Falkovich, M. A. L. Moura, R. S. Silva, P. Artaxo, J. Slanina and M. O. Andreae. 2005. The NH_4^+-NO_3^--Cl^--SO_4^{2-}-H_2O aerosol system and its gas phase precursors at a pasture site in the Amazon Basin: How relevant are mineral cations and soluble organic acids. *Journal of Geophysical Research*, 10: D07303.

Wells K. D. 2007. The Ecology and Behavior of Amphibians. *The University of Chicago Press*, Chicago, USA.

Woolbright L. L. 1985. Patterns of nocturnal movement and calling by the tropical frog *Eleutherodactylus coqui*. *Herpetologica*, 41(1): 1-9.

Zina J. and F. B. Haddad. 2005. Reproductive activity and vocalizations of Leptodactylus labyrinthicus (Anura: Leptodactylidae) in southern Brazil. *Biota Neotropica*, 5(2): BN00605022005

SUPPORTING INFORMATION

Supporting S1. Species range delimitation for mechanistic simulations

Polygonal range delimitation

Species range distributions were estimated in the 'rangeBuilder' r-package. This package contains routines that involves drawing lines connecting occurrence points (Delauney triangulation) while discarding connecting lines between relatively distant points longer than a certain multiple (the parameter α) of the average line lengths. As a result, this yields a representation of the space contained by the cloud points (here buffered with a 100 km buffer around points), while allowing outlying poorly represented regions to be removed (see Burgman and Fox 2003 for a deeper explanation of the method). Occurrence points were obtained from the Global Biodiversity Information Facility – GBIF (http://www.gbif.org/; last access on April 4th, 2023) for the *L. fuscus* and *L. mystacinus* species. In the case of *L. macrosternum*, we used georeferenced records from Magalhães et al. (2020) that offers updated and well referenced occurrence data for this species. Before range estimations, occurrence data were subjected to a cleaning procedure to remove suspicious records such us duplicates, old dated (<1950), or unreliable georeference information (i.e., locations within marine waters or suspicious of misidentification given its extreme location respective to the rest of observations). This procedure yielded a total of 2901, 258 and 265 cleaned records for *L. fuscus*, *L. mystacinus* and *L. macrosternum*, respectively (see small panels in Fig. S2.1).

Species distribution modeling

Species distributions were modeled by relating species geographical occurrences to environmental variables via correlative modeling techniques. Georeferenced presence records were the same used for the Polygonal range delimitation but allowing just one species record per grid cell. As a result, we used a total of 562, 168 and 124 records for *L. fuscus*, *L. mystacinus*, and *L. macrosternum*, respectively. Climatic variables were represented by five bioclimatic variables derived from the Worldclim database (http://www.worldclim.org/) version 2.1 (1970-2000 period). The bioclimatic variables were: BIO1 – annual mean temperature; BIO3 – istothermality; BIO8 – mean temperature of wettest quarter; BIO15 – precipitation seasonality; BIO18 – precipitation of warmest quarter. These variables were selected because, (1) they characterize the temperature and precipitation as a whole (BIO1, BIO3, BIO15) or during the period when our model species are field-active (BIO8, BIO18) and (2) they are no collinear variables (Table S2.1)

which prevents redundant information that could hamper subsequent analysis (Heikkinen et al. 2006). To match the spatial resolution of our microclimatic simulations, bioclimatic variables originally downloaded at 5 arc-min (~10 km resolution) were downscaled to 15 km resolution using a bilinear resampling method in the 'raster' r-package.

To construct predictions, we used an ensemble modeling approach in which outputs of multiple predictive models are combined to estimate species potential distributions (Araújo and New 2007). The ensemble was constructed based on six predictive models: climate envelope bioclim (BIOCLIM), mahalanobis distance (Mahalanobis), generalized linear model (GLM), random Forest (RF), support Vector Machine (SVM) and Maximum Entropy (MaxEnt). All models, except the presence-only ones (BIOCLIM and Mahalanobis), require information for locations where the species are absent. Because true absence data are not available for our species, pseudo-absences with equal numbers of occurrences were generated by selecting points at random from the environmental background (Barbet-Massin et al. 2012). Species dataset records (presence/pseudoabsences) were then randomly split into a train/test (70%-30%) scheme in which 70% of the data were used for model training and the remaining 30% for model testing. Models were run under this split-sample scheme 10 times, and their predictive performances were evaluated by using the Area Under the ROC (Receiver Operating Characteristic) Curve (AUC) (Fielding and Bell 1997) and the True Skills Statistic (TSS) (Allouche et al. 2006) from their individually 10-replicate averages. Models with poor predictive performance (AUC < 0.7 and TSS < 0.5; Table S2.2) were removed from the ensemble analysis. Therefore, the final ensemble output was an unweighted average of well-performed models representing species habitat suitability with cell values ranging in a continuous manner from 0 (unsuitable) to 1 (suitable). Suitability maps were then transformed into binary (presence/absence) maps by applying the lowest presence threshold (LPT; Pearson et al. 2007). Finally, distributional LPT maps were superimposed to the range distribution derived from Delauney triangulation (commented above) deriving into new distributional areas outlined by both methods (Fig. S2.1).

Table S1.1. Summary of the correlation analysis among environmental variables. Potential collinearity was diagnosed via pairwise correlations with Pearson's r^2 < 0.7 considered as uncorrelated. BIO 1 = annual mean temperature; BIO 3 = istothermality; BIO 8 = mean temperature of wettest quarter; BIO 15 = precipitation seasonality; BIO 18 = precipitation of warmest quarter.

	BIO 2	BIO 3	BIO 8	BIO 15	BIO 18
BIO 2	1				
BIO 3	-0.51	1			
BIO 8	-0.27	0.44	1		
BIO 15	0.38	0.04	0.14	1	
BIO 18	-0.18	0.34	0.33	-0.22	1

Table S1.2. Models' AUC and TSS performance scores. Evaluated predictive models: climate envelope bioclim (BIOCLIM), generalized linear model (GLM), mahalanobis distance (MAHALANOBIS), Maximum Entropy (MaxEnt), random Forest (RF) and support Vector Machine (SVM). Predictive performance was considered poor when AUC < 0.7 and TSS < 0.5.

species	**model**	**AUC**	**TSS**
L. fuscus	BIOCLIM	0.644	0.276
	GLM	0.631	0.242
	MAHALANOBIS	0.778	0.434
	MaxEnt	0.763	0.411
	RF	0.843	0.55
	SVM	0.817	0.503
L. mystacinus	BIOCLIM	0.835	0.632
	GLM	0.837	0.608
	MAHALANOBIS	0.862	0.63
	MaxEnt	0.884	0.684
	RF	0.888	0.666
	SVM	0.875	0.678
L. macrosternum	BIOCLIM	0.761	0.516
	GLM	0.73	0.454
	MAHALANOBIS	0.812	0.554
	MaxEnt	0.772	0.527
	RF	0.828	0.573
	SVM	0.796	0.564

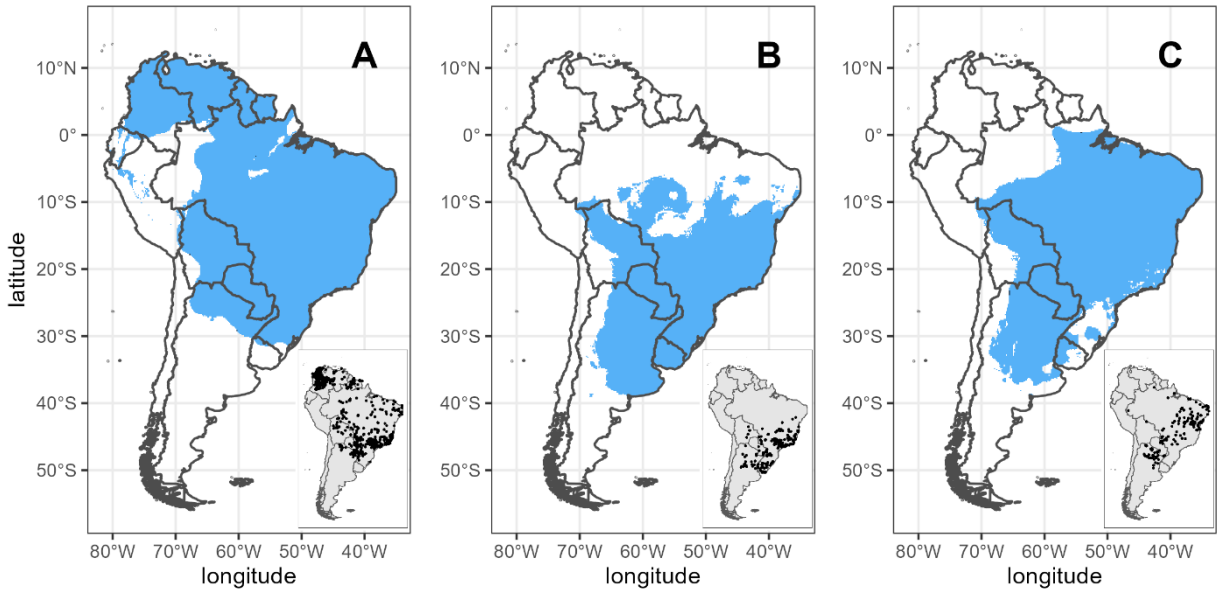

Figure S1.1. Species distributional areas (blue areas) considered for microclimatic simulations on *Leptodactylus fuscus* (**A**), *L. mystacinus* (**B**) and *L. macrosternum* (**C**). Small panels are the presence records (2901, 258 and 265 records in panel A, B, and C, respectively) used to estimate distributional areas derived from Delauney range triangulation and the species distribution modeling approach (see main text and Supporting S2).

Supporting S2. Biophysical model evaluation on agar replicas

Biophysical agar replicas can mimic the physical attributes of an amphibian in steady-state thermal equilibrium with its environment (Bakken et al. 1985), which gives comparable field T_bs to those of living animals (Navas and Araujo 2000). As a result, the agar approach enables operative temperature measures in a continuous manner for daytlight and nighttime conditions over a wider temporal window (various days) and under known local conditions (e.g., soil type, ground-level exposure to sunlight (shade); see Algar et al. 2018). For our intended purpose, this information was very desirable in order to adjust simulations (model parameterization) to field conditions and hence making them more comparable to each other.

We constructed agar replicas obtained from preserved *Rhinella diptycha* toads varying in size (5, 23, 28 and 112g). Agar replicas were made according to standard procedures (Spotila and Berman 1976), except for two alterations: 1) we colored replicas by adding a small drop of black liquid dye (Xadrez®, Brazil) during the agar preparation and, 2) we used a denser agar concentration (4.7%). The first alteration yielded a better approximation to biophysical expectations for a dark-colored animal while the second offered a mechanically more stable replica aimed for field conditions. We deployed agars in the field considering two microhabitat types: shady (85-90% of ground covered by natural vegetation; agar sizes: 23g and 112g) and sunny (without cover vegetation and exposed to direct sunlight during daytime hours; agar sizes: 5g and 28g). Both microhabitats are located at the campus of the São Paulo State University (22°23'49.7"S, 47°32'36.0"W) which edges a natural preservation area (Edmundo Navarro de Andrade, Rio Claro/SP, Brazil). Agars were monitored continuously with thermal loggers (HOBO Pro, v2 External Temperature) inserted into the internal part of models that were programmed to collect temperature readings at 1-min intervals for six consecutive days (Jun 2020). We carried out daily inspections at 8-hour intervals for weighing (0.0001g accuracy, AR2140 balance, Ohaus Adventurer) and replacing agars by new ones in case they exceed >10% of their initial body mass.

Following fieldwork, we used the biophysical model to run simulations and derive expected hourly T_bs for hypothetical equivalent size agars as the real ones (5, 23, 28 and 112g). We simulated wet-skinned anuran-like models in a water conserving posture under the assumption that one-third of agar surface remains in direct contact with substrate. Agar surface area (A_s) was calculated from the bufonid empirical equation described in Klein et al. (2016): $A_s = 7.956Mass^{0.6772}$, assuming a virtually freely evaporating surface (0.1 s/cm for 'skin' resistance). The rest of the model

parameters were run under the default settings (see Rubalcaba et al. 2019). Based on the georeferenced coordinates of field agar deployments, we extracted from Kearney et al. (2014) the hourly microclimatic profile of air and ground (soil) temperatures, solar radiation, wind speed and relative humidity 1 cm above ground for an average day in Jun assuming shady (90% shade) and sunny (0% shade) conditions. Finally, we computed the expected hourly T_bs for hypothetical agars and compared predictions against field observations (see main text for results).

Supporting S3. Parameterization of the heat model used to solve the heat-mass net flux for a theoretical 9 g *L. fuscus*, 15 g *L. mystacinus* and 57 g *L. macrosternum* to predict their expected T_b at a given location.

Model parameter	value	detail	source/reference
Body mass (g)*	9, 15, 57	average masses for our measured individuals	unpublished data
Total skin surface area (cm^2)*	37.5, 52.6, 128.9	surface area calculated as $8.6856Mass^{0.6652}$	Klein et al. (2016)
Skin resistance (s/cm)*	1.04, 2.29, 2.46	Estimated empirically with the use of 3% agar models	unpublished data
Skin type	1	wet-skinned	-
Air temperature (°C)	-	at 1 cm height	microclim dataset (Kearney et al. 2014)
Ground temperature (°C)	-	soil temperature at 0 cm height	microclim dataset (Kearney et al. 2014)
Solar radiation (W/m^2)	-	-	microclim dataset (Kearney et al. 2014)
Wind speed (m/s)	-	at 1 cm height	microclim dataset (Kearney et al. 2014)
Relative humidity (%)	-	at 1 cm height	microclim dataset (Kearney et al. 2014)
Posture	1	entire dorsal surface exposed to air	-
Proportion of ventral surface	1/3	a proxy proportion for an anuran in a water conserving posture	Klein et al. (2016)
Body heat capacity (J/g/°C)	3.6	default value	-
Delta	60	default value	-

*Values are reported for *L. fuscus*, *L. mystacinus* and *L. macrosternum*, respectively.

Suporting S4. Comparisons of T_bs from biophysical simulations and empirical field observations from biophysical agar replicas.

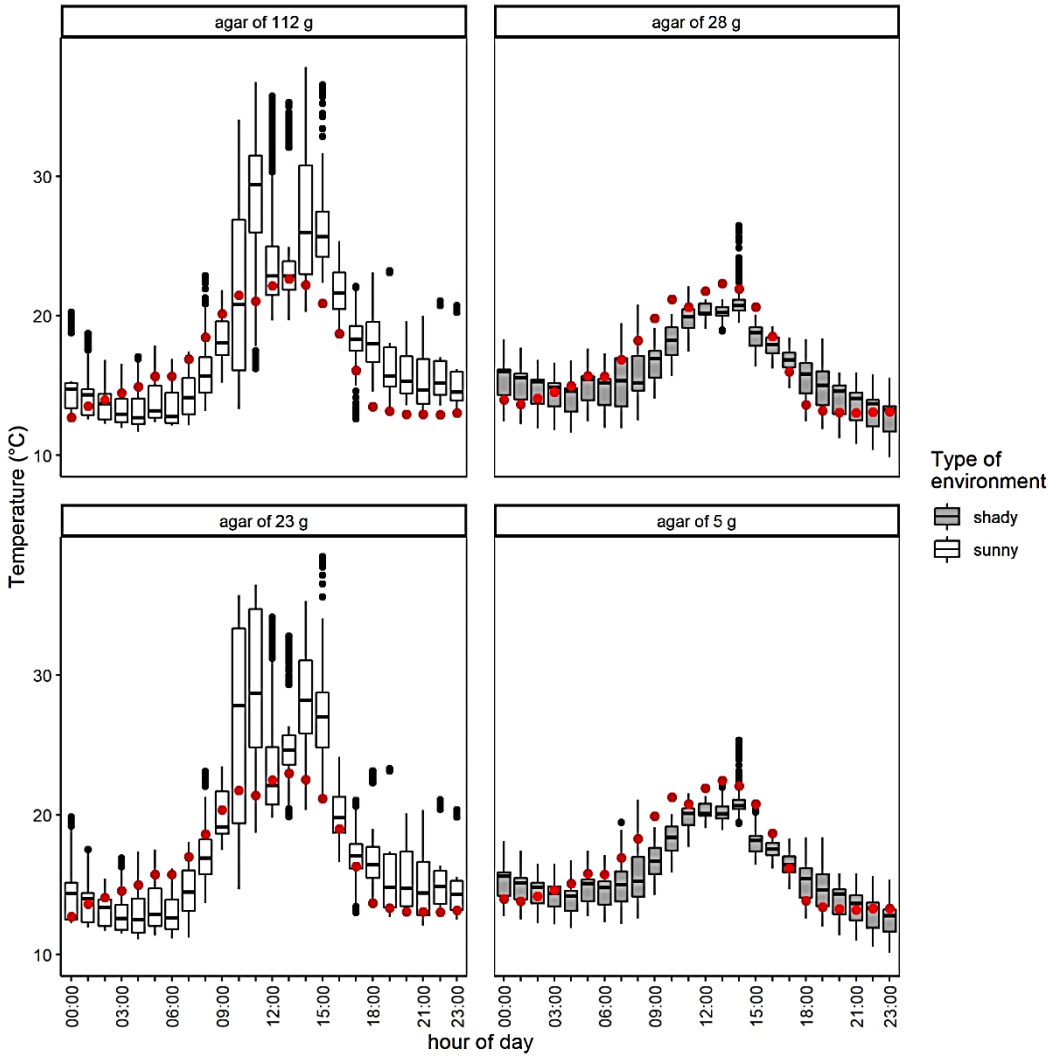

Figure S4.1. Hourly comparison of T_bs collected from agar replicas under field conditions (boxplots) and the T_bs predicted by the biophysical model for equivalent size hypothetical agars (red points). Agars of 23g and 12g deployed over sunny locations are indicated by white boxes, while agars of 5g and 28g were deployed in shady locations are indicated by grey boxes. Black points indicate outliers from field data observations.

Suporting S5. Evaluation between empirical and simulated evaporative water loss (EWL).

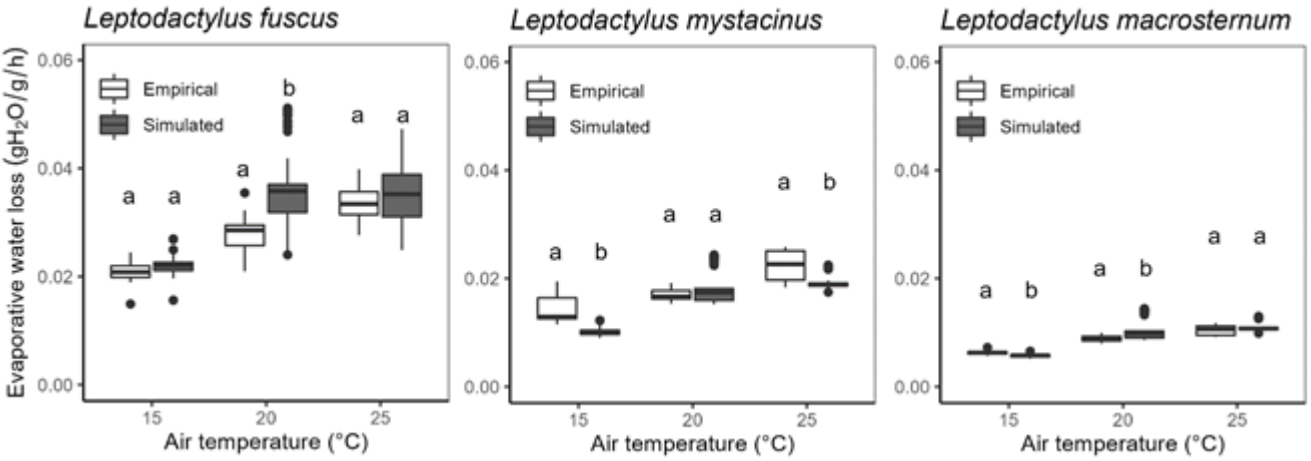

Figure S5.1. Empirical EWL comes from living frogs measured under laboratory conditions while simulated EWL corresponds to the computed EWL predicted by the biophysical model based on physical principles governing mass transfer for equivalent-sized hypothetical frogs. Same lowercase letters indicate a lack of significant differences (P > 0.05) between empirical and simulated EWL within each temperature.

Suporting S6. Nighttime frequency distributions of hours of restriction in activity.

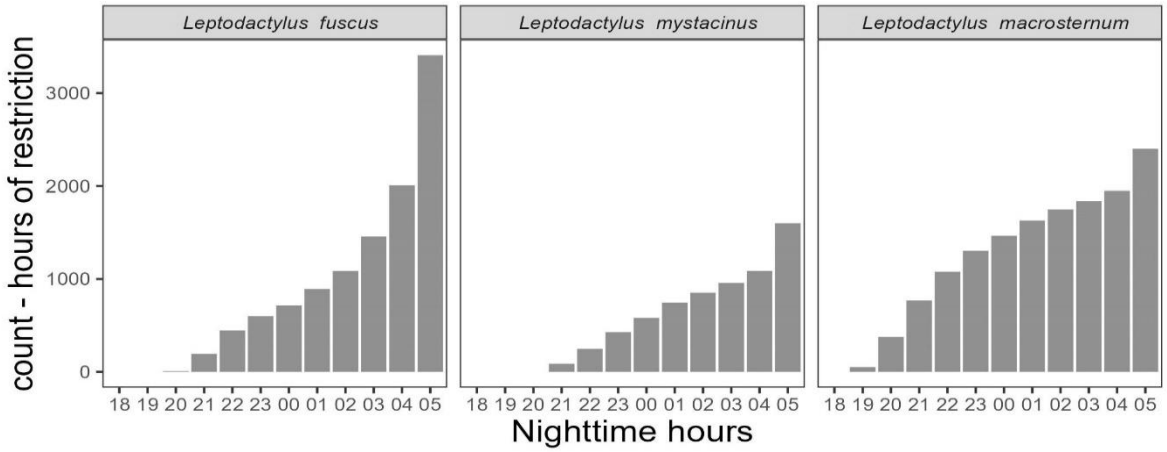

Figure S6.1. Frequency distribution of hours of restriction (Hr) in activity throughout nighttime hours. The Hr refers to locations where animals ceased surface activity because they reached their physiological endpoints (CT_{min} or EWL_{tol}). X-axis represents the whole nightly activity windows considered in our simulations (18:00 - 05:00 h), whereas Hr distribution only correspond to locations where restrictions in activity was detected.

Suporting S7. Body temperature frequency distributions from mechanistic modeling estimates.

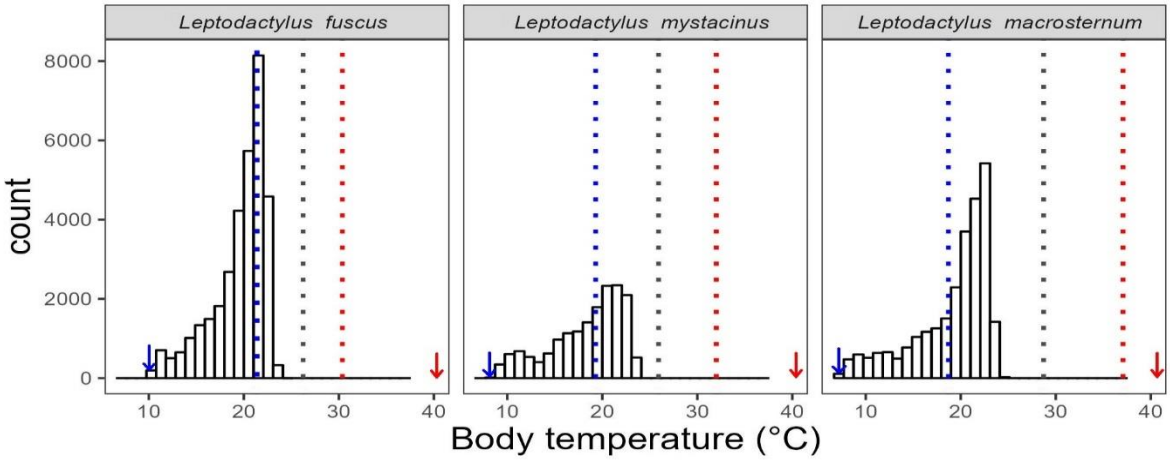

Figure S7.1. Body temperature (T_b) distributions correspond to predicted T_bs by the biophysical model only for surface active animals during the nighttime hours (temporal windows for activity). Vertical dotted lines indicate the optimal temperature for performance, T_{opt} (gray), and the B_{80} lower (blue) and upper (red) limits. Arrows indicate the critical thermal minimum (blue) and maximum (red). Maximum predicted T_bs were 24.1, 24 and 24.6°C for the respectively *L. fuscus*, *L. mystacinus* and *L. macrosternum*, while the minimum predicted T_bs equate their critical thermal minimum (CT_{min}) (see also Figure 1 in main text).

Suporting S8. Physiological constraint predicted for animals during daylight hours.

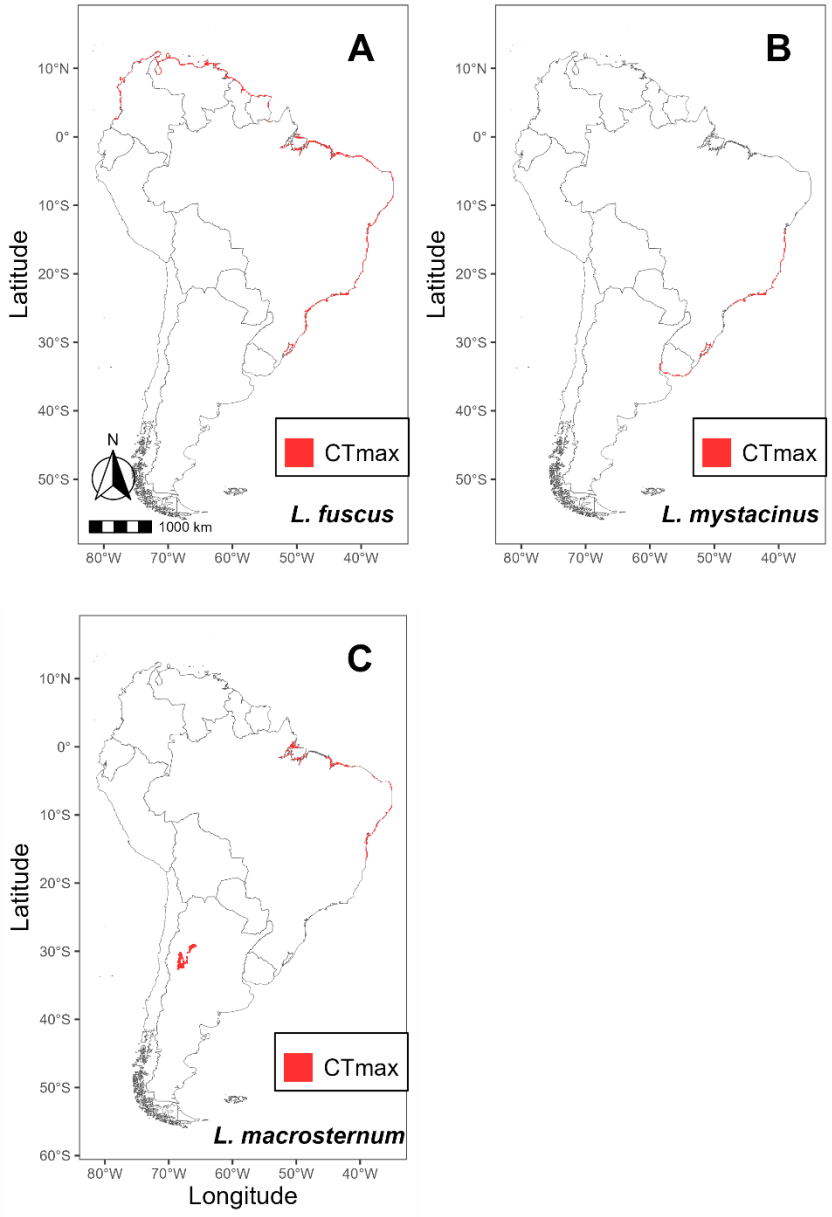

Figure S8.1. Indicated areas represent locations in which animals exceeded their physiological endpoint during daytime. In this case, physiological constraint was the sole function of the critical thermal maximum (CT_{max}). Note that during daytime, animals are assumed to be underground regufia (see main text).

SUPPORTING INFORMATION REFERENCES

Algar A. C., K. Morley and D. S. Boyd. 2018. Remote sensing restores predictability of ectotherm body temperature in the world's forests. *Global Ecology and Biogeography*, 27(12): 1412-1425.

Allouche O., A. Tsoar and R. Kadmon. 2006. Assessing the accuracy of species distribution models: prevalence, kappa and the true skill statistic (TSS). Journal of Applied Ecology, 43(6): 1223-1232.

Anderson R.C.O, R.P. Bovo and D.V. Andrade. 2018. Seasonal variation in the thermal biology of a terrestrial toad, *Rhinella icterica* (Bufonidae), from the Brazilian Atlantic Forest. *Journal of Thermal Biology*, 74: 77-83.

Araújo M. B. and M. New. 2007. Ensemble forecasting of species distributions. *Trends in Ecology and Evolution*, 22(1): 42-47.

Bakken G. S., W. R. Santee and D. J. Erskine. 1985. Operative and standard operative temperature: tools for thermal energetics studies. *American Zoologist*, 25: 933-943.

Barbet-Massin M., F. Jiguet, C. H. Albert and W. Thuiller. 2012. Selecting pseudo-absences for species distribution models: how, where and how many? *Methods in Ecology and Evolution*, 3: 327-338.

Eiter T. and H. Mannila. 1994. Computing discrete Fréchet distance. Technical Report CD-TR 94/64, Christian Doppler Laboratory for Expert Systems, Technical University Vienna, Austria,

Fielding A. H. and J. F. Bell. 1997. A review of methods for the assessment of prediction errors in conservation presence/absence models. Environmental Conservation, 24(1): 38-49.

Heikkinen R. K., M. Luoto, M. B. Araújo, R. Virkkala, W. Thuiller and M. T. Sykes. 2006. Methods and uncertainties in bioclimatic envelope modelling under climate change. *Progress in Physical Geography*, 30(6): 751-777.

Kearney M.R., A.P. Isaac and W.P. Porter. 2014. microclim: global estimates of hourly microclimate based on long-term monthly climate averages. *Scientific Data*, 1:140006.

Kearney M.R. and W.P. Porter. 2020. NicheMapR – an R package for biophysical modelling: the ectotherm and Dynamic Energy Budget models. *Ecography*, 43: 85-96.

Klein W., L. Dabés, V.M.G. Bonfim, L. Magrini and M.F. Napoli. 2016. Allometric relationships between cutaneous surface area and body mass in anuran amphibians. *Zoologischer Anzeiger - A Journal of Comparative Zoology*, 263: 45-54.

Magalhães F.M., Lyra M.L., Carvalho T.R., Baldo D., Brusquetti F., Burella P., Colli G.R., Gehara M.C., Giaretta A.A., Haddad C.F.B., Langone J.A., López J.A., Napoli M.F., Santana D.J., Sá R.O., Garda A.A. 2020. Taxonomic review of South American butter frogs: phylogeny, geographic patterns, and species delimitation in the *Leptodactylus latrans* species group (Anura: Leptodactylidae). *Herpetological Monographs*, 34: 131-177.

Navas C. A. and C. Araujo. 2000. The use of agar models to study amphibian thermal ecology. *Journal of Herpetology*, 34(2): 330-334.

O'Connor M. P. 2000. Extracting operative temperatures from temperatures of physical models with thermal inertia. *Journal of Thermal Biology*, 25: 329-343.

Pearson R. G., C. J. Raxworthy, M. Nakamura and A. T. Peterson. 2007. Predicting species distributions from small numbers of occurrence records: a test case using cryptic geckos in Madagascar. *Journal of Biogeography*, 34: 102-117.

Rubalcaba J.G., S.F. Gouveia and M.A. Olalla-Tárraga. 2019. Upscaling microclimatic conditions into body temperature distributions of ectotherms. *The American Naturalist*, 193(5): 677–687.

Spotila J. R. and E. N. Berman. 1976. Determination of skin resistance and the role of the skin in controlling water loss in amphibians and reptiles. *Comparative Biochemistry and Physiology A*, 55: 407-411.

CHAPTER III

THERMAL AND WATER BALANCE THROUGH ONTOGENY IN A NEOTROPICAL FROG AND ITS FORECASTED SENSITIVITY TO CLIMATE CHANGE

Luis M. Senzano[1], Denis V. Andrade[1]

[1]Laboratório de Biologia Experimental e Integrativa, Departamento de Biodiversidade, Universidade Estadual Paulista, Rio Claro, São Paulo, Brazil

ABSTRACT

Although the most dramatic changes in the biology of amphibians are indubitably associated to metamorphosis, even at the post-metamorphic stage many species can exhibit significant shifts in several functional attributes that can strongly impact their thermal biology and water balance throughout ontogeny. These changes are likely consequential not only to their contemporary pattern of habitat occupation but also to how they will respond to future changes in the environment, particularly those associated with global climate change. Here, we measured selected parameters relevant to the thermal biology and water balance in juveniles and adults of the Neotropical frog, *Leptodactylus macrosternum*. We then explored the potential consequences of these ontogenetic changes in determining the species vulnerability to climate changing conditions under present-day and future (2041-2060) ground-level microclimate scenarios, using biophysically based modeling techniques. Our mechanistic assessment suggests that juveniles may be particularly susceptible to experiencing more stringent constraints in activity than adults. This result was associated to the greater thermal sensitivity to colder temperatures exhibited by juveniles. However, the buffering capacity of refuge use against temperature extremes and desiccation may ameliorate these detrimental effects. Finally, our forecasting models indicates that *L. macrostenum* will face considerable contraction in their area of distributuion under future scenarios of climatic change, even though they may expand the occupation of some specific marginal areas of their current distribution. Our study points out the importance of considering thermal and water sensitivity through ontogeny in amphibians, and the importance of incorporating these changes as relevant functional attributes in the assessment of species to climate change.

INTRODUCTION

As ectotherms, most aspects of anuran physiological and behavioral processes are governed by environmental temperatures. Increases in body temperature (T_b), up to a certain level, enhance rate processes such as feeding, digestion, energy assimilation, and growth (reviewed in Wells 2007). Likewise, locomotor performance typically remains optimal at warmer temperatures, although it rapidly becomes disorganized if that optimal level is exceeded (Huey and Stevenson 1979). Despite the beneficial consequences of warmer conditions, water loss through evaporation increases with temperature, resulting in an important compromise between body temperature regulation and the maintenance of water balance. Indeed, amphibians are well known for being susceptible to excessive rates of evaporative water loss (EWL) given their usually highly permeable skin, which can lead to dehydration and all the deleterious consequences associated with it (O'Connor and Tracy 1992, Tracy et al. 1993). These considerations, combined with the fact that even minor changes in T_b and/or hydration state can lead to short-term reductions in performance capacity, underlie the central importance of adequately modulating the potential trade-offs between the regulation of body temperature and body water balance (Köhler et al. 2011).

The organismal sensitivity to changes in thermal and water conditions will vary as a function of body size, primarily because body surface area decreases relative to body volume as body size increases. This bears important implications for exchange processes that occurs across surfaces, such as heat exchange and water evaporation. Indeed, if smaller juveniles have similar skin resistance (R_s) to evaporation as adults, juveniles can be anticipated to experience higher mass-specific EWL, putting them at a greater risk of dehydration than adults (Gillis 1979, Degani and Warburg 1984). Differences in body size are also known to affect anuran locomotor performance (Wilson 2001, Enriquez-Urzelai et al. 2018) and critical thermal limits in some species (Cupp 1980, Navas et al. 2007, Enriquez-Urzelai et al. 2019, Ruthsatz et al. 2022, but see Enriquez-Urzelai et al. 2018). Thus, environmental constraints, particularly those related to the thermal and hydric attributes of the habitat, can be expected to interact with body size, resulting in varying levels of restriction as the animal's body size changes throughout ontogenetic growth.

There is a growing interest in how organisms will respond to the ongoing impacts of climate change. Climate change is not expected to affect all ontogenetic stages in the same manner. The morphological and physiological attributes of anurans throughout ontogeny (e.g., size changes during juvenile growth into adulthood) can result in differentiated responses to changes in

environmental drivers. For example, rising temperatures can restrict potential activity time in amphibians, and the magnitude of such constraint can be body size-dependent (Newman and Dunham 1994, Peterman et al. 2013). This may confer differential levels of exposure risks to ambient stressors between juvenile and adults, which can result in stage-specific susceptibility to climate change. Nocturnal behavior may buffer various species from threatening daytime temperatures; however, water loss is still an ongoing process capable of constraining activity even under conditions considered thermally suitable. Understanding the constraints and trade-offs regarding thermal and water balance regulation in different developmental stages will be central in identifying possible underlying mechanisms mediating anuran responses to climate change.

Here, we examine variations in thermal and water physiology emerged during the transitional stage from juvenile to adulthood in a model anuran, *Leptodactylus macrosternum*, and evaluate their potential consequences under projected changes in climate. This ground-dwelling frog exhibits nocturnal behavior and is widely distributed in tropical and subtropical regions of South America (Magalhães et al. 2020). Amphibians in this region are particularly vulnerable to climate-driven droughts (Lawler et al. 2009), and this region is expected to experience markedly warming trends and moisture reductions under future climate projections (Anjos et al. 2021). We hypothesized that projected warmer and drier conditions will exert constraining effects on the activity time in both juvenile and adult frogs, but these constraints may have larger effects on juveniles due to the physiological constraints associated with their smaller body size. To address this hypothesis, we experimentally collected physiological information on thermal, hydric, and performance attributes of juvenile and adult members of *L. macrosternum*. We then integrated this information via a biophysical model (Rubalcaba et al. 2019a) into the hourly ground-level conditions for present day and future microclimates (2041-2060) (CMIP6, Erying et al. 2016) through a microclimatic modeling procedure (Kearney and Porter 2017). This procedure enabled us to quantify ontogenetic-specific activity budgets, shifts in present-day and future habitat suitability, and ultimately, the ontogenetic-specific vulnerability to climate change.

METHODS

Animal collection and laboratory housing conditions

Field searches were conducted during the hot, rainy season (March) of 2022 in the municipality of Barbosa (21°15'01" S, 49°54'53" W, 371 m a.s.l.), São Paulo, Brazil. We searched for active animals at night between 07:00 and 00:00 h. Observed animals were captured by hand and their field body temperature (T_{field}) immediately recorded with a quick-reading digital thermometer (Incoterm, model 6132, 0.1°C accuracy) inserted into de cloaca. At the time of capture, we also recorded substrate temperature of animal's site collection with a hand-held infrared thermometer (62 Mini IR, Fluke; 0.1°C accuracy), and the temperature and relative humidity of air 1 cm above ground with a psychrometer device (PCE-320, PCE Instruments, accuracy 0.1%). Animals were then put into individual plastic containers and taken to the laboratory of animal physiology at the university of at the São Paulo State University (Rio Claro, SP, Brazil).

In the laboratory, all animals were kept individually in plastic boxes (40×30×25 cm) with free access to water and shelter. Air-conditioned room temperature was maintained at 24-26°C and a photoperiod set by natural light from a large glass window. Animals were fed once weekly on mealworms (*Tenebrio* sp.), allowing a fasting period of 4 d before any experimental trial. Animal collection was issued by the Instituto Chico Mendes da Conservação da Biodiversidade, Brazil (JCMBIO- MMA, no. 22028-1) and procedures and experimental protocols herein described are already approved by the UNESP-IB/Rio Claro Animal Ethic and Committee (Comissão de Ética no Uso Animal, CEUA; protocol no. 5909, approval no. 27/2019).

We collected a total of 20 frogs that were classified as either juvenile or adult based mainly on their body size, as this was the most obvious morphometric characteristic for age discrimination among individuals. Small frogs with body masses lower than 15g and 57 mm snout-vent length (SVL) were considered juveniles, whereas larger frogs (>40 g body mass and 72 mm SVL) were considered fully mature adults. Hence, we distinguished a total of 13 juveniles (mean ± s.d. of 11.33 ± 2.8 g body mass; 49.26 ± 3.52 mm SVL) and 7 adults (53.25 ± 7.28 g body mass; 80.97 ± 4.2 mm SVL). The lack of information on morphological diagnostic features for sexual dimorphism throughout ontogeny in this species prevent us from making reliable sex discrimination on juveniles and, for this reason, we did not discriminate sex within age classes.

Experimental protocols

We first determined the T_{pref} between 48 to 96h after the arrival of animals to the laboratory, in which Individuals chosen at random were measured each day with the use of custom-made thermal gradients. After this, we determined the locomotor performance at 6 temperatures levels (10, 15, 20, 25, 30 and 35°C), selecting a daily temperature in random order. Both T_{pref} and locomotor trials were conducted at night, between 18:00 and 11:00h. After the completion of this first series, animals were allowed to rest four days for recovery and feeding. We then proceeded to determine EWL and WU measurements, both determined on different days. We finally determined the dehydration tolerance (EWL_{tol}), CT_{min}, and CT_{max}, all measured in separate days at least three days apart and in this same order. The EWL, WU, EWL_{tol}, CT_{min} and CT_{max}, were determined during the daytime, between 09:00 and 17:00h.

Before experimental trials, all animals were put individually inside plastic containers (7x14x10 cm) containing dechlorinated tap water and remained inside a climatic chamber BOD (Eletrolab®, São Paulo, SP, Brazil; model EL101/2RS) for 2 hours. After this period, they were removed from cages and induced to urinate by gently pressing their abdominal region. Finally, they were blotted with paper tissue and weighed with a high-precision balance (0.0001g accuracy, model AR2140, Ohaus Adventurer). These procedures ensured that animals were fully hydrated and thermal equilibrated at the target experimental temperatures at the beginning of trials. Except for locomotor performance that was assessed at 6 temperature levels (see above), all physiological measurements used 25°C as the acclimation starting temperature. Animals were chosen at random for trials, but care was taken to ensure that both juveniles and adults were consistently represented throughout daily measurements. Individuals were subjected to just one experimental trial per day, and in cases of unsuccessful attempts (e.g., excessive animal movement during EWL measurements or animals that jumped out of the arena during locomotor trials), the data was discarded, and the individual was tested again in a different day.

Physiological measurements

The protocol for the laboratory physiological measurements were similar to those described earlier (see Chapter one), but here we describe them briefly. The T_{pref} was determined in a custom-made cylindrical thermal gradient made of steel sheets (60 cm height, 65 cm diameter) placed on top of a copper sheet covered with a black non-woven fabric. A heat source (THG Heat Inc.; heat tape THG 4") at one end, and a set of frozen synthetic ice packs (17x2.5x9.5cm) on the opposite

side generated thermal gradient ranging from 7 to 38°C. The arenas' floor was periodically sprayed with water to allow a uniform distribution of moisture. Animals were released in the middle portion of the thermal gradient and were left undisturbed for 2h in the darkness. After this period, frog's cloacal temperature was measured with a digital thermometer (Incoterm Industry Ltda, Porto Alegre, RS, Brazil, model 6132, 0.1°C accuracy), assuming this measure as the frog´s preferred body temperature.

Locomotor performance was determined from jumping measurements conducted in a 5-m long by 1 m wide jumping arena built with plywood boards settled in an air-conditioned room. Acclimated animals at the test temperature (see experimental protocols) were taken from the climatic chamber one at a time, blotted with paper tissue while inducing urination, and released at one end of the arena. Animals were allowed to jump 5 consecutive times, while we manually marked the location of jump landings with a piece of chalk. Immediately after this, animals' cloacal temperature was recorded with the digital thermometer. The length of each jump was measured with a steel tape measure (model FLF519, Uyustools) from the distance between chalk marks. Based on individuals' longest distance jumped at each test temperature we produced thermal performance curves (TPC) and extracted their optimal temperature for locomotion (T_{opt}) and their thermal performance breadth (B_{80}; the range of T_bs across which jumping ability remains at least 80% of its maximum capacity) (Supporting S1).

Rates of EWL were determined by using an open flow-through system settled inside a climatic chamber BOD (same as above) set at 25°C. The system consisted of a sealed acrylic chamber with an inlet port at the top connected to a mas flow controller (Sable Systems International, Inc., Las Vegas, NV, USA; model SS-4 Subsampler) and to a silica-filled chamber that removed room air humidity before passing through the chamber. A dry airflow was pumped at 21.6 cm^3/s through the inlet port, and an RH analyzer (Sable Systems International, Inc., Las Vegas, NV, USA, model RH-300) connected to an outlet port continuously monitored the RH leaving the chamber, with data being digitally recorded via a U/I unit (Sable Systems International, Inc., Las Vegas, NV, USA; model UI-2). Animals were transferred to the acrylic chamber and were left undisturbed until obtain a minimum of 15 min of steady-state RH recordings after 1 hour of initiated the trial. After a successful trial, we immediately measured the dorsal skin temperature using an infrared thermometer (62 Mini IR, Fluke, 0.1°C accuracy). Baseline measurements with the empty chamber were collected before and after any trial. Area-specific rates ($\mu gH_2O/cm^2/s$) were calculated by

dividing the absolute EWL ($\mu gH_2O/s$) obtained from measurements by the proportion of body surface area exposed to air (Supporting S2). To estimate the skin resistance (R_s) to evaporation from both juveniles and adults, we used the same EWL measurement protocol but applied to equivalent-sized biophysical models made of 3% agar solution that lose water freely while mimicking the shape and size of living animals (refers to Supporting S2 for further details).

The WU was determined as the water absorption capacity through the pelvic patch. At the beginning of each trial, fully hydrated animals were weighed with the high-precision balance (described above) with their urinary bladder emptied, and then were exposed to a desiccating procedure within a wind tunnel settled inside the climatic chamber BOD set at 25°C. Wind tunnel consisted of a piece of polyvinyl chloride (PVC) pipe (10 cm diameter, 20 cm length) arranged horizontally in front an electric fan that blew room air at a constant rate of 3.8 m/s (Kestrel® Instruments, Boothwyn, PA, USA; wind meter model: Kestrel 3000). Animals were removed from wind tunnels when they lost 10% of their initial fully hydrated mass and were transferred to another plastic container containing about 0.5 cm deep water. At 2-min intervals, animals were removed, blotted with paper tissue, and weighed, repeating this procedure six consecutive times. We calculated area-specific WU rates ($\mu gH_2O/cm^2/s$) from the regression slope of body mass gained against rehydration time, divided by one-third of frog´s total skin surface (described above), a surface proportion that represents the ventral region in direct contact with water.

Dehydration tolerance was determined by exposing animals to the same dehydrting procedure previously described for WU trials, but this time animals were allowed to dehydrate until the point of rightning reflex loss when flipped on their back (Gillis 1979). At this point, animals were reweighed again, and the dehydration tolerance was calculated as the percentage (%) of body mass lost relative to the frog's fully hydrated body mass.

For determining critical thermal minimum (CT_{min}) and maximum (CT_{max}), thermally acclimated animals at 25°C (see experimental procedures) were gradually cooled (CT_{min}) or heated (CT_{max}) with a programmable BOD climatic chamber at a rate of 1°C/10 min until frogs were unable to right themselves within 10 sec after being flipped (rightning reflex loss). At this point, animals' cloacal T_b was measured with a quick-reading digital thermometer (Incoterm Industry Ltda, Porto Alegre, RS, Brazil, model 6132, 0.1°C accuracy), assuming this measure as the animals' critical thermal limits. We always measured CT_{min} before CT_{max}, three days apart.

Mechanistic forecasting

Microclimate data for present-day and future climates

Present-day and future microclimates were built based on the microclimate model available in the 'NicheMapR' r-package (Kearney and Porter 2017). Present-day microclimates were generated using the '`micro_global`' function of the NicheMapR package, which can estimate hourly profiles of ground-level conditions derived from coarse monthly climatology (1961-1990), such as mean temperature and temperature range, wind speed, relative humidity, cloud cover, precipitation, and elevation (New et al. 2002). We generated 24-h profiles of 1 cm air temperature, wind speed, relative humidity, solar radiation, and substrate and underground (5 cm depth) temperatures at a 15 km spatial resolution for an average day of each month. All these microclimatic variables were generated under different shading conditions (0, 25, 50, 75 and 90% shade). To forecast future microclimates, we obtained monthly maximum and minimum temperatures and precipitation for 2041-2060 (5 arc-min spatial resolution) from a future global climate model (GCM = ACCESS-CM2) of the CMIP6 project (Erying et al. 2016) under an intermediate emission scenario (SSP3-70) available at the WorldClim Database (http://www.worldclim.org/). Future temperature and precipitation data were resampled to 15 km resolution using bilinear interpolation, and the resulting output was used as input to generate a new global climate database (detailed in Kearney and Porter 2017) with the use of the '`build.global.climate`' function in the 'NicheMapR' package. We re-run the '`micro_global`' function with this new global climate database to downscale future climatology from monthly averages into hourly estimates of future microclimates as previously done for present-day. We run future microclimatic estimates five times, each time assuming a different shading condition (0, 25, 50, 75 and 90% shade).

Our species exhibit a wide distribution (Magalhães et al. 2020) spanning from closed-canopy forests in the south (the Atlantic Forest biome) to open habitats in its northern distribution (the Catinga biome). For this reason, we assigned cell-specific values of shading conditions for present-day and future microclimates. To do so, we resampled a 30-m tree cover map (Hansen et al. 2013) to 15 km resolution, and the continuous output (0 to 100%) was reclassified into five canopy classes: 0% canopy cover (0-20%), 25% canopy cover (21-40%), 50% canopy cover (41-60%), 75% canopy cover (61-80%) and 90% canopy cover (81-100%). We overlapped this discretized canopy map to rasterized versions of present-day and future microclimates, and then we decomposed grid rasters into individually cell-based layers, each cell layer containing all possible combinations

of shading conditions for each monthly day. Finally, we derived new microclimate rasters assigning each grid cell to its best-fitting shading condition (based on the canopy map) so that it only retained its most representative values of microclimate conditions assuming either 0%, 25%, 50%, 75% or 90% canopy shade. We used the same tree cover data for present-day and future microclimates for comparative and methodological consistency.

Aside from differences in vegetation structure, a second issue arises because of the potential for phenological variations in activity in this species. For example, the activity period of *L. macrosternum* differs between its southern and northern distributions, beginning in December in the former (Prado et al. 2000) and May in the latter (Gondim 2021, Chaves et al. 2021), coinciding with the rainy months in these regions (Alvarez et al. 2014). To account for this phenological pattern, the activity period in each grid cell was limited to the wettest month, which may also be the best time of year for frogs to be active. To do this, the microclimate rasters were once decomposed (using a similar process to that described above for canopy shade), but this time, just the month with the greatest value of average RH (assumed to be the wettest month) was maintained at each location.

Biophysical modeling and environmental restrictions

To evaluate the species at the microhabitat scale, we solved the expected inflows and outflows of heat energy expected for animals' T_b with the use of the biophysical model described in Rubalcaba et al. (2019a). This biophysical model computes the heat and water exchanges of an ectotherm model with its inmediate microclimate to derive core body temperature estimates, and it has been suscefully used in both reptiles (Rubalcaba et al. 2019a, Rubalcaba et al. 2019b) and amphibians (Greenberg and Palen 2021, see also Chapter 2). We calculated the hourly T_b distribution for a theoretical 11 g juvenile and 57 g adult *L. macrosternum*, and the biophysical model's input parameters were based on age-specific values of morphological, physiological, and performance attributes (Supporting S3).

We simulated simple behavioral responses of activity (inactive or active states) based on thermal and hydric thresholds bounding temperature-dependent probabilities of activity dictated by the organismal performance capabilities (derived from empirical TPCs). As the frogs are nocturnal, we allowed the possibility of surface activity across all nighttime hours (18:00 - 05:00 h) and assumed an inactive state (i.e., a sheltered animal) during the daylight hours (06:00 - 17:00). Based on the burrow characteristics of other *Leptidactyluys* congeners (Solano 1887, Silva and Giaretta 2008,

Martins 1988, Oliveira-Filho and Giaretta 2008) we assumed animals to be 5-cm deep and fully hydrated when sheltered. The hourly substrate temperature 5 cm below surface was used as a proxy measure for sheltering T_bs since animals may attain thermal equilibrium with their shelter (see Smits 1984). During activity, we set the lower (B_{80} lower) and upper (B_{80} upper) limits of the B_{80} as the T_bs between which animal's performance is optimal (Huey and Stevenson 1979), and thus they are always surface active (100% probability of activity), whereas CT_{min} and CT_{max} were the critical thermal limits at which animals cease activity due to locomotor impairment (0% probability of activity). Beyond the B_{80} limits but between CT_{min} and CT_{max} thresholds, we adopted a continuous transitional model following the descending portions of empirical TPCs, which resulted in a smoothly model describing animals' probability of activity (Gunderson and Leal 2016). We incorporated hydric constraints on activity by computing the hourly cumulative EWL (gH_2O/h) starting from shelter emergence (assuming fully hydration) until it was equivalent to the animals' dehydration tolerance (EWL_{tol}), assuming no further activity beyond this point. Hence, regardless of T_b and hydration state, surface activity could be curtailed anytime if animals experienced harmful temperatures (CT_{min} or CT_{max}), chronic hydric deficit (EWL_{tol}) or it was no longer nighttime. We also removed grid cells where frogs exceeded their CT_{min} or CT_{max} when sheltered (either day or night), as we assumed no viable populations in these locations in the context of our simulations.

To forecast the potential consequences of climate warming on animals, we computed the hours of restrictions in activity (Hr), a metric that measures the length of nighttime hours when ambient conditions exceed animal's physiological limits. The Hr is based on the rationale that declines in foraging activity eventually leads to energy imbalances, which impair ecological functions such as growth, reproduction, and fitness (Ceia-Hasse et al. 2014, Garcia et al. 2019). As a complementary approach, we produced suitability maps for present-day and future microclimate scenarios as a function of age-specific thermal, water and performance traits. This was accomplished by first producing separate suitability maps of temperature (derived from the temperature-dependent probabilities of activity) and water (based on the potential for water loss dehydration) (see details on Supporting S4). These maps were then overlaid to produce a derived map representing the overall habitat suitability for present-day and future scenarios as a function of age-specific thermal requirements and water needs, with scores ranging between 0 in locations where activity is impeded due to thermal or hydric restrictions, and 1 where animals can maintain an optimal range of T_bs while maintaining a good hydration level. This approach allowed us to better evaluate age-specific projected changes in the geographical extent of suitable habitats and potential

distributional shifts. For proper visualization, we additionally mapped predicted distributional shifts into three categories: (i) contraction areas (future lost areas respective to current distribution), (ii) expansion areas (future gained areas respective to current distribution) and (iii) unchanged areas (areas occupied by the species currently and in future projections).

Statistical analysis

Before all analysis, we checked for distribution assumptions of normality and homoscedasticity using the Shapiro-Wilk and Levene tests, respectively. Because body mass effects on EWL was significant ($p = 0.039$), we used one-way ANCOVA analysis to evaluate differences in EWL, with age (juveniles vs. adults) as an independent factor, body mass as a covariate, and EWL as the response variable. For the reminder parameters (T_{pref}, T_{opt}, R_s, WU, EWL_{tol}, CT_{min} and CT_{max}), in which body mass influence was not significant ($p > 0.05$), we used unpaired *t*-test to identify differences between juveniles and adults. All analyses were performed in R (v3.3.6; http://www.R-project.org/) employing RStudio (v1.2.5033; http://www.rstudio.com/). In all cases, a significant level of $p < 0.05$ was used. Unless otherwise stated, all values are presented as means ± SD (standard deviation).

RESULTS

Physiological parameters

Juveniles exhibited a significantly higher T_{field} than adults ($t_{(15)}$ = 2.32, P = 0.03; Fig. 1 A), but they did not differed on their T_{pref} ($t_{(18)}$ = 1.65, P = 0.116; Fig. 1B). On the other hand, T_{opt} for locomotion was higher on adults ($t_{(18)}$ = -2.24, P = 0.038; Fig. 1C) (see Table 1). The CT_{min} was significantly lower in juveniles than adults ($t_{(18)}$ = 4.72, P < 0.001; Fig. 1D), but they did not differ in their CT_{max} ($t_{(17)}$ = -1.88, P = 0.076; Fig. 1E). Rates of EWL were significantly greater in juveniles than adults ($F_{(1,17)}$ = 36.17, P < 0.001; Fig. 2A), which was accompanied with a lower R_s in the juveniles ($t_{(18)}$ = -2.66, P = 0.016; Fig. 2B). Juveniles tolerated higher levels of EWL_{tol} than adults ($t_{(18)}$ = -4.59, P < 0.001; Fig. 2C), and they also had a higher capacity for rehydration than adults ($t_{(18)}$ = 5.95, P = 0.02; Fig. 2D).

Mechanistic forecasting

When forecasting the consequences of climate change on the hours of restrictions (Hr) in activity, our mechanistic model predicts for juveniles a mean Hr of 6.06 hours (SD = ± 3.46 hours) and 6.42 hours (SD = ± 3.32 hours) for the present-day and future scenarios, respectively (Fig. 3). Adults had comparatively lower values of Hr than juveniles, with a mean Hr of 5.16 hours (SD = ± 2.69 hours) and 5.03 hours (SD = ± 3.32 hours) for the present-day and future scenarios, respectively (Fig. 3). Mechanistic models show the most suitable habitats for both adults and juveniles near the coast, but also in the northermost parts for adult frogs (Fig. 4A, 4B). Suitability forecasts for the period 2041-2060 remained similar respective to present-day for both juveniles and adults (Fig. 4C, 4D), although some areas in the central regions showed a contraction trend for both juveniles (5.7%) and adults (1.72%) (Fig. 4E, 4F). However, mechanistic models also predict the potential colonization of new areas for both juveniles (3.7%) and adults (0.86%), with most of it concentrated in their southern distributions (Fig. 4E, 4F).

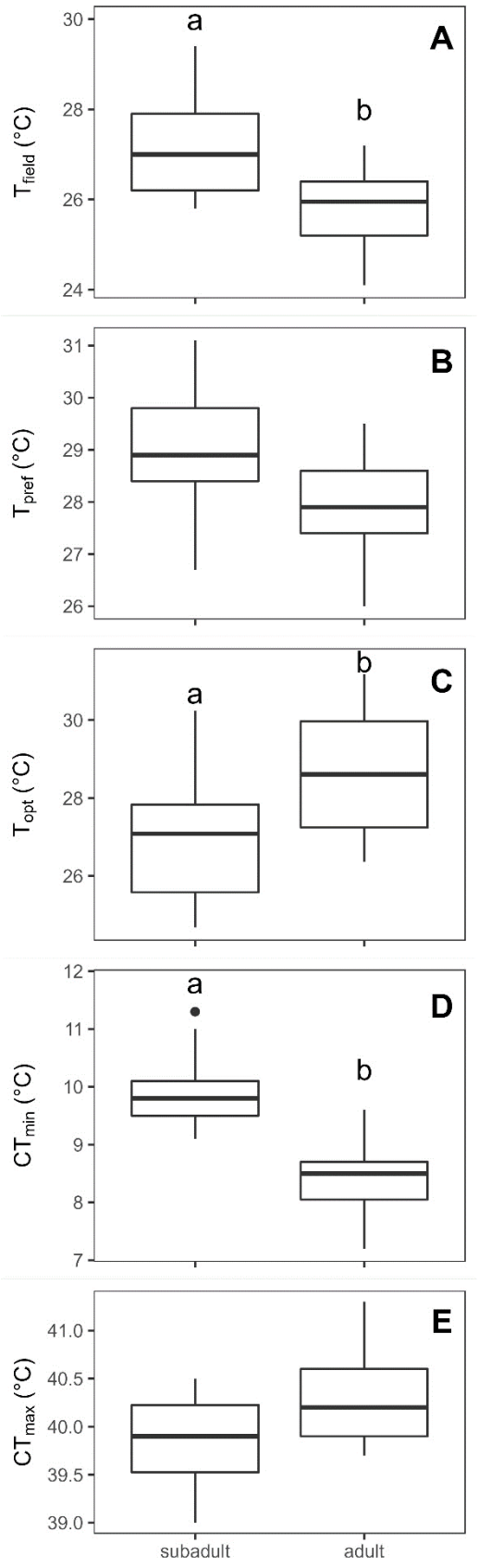

Figure 1. Field body temperature (T_{field}; **A**), preferred body temperature (T_{pref}; **B**), optimal temperature for locomotion (T_{opt}; **C**), critical thermal minimum (CT_{min}; **D**), and critical thermal maximum (CT_{max}; **E**) of juvenile and adult *L. macrosternum* frogs. Different lowercase letters indicate a statistically significant difference between groups. Boxplot lines indicate medians, the lower and upper borders represent the 25th and 75th percentiles, whiskers are the minimum and maximum range values.

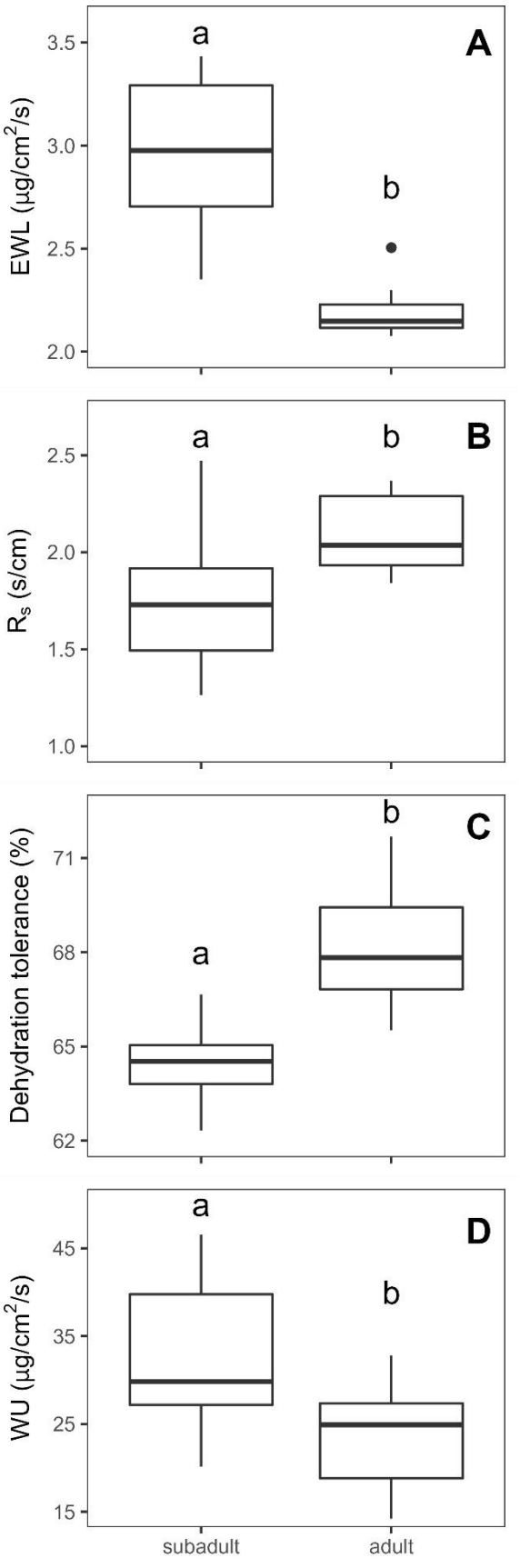

Figure 2. Evaporative water loss (EWL; **A**), skin resistance to evaporation (R_s; **B**), dehydration tolerance (**C**), and water uptake (WU; **D**) of juvenile and adult *L. macrosternum* frogs. Different lowercase letters indicate a statistically significant difference between groups. Black point indicates an outlier observation.

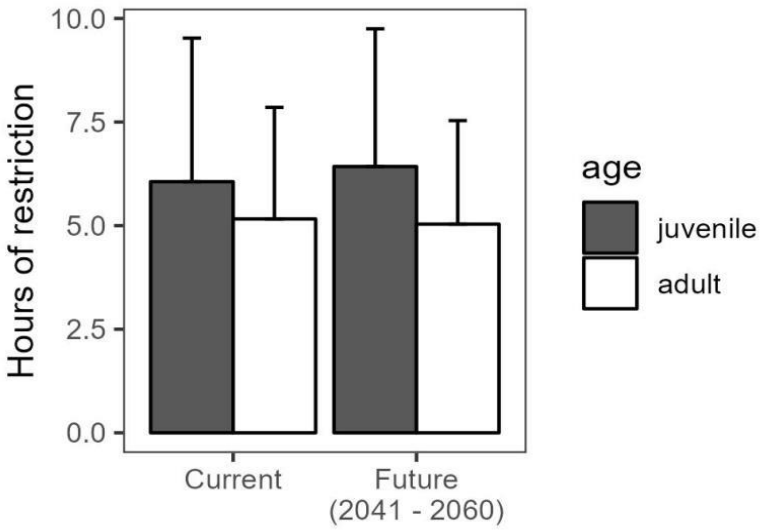

Figure 3. Hours of restriction in activity throughout nighttime hours for juveniles and adults of *L. macrosternum*. Bar charts indicate the mean ± the standad deviation (s.d.).

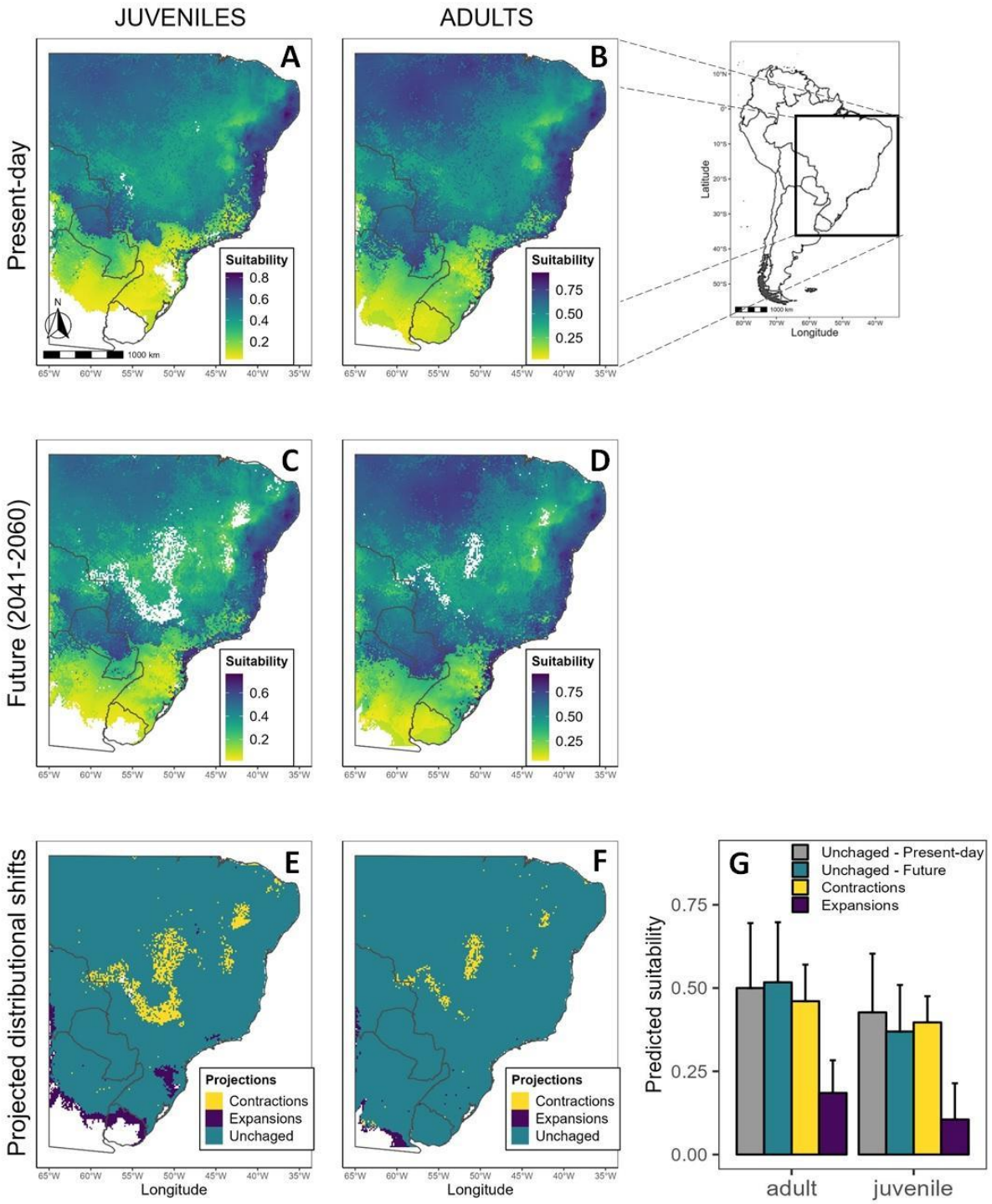

Figure 4. Overall habitat suitability for present-day (A, B) and future scenarios (C, D) as a function of age-specific thermal requirements and water needs. Panels E and F show predicted distributional shifts of contractions, expanstions and unchaged areas respective to present-day distributions of *L. macrosternum* juveniles and adults. Panel G shows the predictive suitability expected to each distributional shift category.

Table 1. Summary of the physiological traits determined for juveniles and adults of *L. macrosternum*. Evaporative water loss (EWL); skin resistance (R_s); dehydration tolerance (EWL_{tol}); water uptake (WU); Field body temperature (T_{field}); preferred body temperature (T_{pref}); optimum temperature for locomotion (T_{opt}); lower end of thermal performance breadth (B_{80} lower); upper end of thermal performance breadth (B_{80} upper); critical thermal minimum (CT_{min}); critical thermal maximum (CT_{max}).

trait	unit	N	mean	s.d.
Juveniles				
EWL	$\mu gH_2O/cm^2/s$	13	2.96	0.35
R_s	s/cm	13	1.74	0.32
EWL_{tol}	%	13	64.14	1.72
WU	$\mu gH_2O/cm^2/s$	13	31.18	9.84
T_{field}	°C	11	27.19	1.24
T_{pref}	°C	13	28.92	1.36
T_{opt}	°C	13	26.09	1.99
B_{80} lower	°C	13	19.87*	
B_{80} upper	°C	13	32.94*	
CT_{min}	°C	13	9.96	0.68
CT_{max}	°C	12	39.85	0.49
Adults				
EWL	$\mu gH_2O/cm^2/s$	7	2.20	0.15
R_s	s/cm	7	2.09	0.22
EWL_{tol}	%	7	68.22	2.20
WU	$\mu gH_2O/cm^2/s$	7	23.46	6.64
T_{field}	°C	6	25.78	1.1
T_{pref}	°C	7	27.92	1.16
T_{opt}	°C	7	28.65	1.76
B_{80} lower	°C	7	18.98*	
B_{80} upper	°C	7	35.34*	
CT_{min}	°C	7	8.40	0.75
CT_{max}	°C	7	40.31	0.56

Asterisks represent trait unique (not mean) values derived from the age-specific performance functions described on Supporting S1.

DISCUSSION

Postmetamorphic variations in body size may have important implications in the vulnerability of amphibians to climate warming. Here, we showed that some parameters related to the thermal and water physiology of *L. macrosternum* frogs undergo ontogenetic size changes, and these differences affected the projected species distributions under changing climatic conditions. Our results also show that juveniles may be particularly susceptible to experiencing more stringent constraints in activity than adults due to their greater thermal sensitivity to colder temperatures.

Ontogenetic changes in thermal and water balance traits

We found that juveniles of *L. macrosternum* exhibited higher values of T_{field} than adults, which agrees with some previous reports in other anuran species (Smits 1984, Navas et al. 2007, Sanabria et al. 2003, 2013; but see Carey 1978). The tendency for selecting warmer temperatures by juvenile anurans has been suggested as a thermoregulatory response aiming digestive efficiency, faster ontogenetic development and/or the promotion of locomotor performance (Lillywhite et al. 1973, Carey 1978, Tracy et al. 1993, Browne and Edwards 2003, Goldstein et al. 2017). Thus, any thermal gain as a result of an elevated T_{field} may translate into thermal benefits as long as body hydration do not become an issue (O'Connor and Tracy 1992, Tracy et al. 1993). Under laboratory conditions, however, T_{pref} remained similar between age classes, although juveniles' T_{pref} was on average 1°C warmer than that of the adults. A similar lack of T_{pref} difference between juveniles and adults is also reported for the European frog, *Rana temporaria* (Enriquez-Urzelai et al. 2018). However, simultaneous comparisons of T_{pref} between juvenile and adult anurans are virtually absent in the literature, which preclude broad generalizations to be made. In the specific case of *L. macrosternum*, the evidence points out that, since T_{pref} did not vary considerably, the differences in T_{field} might be related to the influence of body size, especially differences in volume to surface ratios, to heat exhcnnge dynamics, or differences in micro-habitat selection driven by other, non-thermal, factors.

Adults of *L. macrosternum* exhibited a higher T_{opt} (28.65°C) than juveniles (26.09°C), however, the T_{opt} of the later was closer (1.1°C) to their T_{field} (27.2°C) whereas adults' T_{opt} exceeded by about 3°C their T_{field} (25.8°C). This indicates that under nautral settings, juveniles seem to operate at T_bs that approximate their peak performance, whereas adults do not. Based on field and laboratory observations, some previous reports showed that T_bs of some species' tadpoles and juveniles tend to match the range of temperatures at which optimal locomotor performance is promoted

(O'Connor and Tracy 1992, Tracy et al. 1993, but see Sanabria et al. 2015) and the closeness beween T_{opt} and T_{field} observed in juvenile *L. macrosternum* reinforce these observations. During the juvenile stage, juveniles tend to be active foragers (Lima and Magnusson 2000), are more vulnerable to predation, and hence more likely to engage in locomotory escape behaviors (Wassersug and Sperry 1977, Heinen and Hammond 1997, Vonesh 2005). Furthermore, they are often regarded as the primary long-distance dispersers in anuran populations (Pittman et al. 2014). As such, a T_{field} that would allow juveniles to maximize their jumping abilities might be particularly helpful in supporting these ecological locomotory activities. In the case of adults, their peak performance occurred well above their T_bs exhibited in the field. Adult anuran T_{field} has found to match the maximal capacity for locomotion in some species (Putnam and Bennett 1981) but not in others (John-Alder et al. 1988).

Variations in thermal traits throughout ontogeny presumably reflect changing physiological requirements in response to environmental drivers as maturation occurs, and different physiological processes can exhibit differences in thermal optima (reviwed by Sinclair et al. 2016). In this sense, the T_{field} of adult *L. macrosternum* may reflect tradeoffs in thermal optima in which other thermally dependent functions may be favored at the cost of suboptimal temperatures for peak jumping performance. The suboptimality of T_{field} for promoting peak performance on adults might not necessary be interpreted as detrimental, as the range of temperatures over which 80% of maximal performance (i.e., the B_{80} lower and upper limits) still overlaping the range of T_{field} exhibited by both juveniles and adults (see Table 1). Finally, there might be other ecologically relevant drivers affecting habitat selection by juveniles and adults and that are not directly related to locomotor performance and/or temperature, among which the most prominent is likely the ennngagment in reproductive activity by the adults. The availability of reproductive partners, calling activity, mating, territorial disputes, pre and post-copulatory behaviors are all crucial components for the adult stage that might influence the attainment of T_{pref} under natural settngs.

Age classes differed on their CT_{min}, but not on their CT_{max}. In general, anurans exhibit a tendency for conservatism in CT_{max} and a relatively higher lability in CT_{min} (Pintanel et al. 2019, Bodensteiner et al. 2021) and our results conform to this pattern. However, the influence of ontogenic size variation on thermal tolerance has been explored in very few species and still remains uncertain. Depending on the species, CT_{max} is reported to be higher in adults (Cupp 1980, Sherman 1980), in juveniles (Cupp 1980, Navas et al. 2007) or no difference has been found between them, as in our

case. The situation of CT_{min} is even worse, since CT_{min} comparisons between juvenile and adults are virtually non-existent in the literature. Although it has been hypothesized that juveniles of some freeze tolerant frog species in temperate regions may be less cold-tolerant than adults (Storey and Storey 1985), this may not be comparable to our results as most of the physiological processes against freezing generally occurs at sub-zero temperatures (for review see Storey and Storey 2017), and *L. macrosternum* frogs only inhabit tropical and subtropical regions. Thus, the mechanisms underlying the lower cold tolerance of *L. macrosternum* juveniles remain uncertain and comparisons are difficult because of the non-existence data on tropical anurans.

As expected, rates of EWL were greater in juveniles than adults. This implies that juveniles should experience faster dehydration rates than adults, hence minimising EWL must be proportionally more relevant for the small-sized juveniles. Water economy through increased R_s is known to occur among different anuran species, particularly those differing in habitat preference (Young et al. 2005, Tracy et al. 2010), but reports on variations in R_s between juvenile and adults are surprisingly scarce. The only published report on ontogenetic R_s we were able to find in the literature reported that R_s peaks in newly metamorphosed *Hyla cinerea* froglets to then decrease during adulthood (Wygoda and Garman 1993), which differs from what we found in *L. macrosternum*, in which juveniles had lower R_s than adults. From a biophysical standpoint, water economy should favor higher values of R_s on adults because EWL is more sensitive to R_s as body size increases (Gouveia et al. 2019), and the higher R_s observed on *L. macrosternum* adults respective to juveniles seem to align with this water-conserving hypothesis. However, despite the higher R_s on *L. macrosternum* adults, the R_s difference between juveniles and adults is very small (0.35 s/cm) and their R_s values fall within the range (1-5 s/cm) typically expected for low skin resistance species (Young et al. 2005, Lillywhite 2006), which includes other leptodactylid species (see Supporting S3 in Senzano et al. 2022). As a result, water evaporates almost freely through the skin of both juveniles and adults, and any difference in EWL mediated by ontogenetically differences in R_s would yield a negligible water economy between them. We shall note that this conclusion is restricted to differences in R_s relative to the general water balance caused by geometric scaling of surface and body volume, which will have important consequences as the animals grow.

The lower Rs and higher surface to volume ratio of *L. macrosternum* juveniles leave them exposed to an increased risk of dehydration and some mechanisms to compensate for this greater

vulnerability might be identified. For example, juveniles tolerated higher levels of bodily water loss than adults, a pattern that coincides with an earlier report (Thorson 1955), but contrasts with others in which the opposite was true (Degani and Warburg 1984, Gillis 1979), or no EWL_{tol} difference was found among differently sized individuals (Nevo 1973, Newman and Dunham 1994). Regardless of whether EWL_{tol} is an ontogenetic dependent process or not, the advantage gained by a higher EWL_{tol} at the juvenile stage may counteract the increased risk of incurring in dehydration due to their greater vulnerability to evaporative water loss. Additionally, the higher rates of WU showed by *L. macrosternum* juveniles may also improve their ability to replenish bodily water losses faster than adults.

Present-day and forecasted habitat suitability

For the present-day scenario, our data predict suitable habitats for both juveniles and adults at lower latitudes and along coastlines of South America (Fig. 10A and 10B). These regions are mostly defined by habitats with closed-canopy forests, such as the Amazon biome in the northern and the Atlantic Forest biome in coastal areas, and the semi-open canopy savannas of the Cerrado biome in central regions. Although not directly quantified here, the buffering effect of canopies against temperature extremes and high variations in humidity may provide relatively stable ground-level conditions (Oyamaguchi et al. 2018), which may lead our models to predict suitable microclimates (lower risks of thermal and hydric stress). Still, some regions predicted as suitable by our models do not coincide with the current known distribution of the species (Magalhães et al. 2020), as is the case of northernmost (Amazonian) and southeastern coastal areas (southern Atlanctic Forest). Since our models consider both thermal and water constraints to infer habitat suitability, the thermal and water ambient conditions may no longer be the major limiting factors in these regions. Instead, other factors not considered here, such as seasonal environmental drivers on reproductive cycles (Chaves et al. 2021), possible interspecific competition (Baia et al. 2020) or, perhaps, dispersal biogeographical events in the past related to the Cerrado biome (see Werneck et al. 2012) may explain the virtually absence of *L. macrosternum* in these predicted thermally suitable areas. By contrast, large parts toward the southern edge of the species' geographical range were estimated to be poorly suitable for both juveniles and adults (Fig. 10A and 10B). Except for small portions of the semiarid Chaco biome, these southern areas are not considered drought-vulnerable habitats (Ganem et al. 2022), which is consistent with our hydric suitability predictions, in which hydric constraints are predicted to be minimal in these areas (Supporting S4). Instead, the

low suitability in southern regions was mostly driven by the low thermal suitability (Supporting S4) resulted from the colder ambient conditions that characterize these southern regions (Anjos et al. 2021).

Our mechanistic assessment indicates that juveniles of *L. macrosternum* will experience longer periods of activity restriction (Hr) than adults (Fig. 9), and because models predict the CT_{min} as the sole driver for limiting surface activity for both age classes (Supporting S5), juveniles' higher Hr was mostly dictated by their greater thermal sensitivity to colder temperatures for both present-day and future scenarios. The inclusion of shelter use in our simulations, however, enabled both juveniles and adults to withstand the colder nightly conditions of southern habitats (Supporting S5), although at suboptimal thermal conditions for optimal performance when surface active. Previous works have pointed out the buffering capacity of refuge use against temperature extremes and desiccation in anurans (e.g., Seebacher and Alford 2002, Oromí et al. 2010, Senanayake et al. 2019) and its potential buffering role to climate change (Enriquez-Urzelai et al. 2020), and our modelled outcomes support this expectation by allowing animals to persist in locations where they otherwise would become extinct (see Supporting S5). However, the temperature buffering capacity of underground shelter is still influenced by the thermal characteristics prevailing above ground, which can have direct consequences on organismal physiological tolerance. For example, shelter temperatures above the upper or below the lower thermal limits tolerated by animals may compromise immediate survival, as was the case for both sheltered juvenile and adult frogs, whose CT_{min} is predicted to limit their presence on colder southern habitats, and for juveniles, due to their CT_{max}, some locations in central regions under current climatic conditions (Supporting S6). This suggests that, despite the clear buffering properties of shelter use, the thermal sensitivity to critical thermal limits may still play a certain role in mediating species distributions and persistence under both current and future climate scenarios (discussed below).

In a climate warming scenario, warmer conditions at higher latitudes will lead to an expansion of suitable temperature conditions southward for both juveniles and adults (Fig. 10C-F), while on the other hand, larger areas in central regions may become climatically unsuitable for species presence, particularly for juveniles. The proportionally larger habitat loss found for juveniles are linked to influence of temperature. Indeed, according to our models, the projected contractions seem in the central regions of projected distribution in juveniles of *L. macrosternum* were solely a

function of animals reaching their CT_{max} (an event only detected during daylight hours), whereas CT_{min} (only detected during nocturnal hours) was the sole limiting factor for the species presence in southern regions (Supporting S6). As such, the slightly lower CT_{max} of juveniles (about 0.5°C lower than adults) renders them more susceptible to heat stress during the daytime, even if the shelter use buffering is considered (see previous paragraph). Climate warming may also offer new climatically suitable habitats by the elevation of nightly temperatures (McMunn and Pepi 2022). However, the suitability of these expansion areas was predicted to be very low, and do not even approach the present day suitability values for the areas projected to become unsuitable (Fig. 10G). Consequently, we might expect *L. macrosternum* to experience larger contracting distributional shifts in central regions with only marginal gains on its southern edge, where ambient conditions are close to species' thermal tolerance thresholds.

Although our modeling approach integrates important intrinsic (age-specific temperature and water sensitivity) and extrinsic (ground-level microclimate) aspects driving the complexities of animal-environment interactions, some considerations must be taken into account when interpreting our modeling predictive outputs. For example, our models were conceived to match the wettest periods of year when humid conditions are optimal and that generally coincides with frogs' peak activity (see methods section). This, however, may underestimate the potential role of evaporative water loss as a limiting factor in our estimates. Additionally, juveniles and adults engage on different ecological activities and behaviors that might be consequential to the assessment of their vulnerability to climate change. For example, adults tend to remain near their aquatic breeding habitats, while juveniles are considered the main populational dispersers (Pittman et al. 2014) whit dispersal activities often covering diurnal hours (e.g., Navas et al. 2007). Thus, desiccation risks may restrict surface activity more markedly on juvenile frogs under current and future conditions (see Child et al. 2009, Bartelt et al. 2010). Additional factors not considered here, such as the capacity for physiological and behavioral plasticity (Riddell et al. 2018), climate-induced body size changes (Sheridan et al. 2022), or the thermal and hydric sensitivity during larvae stages, including their potential carry-over effects on adulthood (Rudin-Bitterli et al. 2020, Ohmer et al. 2023), will likely influence the ability of a species to persist in projected changing environments. Despite these limitations, which are an expected challenge inherent to any current mechanistic approach, our mechanistic predictions still offering ecologically robust projections by capturing key processes though to be biologically relevant, and at scales over which microclimatic conditions are most likely to have direct impacts on organismal responses to climate change.

REFERENCES

Alvarez C. A., J. L. Stape, P. C. Sentelhas, J. L. M. Gonçalves and G. Sparovek. 2014. Köeppen's climate classification map for Brazil. Meteorologische Zeitschrift 22(6): 711-728.

Anjos L. J. S., E. B. Souza, C. T. Amaral, T. K. Igawa and P. M. Toledo. 2021. Future projections for terrestrial biomes indicate widespread warming and moisture reduction in forests up to 2100 in South America. *Global Ecology and Conservation*, 25: e01441.

Baia R. R. J., P. R. Sanches, F. P. Santos, A. C. Florentino and C. E. Costa-Campos. 2020. Diet overlap of three sympatric species of *Leptodactylus* Fitzinger (Anura: Leptodactylidae) in a Protected area in the Brazilian Amazon. *Cuadernos de Herpetología*, 34(2): 175-184.

Bartelt P. E., R. W. Klaver and W. P. Porter. 2010. Modelling amphibian energetics, habitat suitability, and movements of western toads, *Anaxyrus* (=*Bufo*) *boreas*, across present and future landscapes. *Ecological Modelling*, 221(22): 2675-2686.

Bodensteiner B. L., G. A. Agudelo-Cantero, A. Z. A. Arietta, A. R. Gunderson, M. M. Muñoz, J. M. Refsnider and E. J. Gangloff. 2021. Thermal adaptation revisited: How conserved are thermal traits of reptiles and amphibians? *Journal of Experimental Zoology A*, 335(1): 173-194.

Browne R. K. and D. L. Edwards. 2003. The effect of temperature on the growth and development of the endangered green and golden bell frog (*Litoria aurea*). *Journal of Thermal Biology*, 28(4): 295-299.

Carey C. 1978. Factors affecting body temperatures of toads. *Oecologia*, 35: 197-219.

Ceia-Hasse A., B. Sinervo, L. Vincente and H. M. Pereira. 2014. Integrating ecophysiological models into species distribution projections of European reptile range shifts in response to climate change. *Ecography*, 37: 1-10.

Chaves M. F., G. J. B. Moura, J. S. Baptista, A. P. Dantas, V. W. Texeira and A. A. C. Teixeira. 2021. Environmental and abiotic factors interfere in *Leptodactylus macrosternum* (Anura, Leptodactylidae) reproduction despite no changes in sexual hormones levels. *Research, Society and Development* 10(8): e46110817627.

Child T., B. L. Phillips and R. Shine. 2009. Does desiccation risk drive the distribution of juvenile cane toads (*Bufo marinus*) in tropical Australia? *Journal of Tropical Ecology*, 25: 193-200.

Cupp P. V. 1980. Thermal tolerance of five salientian amphibians during development and metamorphosis. *Herpetologica*, 36(3): 234-244.

Degani G. and M. R. Warburg. 1984. Changes in concentrations of ions and urea in both plasma and muscle tissue in dehydrated Hylid anuran. *Comparative Biochemistry and Physiology Part A*, 77(2): 357-360.

Erying V., S. Bony, G. A. Meehl, C. A. Senior, B. Stevens, R. J. Stouffer and K. E. Taylor. 2016. Overview of the coupled model intercomparison project phase 6 (CMIP6) experimental design and organization. *Geoscientific Model Development*, 9: 1937-1958.

Enriquez-Urzelai U., A. S. Palacio, N. M. Merino, M. Sacco and A. G. Nicieza. 2018. Hindered and constrained: limited potential for thermal adaptation in post-metamorphic and adult *Rana temporaria* along elevational gradients. *Journal of Evolutionary Biology*, 31(12): 1852-1862.

Enriquez-Urzelai U., M. Sacco, A. S. Palacio, P. Pintanel, M. Tejedo and A. G. Nicieza. 2019. Ontogenetic reduction in thermal tolerance is not alleviated by earlier developmental acclimation in *Rana temporaria*. *Oecologia*, 189: 385-394.

Enriquez-Urzelai U., R. Tingley, M. R. Kearney, M. Sacco, A. S. Palacio, M. Tejedo and A. G. Nicieza. 2020. The roles of acclimation and behaviour in buffering climate change impacts along elevational gradients. *Journal of Animal Ecology*, 89: 1722-1734.

Ganem K. A., Y. Xue, A. A. Rodrigues, W. Franca-Rocha, M. T. Oliveira, N. S. Carvalho, E. Y. T. Cayo, M. R. Rosa, A. C. Dutra and Y. E. Shimabukuro. 2022. Mapping South America's drylands through remote sensing—A review of the methodological trends and current challenges. *Remote Sensing*, 14(3): 736.

Garcia R. A., J. L. Allen and S. Clusella-Trullas. 2019. Rethinking the scale and formulation of indices assessing organism vulnerability to warmer habitats. *Ecography*, 42: 1024-1036.

Gillis J. E. 1979. Adaptive differences in the water economies of two species of Leopard frogs from eastern Colorado (Amphibia, Anura, Ranidae). *Journal of Herpetology*, 13(4): 445-450.

Goldstein J. A., K. S. Hoff and S. D. Hillyard. 2017. The effect of temperature on development and behaviour of relict leopard frog tadpoles. *Conservation Physiology*, 5: cow075.

Gondim P. M. 2021. Indicadores de estresse ambiental em populações de *Leptodactylus macrosternum* (Leptodactylidae) e *Scinax x-signatus* (Hylidae) em ambientes agrícolas no semi-árido brasileiro. PhD dissertation. Universidade Federal do Ceará, Brazil.

Gouveia S.F., R.P. Bovo, J.G. Rubalcaba, F.R. Silva, N.M. Maciel, D.V. Andrade and P.A. Martinez. 2019. Biophysical modeling of water economy can explain geographic gradient of body size in anurans. *The American Naturalist*, 193(1): 51-58.

Greenberg D.A. and W.J. Palen. 2021. Hydrothermal physiology and climate vulnerability in amphibians. *Proceedings of the Royal Society B*, 288: 20202273.

Gunderson A.R. and M. Leal. 2016. A conceptual framework for understanding thermal constraints on ectotherm activity with implications for predicting responses to global change. *Ecology letters*, 19: 111-120.

Hansen M.C. et al. 2013. High resolution global maps of 21st-century forest cover change. Science, 342(6160): 850-853.

Heinen J. T. and G. Hammond. 1997. Antipredator behaviors of newly metamorphosed green frogs (*Rana clamitans*) and leopard frogs (*R. pipiens*) in encounters with eastern garter snakes (*Thamnophis s. sirtalis*). *The American Midland Naturalist*, 137: 136-144.

Huey R.B. and R.D. Stevenson. 1979. Integrating thermal physiology and ecology of ectotherms: a discussion of approaches. *American Zoologist*, 19(1): 357-366.

John-Alder H. B., P. J. Morrin and S. Lawler. 1988. Thermal physiology, phenology, and distribution of tree frogs. *The American Naturalist*, 132(4): 506-520.

Kearney M.R. and W.P. Porter. 2017. NicheMapR – an R package for biophysical modelling: the microclimate model. *Ecography*, 40: 664-674.

Köhler A., J. Sadowska, J. Olszewska, P. Trzeciak, O. Berger-Tal and C.R. Tracy. 2011. Staying warm or moist? Operative temperature and thermal preferences of common frogs (*Rana temporaria*), and effects of locomotion. *Herpetological Journal*, 21: 17-26.

Lawler J. J., S. L. Shafer, B. A. Bancroft and A. R. Blaustein. 2009. Projected climate impacts for the amphibians of the western hemisphere. *Conservation Biology*, 24(1): 38-50.

Lertzman-Lepofsky G.F., A.M. Kissel and B. Sinervo. 2020. Water loss and temperature interact to compound amphibian vulnerability to climate change. Global Change Biology, 26(9): 4868-4879.

Lillywhite H. B., P. Licht and P. Chelgren. 1973. The role of behavioral thermoregulation in the growth energetics of the toad, *Bufo boreas*. *Ecology*, 54(2): 375-383.

Lillywhite H. B. 2006. Water relations of tetrapod integument. *Journal of Experimental Biology*, 209: 202-226.

Lima A. P. and W. E. Magnusson. 2000. Does foraging activity change with ontogeny? An assessment for six sympatric species of postmetamorphic litter anurans in Central Amazonia. *Journal of Herpetology*, 34(2): 192-200.

Magalhães F.M., Lyra M.L., Carvalho T.R., Baldo D., Brusquetti F., Burella P., Colli G.R., Gehara M.C., Giaretta A.A., Haddad C.F.B., Langone J.A., López J.A., Napoli M.F., Santana D.J., Sá R.O., Garda A.A. 2020. Taxonomic review of South American butter frogs: phylogeny, geographic patterns, and species delimitation in the *Leptodactylus latrans* species group (Anura: Leptodactylidae). *Herpetological Monographs*, 34: 131-177.

Martins M. 1988. Biologia reprodutiva de *Leptodactylus fuscus* em Boa Vista, Roraima (Amphibia: Anura). Revista Brazileira de Biologia 48(4): 969-977.

McMunn M. and A. Pepi. 2022. Predicted asymmetrical effects of warming on nocturnal and diurnal soil-swelling ectotherms. *The American Naturalist*, 199(2): 302-312.

Navas C. A., M. M. Antoniazzi, J. E. Carvalho, H. Suzuki and C. Jared. 2007. Physiological basis for diurnal activity in dispersing juvenile *Bufo granulosus* in the Caatinga, a Brazilian semi-arid environment. *Comparative Biochemestry and Physiology Part A*, 147(3): 647-657.

Nevo E. 1973. Adaptive variation in size of cricket frogs. *Ecology*, 54(6): 1271-1281.

New M., D. Lister, M. Hulme and I. Makin. 2002. A high-resolution data set of surface climate over global land areas. *Climate Research*, 21: 1-25.

Newman R. A. and A. E. Dunham. 1994. Size at metamorphosis and water loss in a desert anuran (*Scaphiopus couchii*). *Copeia*, 2: 372-381.

O'Connor M. P. and C. R. Tracy. 1992. Thermoregulation by juvenile toads of *Bufo woodhousei* in the field and in the laboratory. *Copeia*, 3: 865-876.

Ohmer M. E. B., T. T. Hammond, S. Switzer, T. Wantman, J. G. Bednark, E. Paciotta, J. Coscia and C. L. Richards-Zawacki. 2023. Developmental environment has lasting effects on amphibian post-metamorphic behavior and thermal physiology. *Journal of Thermal Biology*, 226: jeb244883.

Oliveira-Filho J.C. and A.A. Giaretta. 2008. Reproductive behavior of *Leptodactylus mystacinus* (Anura, Leptodactylidae) with notes on courtship call of other Leptodactylus species. *Iheringia, Série Zoologia*, 98(4): 508-515.

Oromí N., D. Sanuy and U. Sinsch. 2010. Thermal ecology of natterjack toads (*Bufo calamita*) in a semiarid landscape. *Journal of Thermal Biology*, 35: 34-40.

Oyamaguchi H. M., P. Vo, K. Grewal, R. Do, E. Erwin, N. Jeong, K. Tse, C. Chen, M. Miyake, A. Lin and M. Gridi-Papp. 2018. Thermal sensitivity of a Neotropical amphibian (*Engystomops pustulosus*) and its vulnerability to climate change. Biotropica, 50(2): 326-337.

Peterman W. E., J. L. Locke and R.D. Semlitsch. 2013. Spatial and temporal patterns of water loss in heterogeneous landscapes: using plaster models as amphibian analogues. *Canadian Journal of Zoology*, 91: 135-140.

Pintanel P., M. Tejedo, S. R. Ron, G. A. Llorente and A. Merino-Viteri. 2019. Elevational and microclimatic drivers of thermal tolerance in Andean *Pristimantis* frogs. *Journal of Biogeography*, 46(8): 1664-1675.

Pittman S. E., M. S. Osbourm and R. D. Semlitsch. 2014. Movement ecology of amphibians: A missing component for understanding population declines. *Biological Conservation*, 169: 44-53.

Putnam R. W. and A. F. Bennett. 1981. Thermal dependence of behavioral performance of anuran amphibians. *Animal Behaviour*, 29(2): 502-509.

Prado C. P. A., M. Uetanabaro and F. S. Lopes. 2000. Reproductive strategies of *Leptodactylus chaquensis* and *L. podicipinus* in the Pantanal, Brazil. Journal of Herpetology 34(1): 135-139.

Riddell E. A., J. P. Odom, J. D. Damm and M. W. Sears. 2018. Plasticity reveals hidden resistance to extinction under climate change in the global hotspot of salamander diversity. *Science Advances*, 4(7): eaar5471.

Rubalcaba J.G., S.F. Gouveia and M.A. Ollaga-Tárraga. 2019a. Upscaling microclimatic conditions into body temperature distributions of ectotherms. *The American Naturalist*, 193(5): 677-687.

Rubalcaba J.G., S.F. Gouveia and M.A. Ollaga-Tárraga. 2019b. A mechanistic model to scale up biophysical processes into geographical size gradients in ectotherms. *Global Ecology and Biogeography*, 28(6): 793-803.

Ruthsatz k., K. H. Dausmann, M. A. Peck and J. Glos. 2022. Thermal tolerance and acclimation capacity in the European common frog (*Rana temporaria*) change throughout ontogeny. *Journal of Experimental Zoology A*, 337(5): 477-490.

Sanabria E. A., L. B. Quiroga and J. C. Acosta. 2003. Ecología térmica de *Leptodactylus ocellatus* (Linnaeus, 1758) (Anura: Leptodactylidae) en los Bañados de Zonda, San Juan, Argentina. *Cuadernos de Herpetologia*, 17(1-2): 127-129.

Sanabria E. A., L. B. Quiroga, E. Gonzáles, D. Moreno and A. Cataldo. 2013. Thermal parameters and locomotor performance in juvenile of *Pleurodema nebulosum* (Anura: Leptodactylidae) from the Monte Desert. *Journal of Thermal Biology*, 38: 390-395.

Sanabria E. A., C. Y. Rodríguez, C. Vergara, E. Ontivero, M. Banchig, A. L. Navas, M. A. Herrera-Morata and L. B. Quiroga. 2015. Thermal ecology of the post–metamorphic Andean toad (*Rhinella spinulosa*) at elevation in the monte desert, Argentina. *Journal of Thermal Biology*, 52: 52-57.

Senzano L. M., R. P. Bovo and D. V. Andrade. 2022. Empirical estimation of skin resistance to water loss in amphibians: agar evaluation as a non-resistance model to evaporation. *Journal of Experimental Biology*, 225: jeb243941.

Seebacher F. and R. A. Alford. 2002. Shelter microhabitats determine body temperature and dehydration rates of a terrestrial amphibian (*Bufo marinus*). *Journal of Herpetology*, 36(1): 69-75.

Senanayake U. I., S. Siriwardana, D. K. Weerakoon and M. R. Wijesinghe. 2019. Combating extreme tropical seasonality: Use of rock cravices by the critically endangered frog *Nannophrys marmorata* in Sri Lanka. *Herpetological Conservation and Biology*, 14(1): 261-268.

Sheridan J. A., C. D. Mendenhall and P. Yambun. 2022. Frog body size responses to precipitation shift from resource-driven to desiccation-resistant as temperatures warm. *Ecology and Evolution*, 12(12): e9589.

Sherman E. 1980. Ontogenetic change in thermal tolerance of the toad *Bufo woodhousii fowleri*. *Comparative Biochemistry and Physiology A*, 65: 227-230.

Silva W.R. and A.A. Giaretta. 2008. Further notes on the natural history of the South American pepper frog, *Leptodactylus labyrinthicus* (Spix, 1824) (Anura, Leptodactylidae). Brazilian Journal of Biology 68(2): 403-407.

Sinclair B. J., K. E. Marshall, M. A. Sewell, D. L. Levesque, C. S. Willett, S. Slotsbo, Y. Dong, C. D. G. Harley, D. J. Marshall, B. S. Helmuth and R. B. Huey. 2016. Can we predict ectotherm responses to climate change using thermal performance curves and body temperatures? *Ecology Letters*, 19: 1372-1385.

Smits 1984. Activity patterns and thermal biology of the toad *Bufo boreas halophilus*. *Copeia*, 3: 689-696.

Solano H. 1987. Algunos aspectos de la biología reproductiva del sapito silvador *Leptodactylus fuscus* (Schneider) (Amphibia: Leptodactylidae). *Amphibia-Reptilia*, 8: 111-128.

Storey J. M. and K. B. Storey. 1985. Adaptations of metabolism for freeze tolerance in the gray tree frog, *Hyla versicolor*. *Canadian Journal of Zoology*, 63(1): 49-54.

Storey K. B. and J. M. Storey. 2017. Molecular physiology of freeze tolerance in vertebrates. *Physiological Reviews*, 97: 623-665: 623-665.

Thorson T. B. 1955. The relationship of water economy to terrestrialism in amphibians. *Ecology*, 36(1): 100-116.

Tracy C. R., K. A. Christian, M. P. O'Connor and C. R. Tracy. 1993. Behaviuoral thermoregulation by *Bufo americanus*: the importance of the hydric environment. *Herpetologica*, 49(3): 375-382.

Tracy C.R., K.A. Christian and C.R. Tracy. 2010. Not just small, wet, and cold: effects of body size, and skin resistance on thermoregulation and arboreality of frogs. *Ecology*, 91(5): 1477-1484.

Vonesh J. R. 2005. Sequential predator effects across three life stages of the African tree frog, *Hyperolius spinigularis*. *Oecologia*, 143: 280-290.

Wassersug R. J. and D. G. Sperry. 1977. The relationship of locomotion to differential predation on *Pseudacris triseriata* (Anura: Hylidae). *Ecology*, 58: 830-839.

Wells K. D. 2007. The Ecology and Behavior of Amphibians. *The University of Chicago Press*, Chicago, USA.

Wilson R. S. 2001. Geographic variation in thermal sensitivity of jumping performance in the frog *Limnodynastes peronii*. *The Journal of Experimental Biology*, 204: 4227-4236.

Young J.E., K.A. Christian, S. Donnellan, C.R. Tracy and D. Parry. 2005. Comparative analysis of cutaneous evaporative water loss in frogs demonstrates correlation with ecological habits. *Physiological and Biochemical Zoology*, 78(5): 847-856.

SUPPORTING INFORMATION

Supporting S1. Thermal performance curves

The longest distance jumped by each frog at each test temperature was plotted against its corresponding T_b collected at the end of each trial. From this empirical data, we fitted various thermal performance curve (TPC) models available in the 'nls.multstart' and 'rTPC' R-packages following Padfield et al. (2021). We selected the best-fitting curve model for each group based on Akaike Information Criterion scores corrected for small sample sizes (AICc) (Table S1). Then, the TPC models were used to analyze individual TPCs for each frog and estimate its respective T_{opt} as the T_b level in which the animals attained maximum performance (Huey and Stevenson 1979). For subsequente modeling purposes (see main text), we also calculated the thermal performance breadth (B_{80}; the range of T_bs across which jumping ability remains at least 80% of its maximum capacity) from the combined data of all individuals as a general descriptive trait that characterize the overall thermal sensitivity for each age class (Huey and Kingsolver 1989) (Figure S1).

Table S1. Summary of the thermal performance curve (TPC) models fitted to each age class. TPC models are ranked based on their Akaike Information Criterion scores corrected for small sample sizes (AICc), with lower scores indicating a better fit of model to empirical observations. See Padfield et al. (2021) for TPC descriptions, equations, and references therein.

Juveniles		*Adults*	
TPC model	**AICc**	**TPC model**	**AICc**
boatman	767.63	kamykowski	368.13
thomas_2017	768.14	boatman	369.18
kamykowski	768.2	beta	372.62
beta	768.63	joehnk	378.79
briere2	769.2	thomas_2017	378.95
joehnk	769.81	briere2	390.41
ratkowsky	778.55	modifiedgaussian	395.48
quadratic	780.68	quadratic	400.04
modifiedgaussian	790.89	ratkowsky	401.62
weibull	802.23	oneill	415.88
oneill	802.87	weibull	422.7
gaussian	810.48	rezende	428.7
delong	818.11	gaussian	433.03
sharpeschoolhigh	831.57	spain	433.92
pawar	831.57	sharpeschoolhigh	435.11
flinn	853.87	pawar	435.11
rezende	855.64	delong	440.37
spain	864.09	flinn	456.25
hinshelwood	868.06	lactin2	472.92
lactin2	919.48	hinshelwood	603.8
johnson_lewin	1138.7	johnson_lewin	603.8

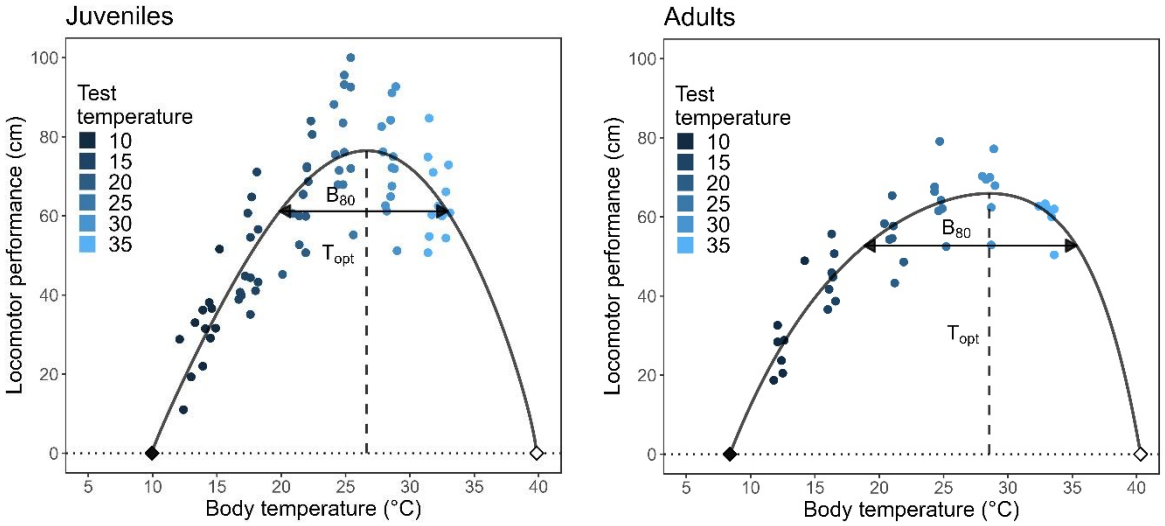

Figure S1.1. Locomotor performance represents the longest distance jumped by each frog at each test temperature. Points indicate individuals' body temperature collected at the end of each temperature trial. Vertical dashed lines indicate the optimal temperature (T_{opt}) and horizontal arrows indicate the thermal performance breadth, B_{80} (the thermal range at which locomotory function remains above 80% of its maximum capacity). Rhombuses indicate the empirically determined critical thermal minimum (black rhombus) and maximum (white rhombus).

Supporting S2. Calculation of evaporative water loss and skin resistance to evaporation

Evaporative wate loss calculations

Relative humidity recordings were converted into water vapor density (WVD) values (g/m^3), and used to calculate absolute EWL ($\mu gH_2O/s$) from the equation: EWL = (VDe − VDi)*F; where VDe and VDi are the WVD of the excurrent and incurrent (baseline) airflow from/to the chamber, respectively, and F is the airflow rate (cm^3/s). Animal exposed surface area (A_s) to evaporation was estimated from the empirical equation described by Klein et al. (2016) for Leptodactylids: $A_s = 8.6856Mass^{0.6652}$, assuming that one-third of agar surface remained in direct contact with substrate. Area-specific EWL rates ($\mu gH_2O/cm^2/s$) were obtained by dividing absolute EWL rates by two-thirds of animals' total skin surface area.

Skin resistance to evaporation

Total resistance (R_T) to evaporation is the combined result of both skin (R_s) and boundary layer (R_b) resistances, thus we used the agar method described by Spotila and Berman (1976) to derive empirical estimations of R_b. Alginate dental impressions obtained from living animals in a water conserving posture were filled with heated 3% agar solution and left to harden. This resulted in agar replicas that lose water freely, while mimicking the shape and size of living animals. Because agar models mimic the shape and size of real frogs in a water conserving posture, agar exposed surface area to evaporation and area-specific EWL rates were calculated in the same manner as real frogs. The R_b component was determined following Spotila and Berman (1976): R_b = VDD/EWL, where R_b (s/cm) is the resistance of the boundary layer of adhered air next to the agar surface, VDD is the water vapor density (WVD) difference ($\mu g/cm^3$) between the saturated WVD at the agar surface temperature, and the partial WVD of air temperature, and EWL is the area-specific water loss rates. The same resistance calculation was used to estimate R_T departing from frogs' area-specific EWL rates. Finally, skin resistance was calculated as $R_s = R_T - R_b$.

Supporting S3. Biophysical model parameterization used for solving inflows and outflows of heat energy expected for a 11 g juvenile and a 57 g adult *L. macrosternum* frog. Lower (B_{80} lower) and upper (B_{80} upper) bounds of thermal performance breadth, critical thermal minimum (CT_{min}) and maximum (CT_{max}), and tolerance to dehydration (EWL_{tol}).

Model parameter	value	detail	source/reference
Body mass (g)*	11, 57	average masses for our measured individuals	unpiblished data
Total skin surface area (cm^2)*	42.8, 128.9	surface area calculated as $8.6856Mass^{0.6652}$	Klein et al. (2016)
Skin resistance (s/cm)*	1.73, 2.09	Estimated empirically with the use of 3% agar models	unpiblished data
Skin type	1	wet-skinned	-
B_{80} lower (°C)*	19.87, 18.98	determined empirically	
B_{80} upper (°C)*	32.94, 35.34	determined empirically	
CT_{min} (°C)*	9.96, 8.4	determined empirically	
CT_{max} (°C)*	39.85, 40.31	determined empirically	
EWL_{tol} (%)*	63.37, 68.22	determined empirically	
Air temperature (°C)	-	at 1 cm height	'`micro_global`' (NicheMapR)
Ground temperature (°C)	-	soil temperature at 0 cm height	'`micro_global`' (NicheMapR)
Solar radiation (W/m^2)	-	-	'`micro_global`' (NicheMapR)
Wind speed (m/s)	-	at 1 cm height	'`micro_global`' (NicheMapR)
Relative humidity (%)	-	at 1 cm height	'`micro_global`' (NicheMapR)
Posture	1	dorsal surface exposed to air	-
Proportion of ventral surface	1/3	proxy proportion for an anuran in a water conserving posture	Klein et al. (2016)
Body heat capacity (J/g/°C)	3.6	default value	-
Delta	60	default value	-

*Values are reported for juveniles and adults, respectively.

Supporting S4. Thermal and hydric suitability maps

We infered thermal suitability of locations by scaling hourly surface activity scores between 0, if animals were unable to engage in activity due to thermal constraints, and 1 if animals achieved at least 6 hours of activity with their T_b kept within their B_{80} limits, time assumed to be sufficient for performing most relevant ecological tasks. This later assumption is based in *Leptodactylus* congeners, where a large proportion of activity occurs primarily during the first half of the night (Woolbright 1985, De-Carvalho et al. 2008, Bardier et al. 2014, Borges-Leite et al. 2015). Hydric suitability was estimated by scaling the total cumulative EWL scores into relative scores between 0, when the cumulative EWL attained EWL_{tol} during the first hour of activity (no activity due to hydric constraints) and 1 if animals were able to conclude all nightime hours with a cumulative EWL approximating its initial state of fully hydration. Note that, since EWL is an unavoidable process, even locations considered highly suitable from a hydric prespective will exhibit values very close to 1, but not 1. We then projected these thermal and hydric suitability outputs onto maps for present-day and future scenarios (Fig. S4.1). Finally, we combined the thermal and hydric suitability maps by multiplying their scores to produce an overall habitat suitability map with scores ranging on a continuous scale between 0, representing locations where activity was curtailed by thermal or hydric restrictions, and 1 representing locations where animals can maintain an optimal range of T_bs (at least 6 hours of activity within their B_{80} limits) while maintaining a good hydration level (see 'Results' section in the main text).

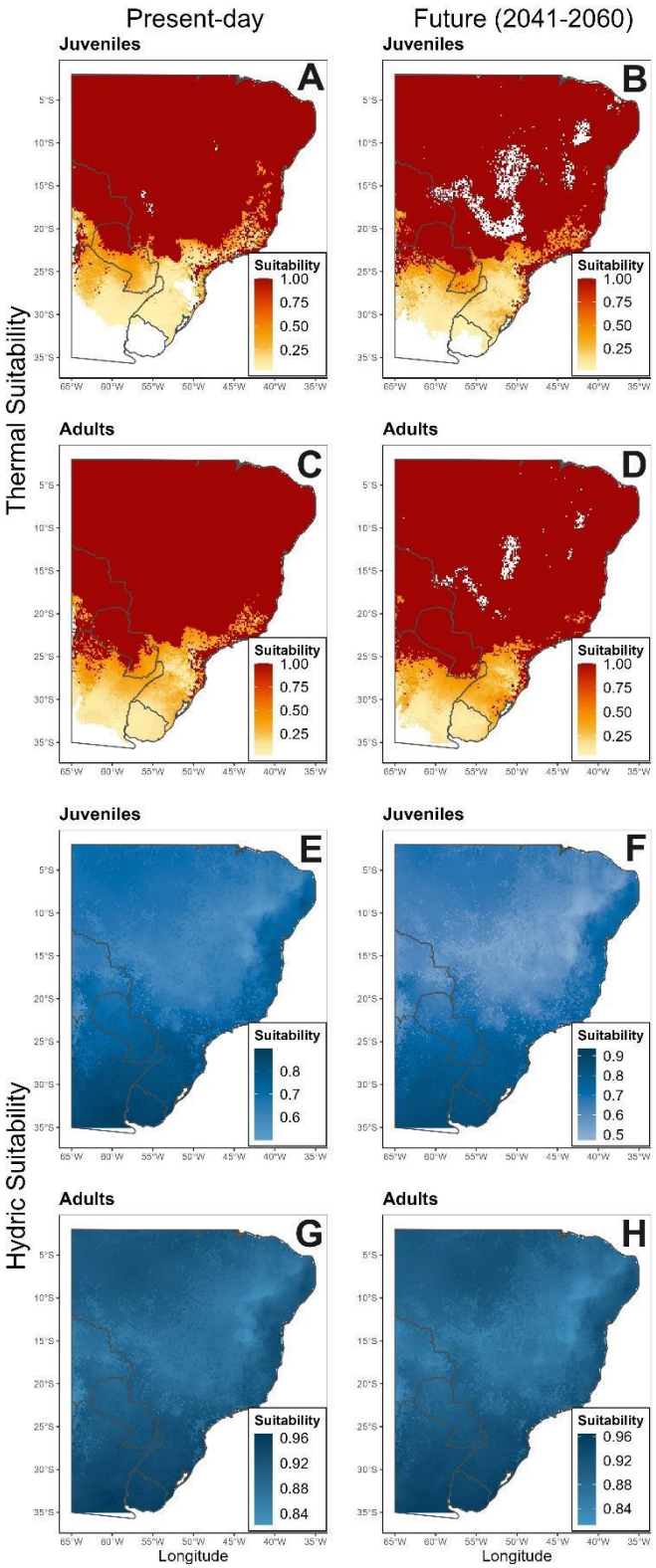

Figure S4.1. Thermal (A-D) and hydric suitability (E-H) maps for present-day and future scenarios for juvenile and adult frogs of *Leptodactylus macrosternum*.

Supporting S5. Physiological limiting constraints on activity time during nighttime hours

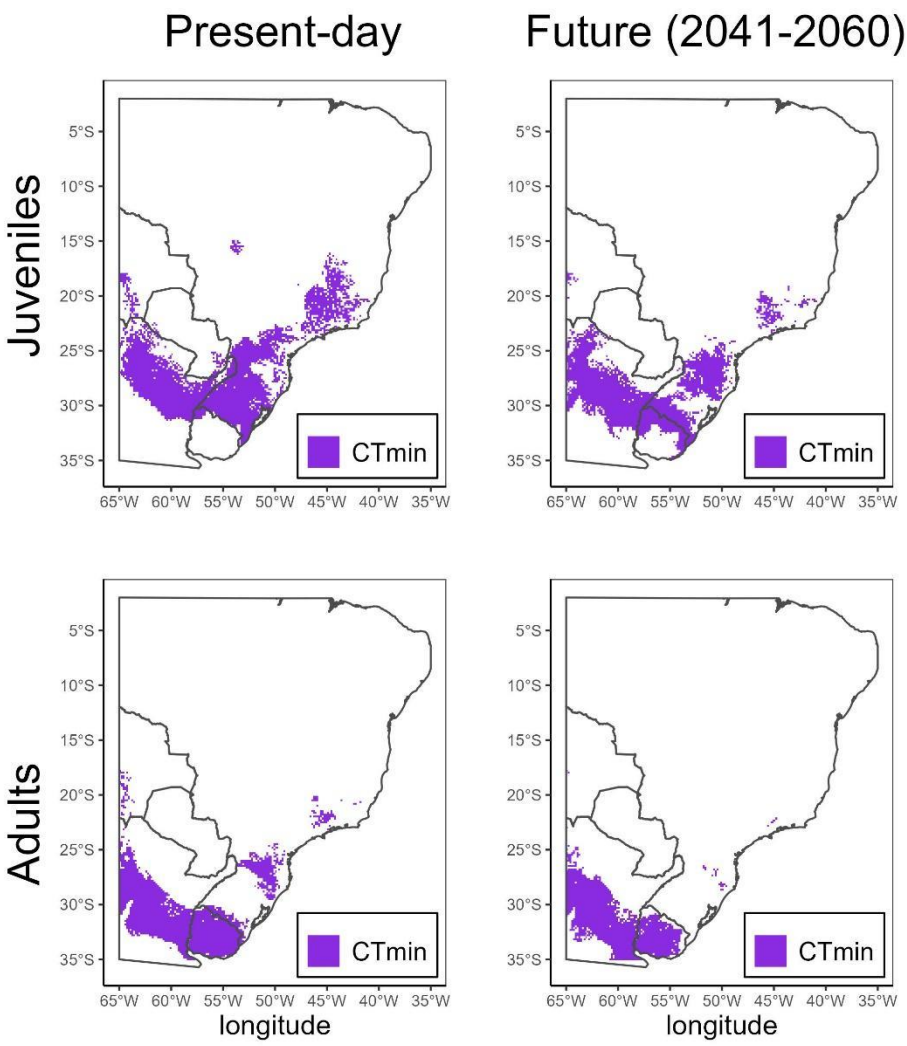

Figure S5.1. Predicted physiological limiting constraints on activity time for both juvenile and adult *L. macrosternum* frogs. The indicated areas represent locations where animals are predicted to experience some level of restriction in activity (Hr) (regardless of the total hours of restriction) throughout nighttime hours (18:00 - 05:00 h). Here, the Hr was predicted to be a sole function of the critical thermal minimum (CT_{min}) for the present-day and future scenario. Additionally, because the premise of shelter use in our simulations permits animals to escape harmful surface conditions (see main text), these areas also represent locations in which species persistence is only possible with the use of underground refugia (i.e., the species could go locally extinct without the buffering effect of shelter use).

Supporting S6. Physiological constraints predicted for animals when sheltered underground

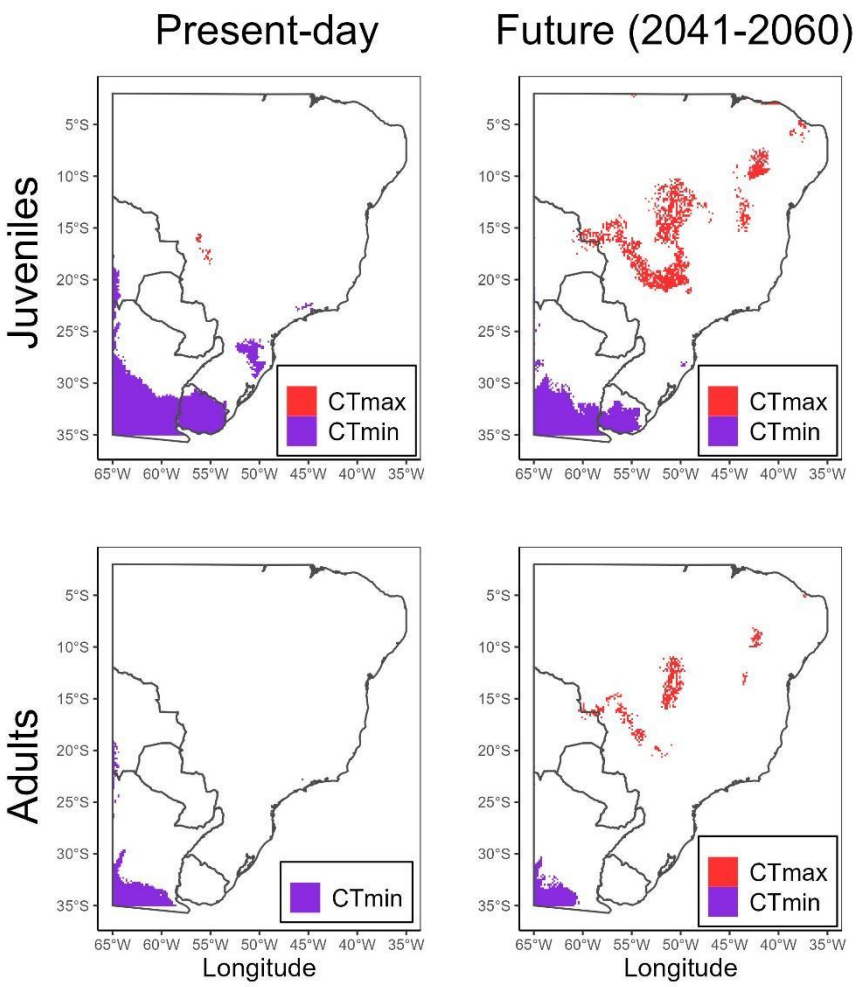

Figure S5.1. Indicated areas represent locations in which frogs exceeded their critical thermal minimum (CT_{min}) and/or maximum (CT_{max}) when sheltered. Note that, in the context of our simulations, a sheltered frog is likely impeded to escape harmful T_bs in case of thermal stress, so these areas simultaneously represent local species absence (present-day scenario) or projected extinctions (future scenarios) in which sheltered frogs (either day or night) attained its critical thermal endpoints. In addition, predicted local extintions led by CT_{min} were detected to occur only during nighttime hours, whereas CT_{max}-induced extinctions only occurred during daylight hours.

SUPPORTING INFORMATION REFERENCES

Bardier C., A. Canavero and R. Maneyro. 2014. Temporal and spatial activity patterns of three species in the *Leptodactylus fuscus* group (Amphibia, Leptodactylidae). *South American Journal of Herpetology*, 9(2): 106-113.

Borges-Leite M. J., J. F. M. Rodrigues, P. M. Gondim AND D. M. Borges-Nojosa. 2015. Reproductive activity of *Adenomera* aff. *hylaedactyla* (Anura: Leptodactylidae) in a coastal area of Brazil. *Animal Biology*, 65: 101-111.

De-Carvalho C. B., E. B. Freitas, R. G. Faria, R. C. Batista, C. C. Batista, W. A. Coelho and A. Bocchiglieri. 2008. História natural de *Leptodactylus mystacinus* e *Leptodactylus fuscus* (Anura: Leptodactylidae) no Cerrado do Brasil Central. Biota Neotropica 8(3): 105-115.

Huey R.B. and R.D. Stevenson. 1979. Integrating thermal physiology and ecology of ectotherms: a discussion of approaches. *American Zoologist*, 19(1): 357-366.

Klein W., L. Dabés, V.M.G. Bonfim, L. Magrini and M.F. Napoli. 2016. Allometric relationships between cutaneous surface area and body mass in anuran amphibians. *Zoologischer Anzeiger - A Journal of Comparative Zoology*, 263: 45-54.

Padfield D., H. O'Sullivan and S. Pawar 2021. rTPC and nls.multstart: a new pipeline to fit thermal performance curves in R. *Methods in Ecology and Evolution*, 12(6): 1138-1143.

Spotila J. R. and E. N. Berman. 1976. Determination of skin resistance and the role of the skin in controlling water loss in amphibians and reptiles. *Comparative Biochemistry and Physiology A*, 55: 407-411.

Woolbright L. L. 1985. Patterns of nocturnal movement and calling by the tropical frog *Eleutherodactylus coqui*. *Herpetologica*, 41(1): 1-9.